Course of Geodynamics

Dr. Magdala Tesauro

Course Outline:

1. Thermo-physical structure of the continental and oceanic crust
2. **Thermo-physical structure of the continental lithosphere**
3. Thermo-physical structure of the oceanic lithosphere and oceanic ridges
4. Strength and effective elastic thickness of the lithosphere
5. Plate tectonics and boundary forces
6. Hot spots, plumes, and convection
7. Subduction zones systems
8. Orogens formation and evolution
9. Sedimentary basins formation and evolution

The current paradigm of plate dynamics is based on the “LAB hypothesis”

- The kinematic entities we call plates (lithosphere) are decoupled from deeper mantle flow by a weak zone of lateral shearing (asthenosphere) within the uppermost mantle
- *The lithosphere-asthenosphere boundary (LAB) marks the base of the tectonic plates*

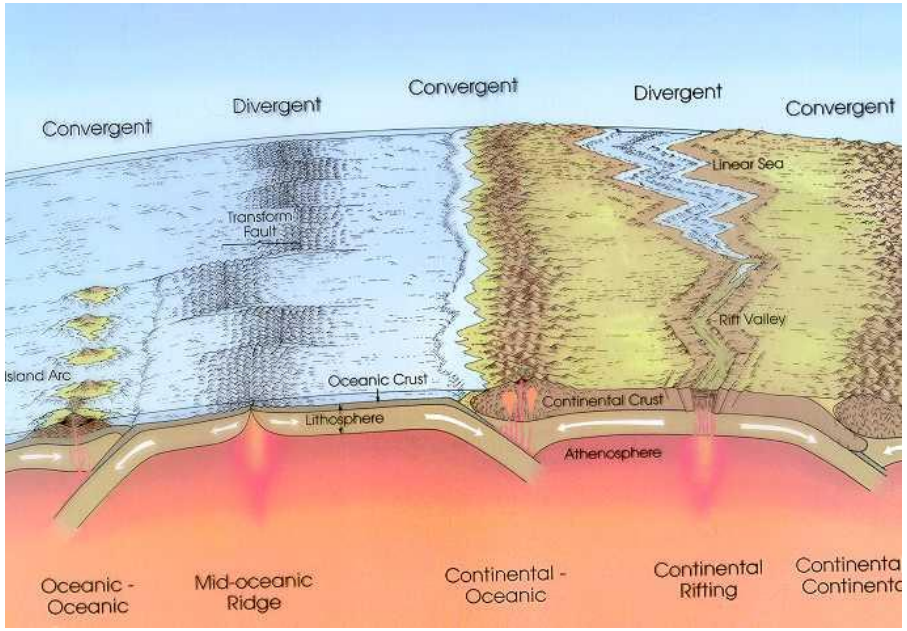

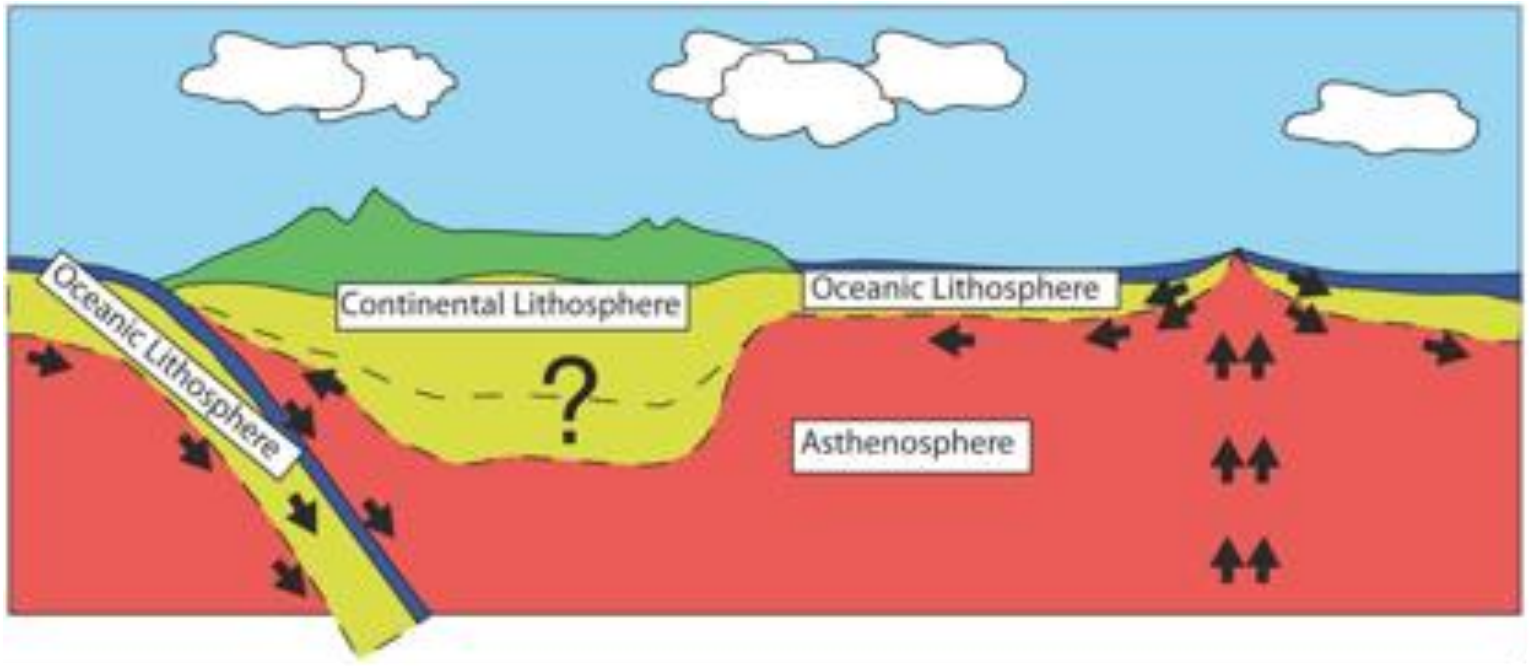

Oceanic and continental lithosphere

Oceanic lithosphere

- Thin
  - Crust: approximately constant (7 km)
  - Lithospheric thickness increases with age (max 100-125 km)
- Young: less than 200 million years
- Heavy: ultimately always subduction
- Enriched in FeO and MgO
- Hardly any heat production

Continental lithosphere

- Thick
  - Crust: 20 – 60 km
  - Lithosphere: 25 – 250 km
- Old: More than 4 billion years
- Light: virtually never subduction
- Enriched in SiO_2
- Substantial heat production

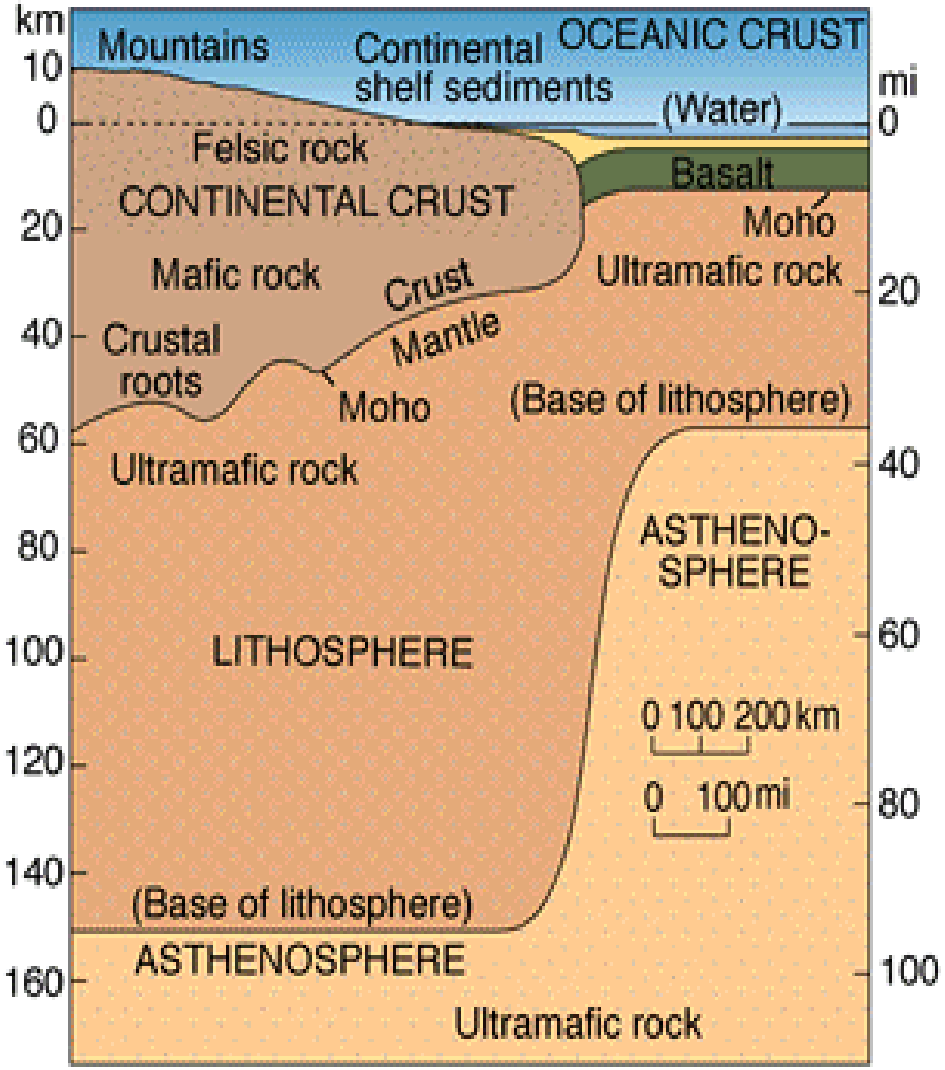

Upper mantle heterogenity detected from seismic tomography

Seismic wave velocity is a function of temperature:

Warm → slower

Cold → faster

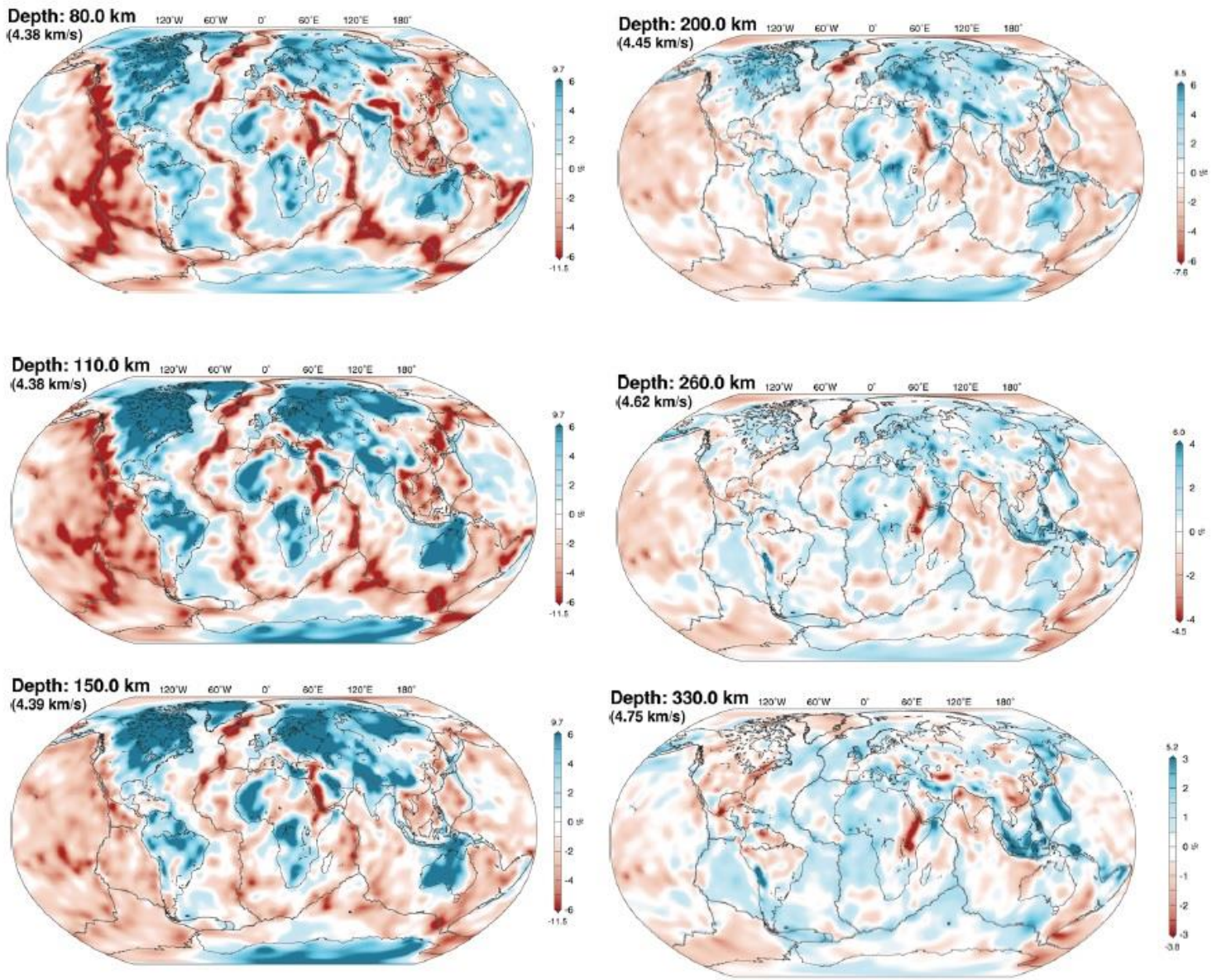

Shear waves anomalies Scaheffer and Lebedev, 2013, Geophys. J. Int., 194

Dependance of seismic velocities in the upper mantle

Anharmonicity: refers to the behaviour of materials in which elastic properties change because of temperature (or pressure) caused by the deviation of lattice vibration from the harmonic oscillator. This process produces thermal expansion (without energy dissipation) and thus elastic properties of materials vary due to the change in mean atomic distances.

Anelasticity: a dissipative process involving viscous deformation. The degree to which viscous deformation affects seismic wave velocities is measured by the attenuation parameter *Q* and depends on the frequency of seismic waves and temperature. Seismic attenuation is described by the "quality factor" Q which quantifies the amount of energy ΔE lost per cycle.

Composition: A decrease in Mg# by 4–5 units (corresponding to a typical difference between Archean to Phanerozoic lithospheric mantle) results in a 1% *S* velocity decrease, in a ~1.4% density increase and in a mantle temperature variation by 220 °C.

Melt: ca. 5% of melt lead to more than a 10% velocity decrease. The amount of melt even beneath the midocean ridges is only ca. 2%, while in the continental lithospheric mantle is even smaller. Indeed, interconnected melt is gravitationally unstable and migrates upwards even at concentrations of <<1%.

Fluids: They may have an indirect effect on velocities by affecting the solidus temperature and enhance anelasticity. We should consider that the amount of water does not exceed 0.03 wt.% of olivine, but at the sites of paleosubduction zones the amount of water in the mantle can increase by 3–10 times due to its downward transport.

Seismic anisotropy: or the dependence of seismic wave speeds on the propagation direction or polarization of the waves. Deformation in the Earth often leads to seismic anisotropy, either through the crystallographic or lattice preferred orientation (CPO, LPO) of anisotropic constituent minerals. Differences in propagation speed between surface waves that are polarized differently (Rayleigh waves vs. Love waves) contain information about radial anisotropy, while the dependence of Rayleigh (or Love)wave velocities upon propagation direction contains information about azimuthal anisotropy.

Anharmonicity and Anelasticity

Seismic velocity and temperature are linearly inversely correlated up to a temperature of about 900°C due to the anharmonicity effect.

At higher temperatures it starts the effect of anelasticity: no linear correlation between velocity and temperatures

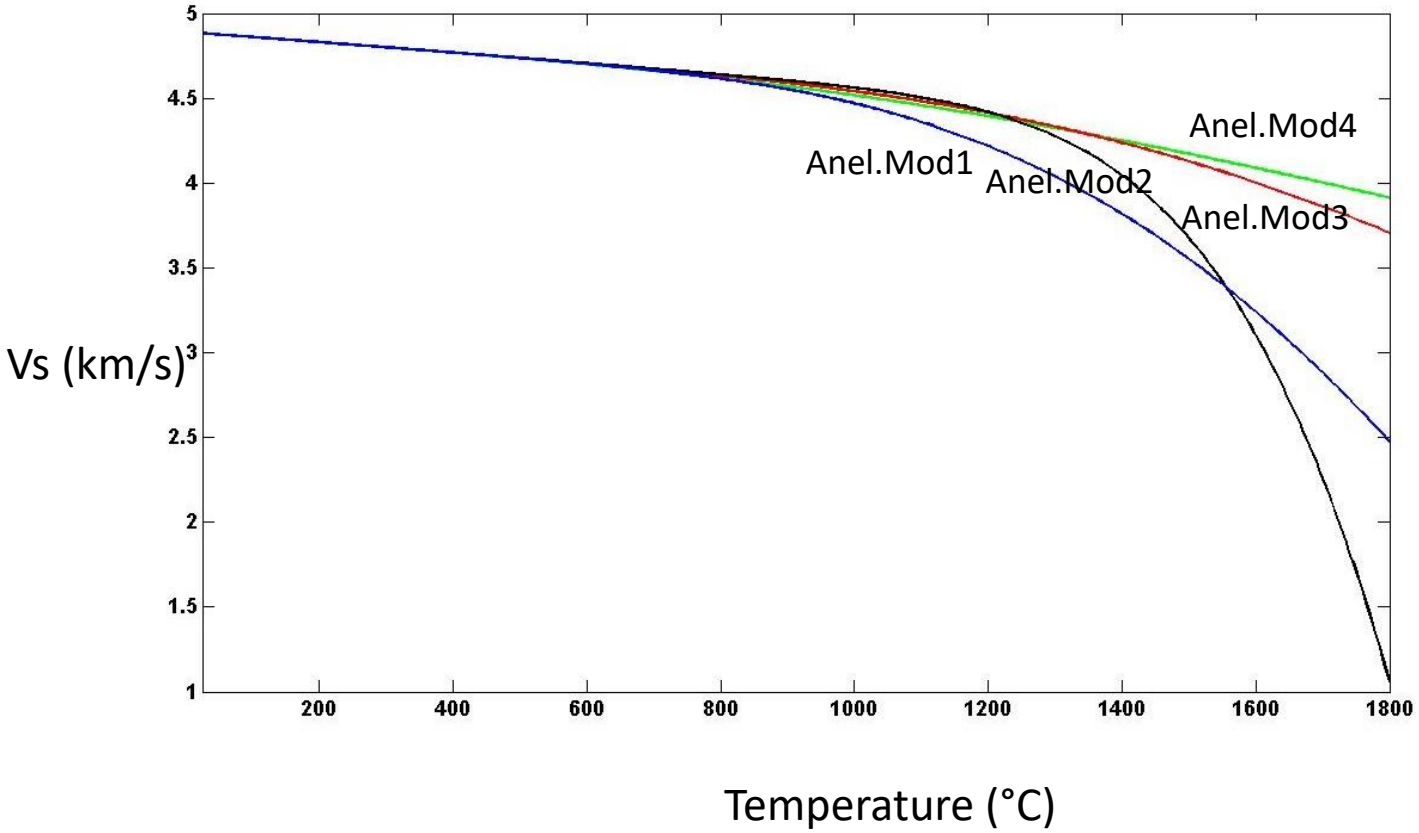

$$V(P, T, X, \omega) = V_{\text{anh}}(P, T, X)\left[1 - \frac{Q^{-1}(\omega, T)}{2\tan(\pi a/2)}\right]$$

V_{ahn}= Synthetic Velocity (anharmonicity effect)

$$Q_\mu = A\,\omega^a \exp(aE^*/RT),\ E^* = H^* + PV^*$$

A is a normalization factor, *ω* the seismic frequency, *a* the exponent describing the frequency dependence of the attenuation, *T* the temperature, *R* the gas constant, *E** the activation energy, *V** the activation volume and *H** the activation enthalpy.

Dependance of seismic velocities on volatiles

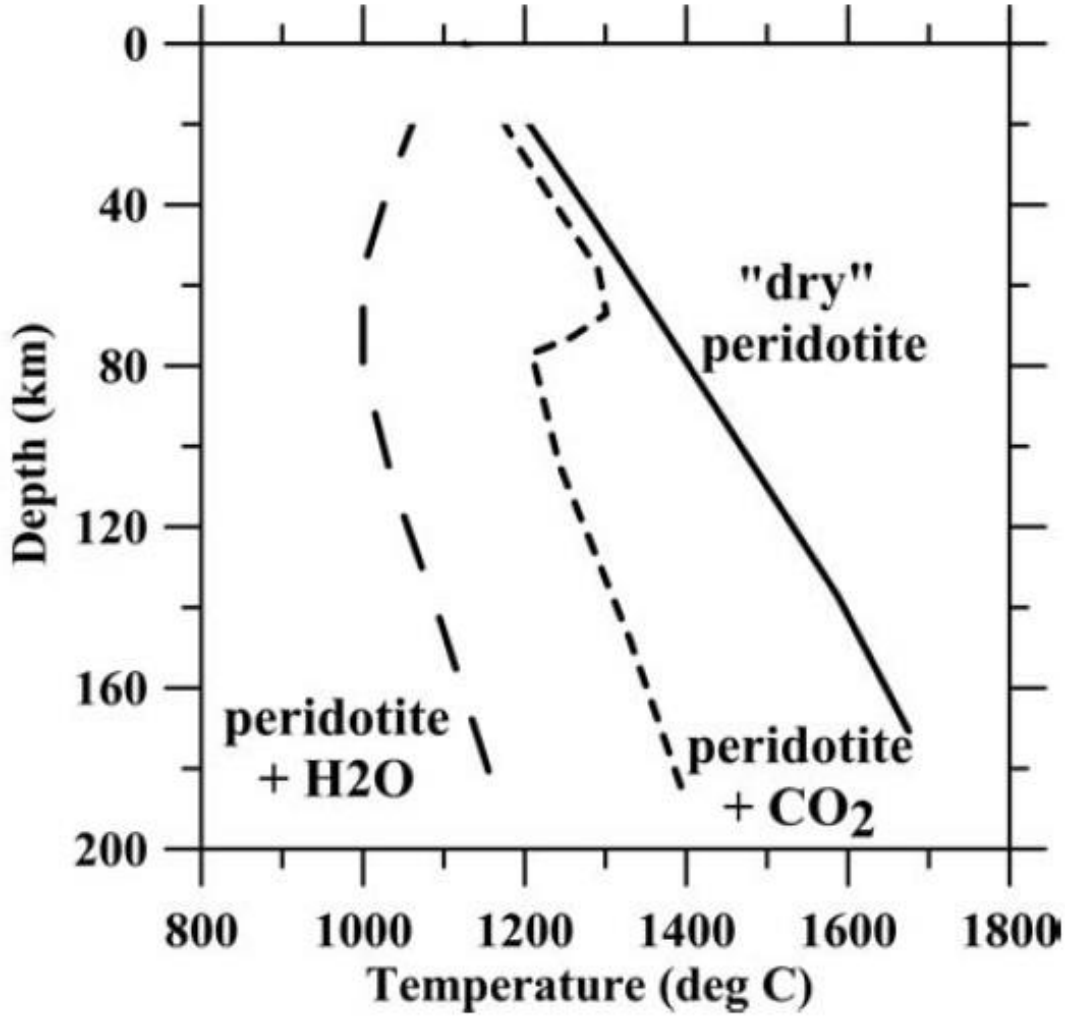

- At a depth > 80 km at high temperatures, the presence of even small volumes of volatiles (water and carbon dioxide) in the upper mantle indirectly reduces seismic velocities by lowering mantle melting temperature.

Global Tectonic Regionalization

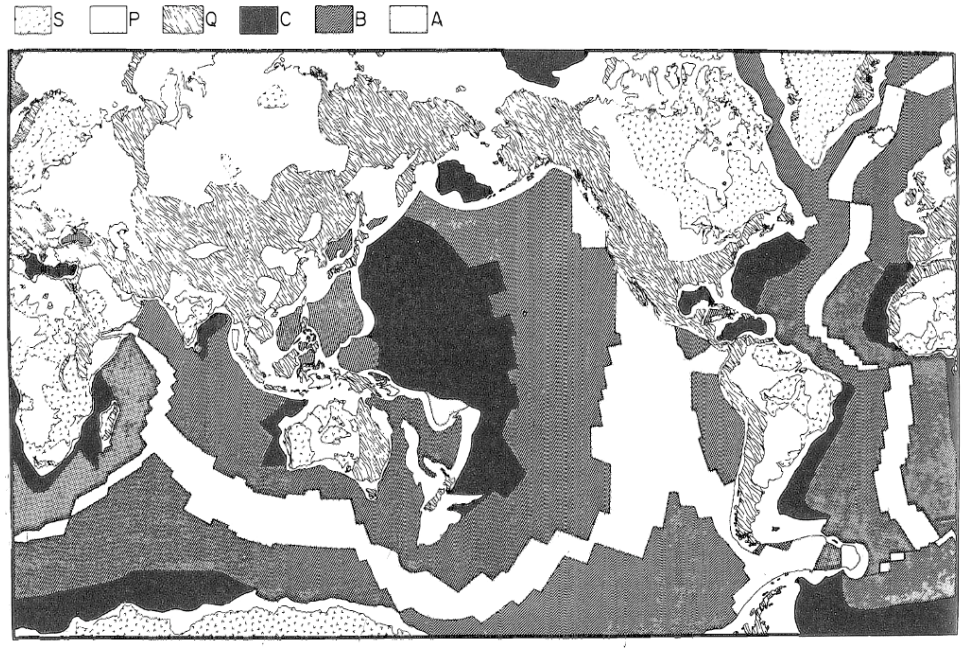

GRT1 (Jordan, 1981)

- Three oceanic regions A, B, C
  - based on lithospheric age
- Three continental regions Q, P, S
  - based on generalized tectonic behavior during the Phanerozoic

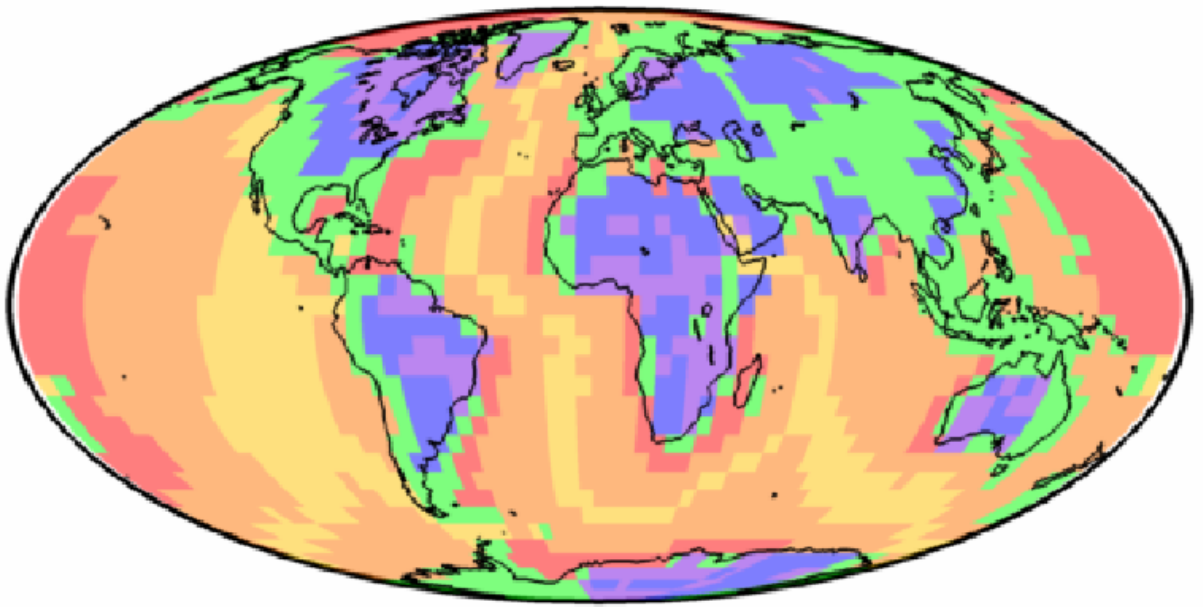

A- Young Oceans
B- Intermediate Oceans
C- Old Oceans
Q- Phanerozoic Orogenic Zones and Magmatic Belts
P- Precambrian Platform
S- Precambrian Shield

Global Tectonic Regionalization

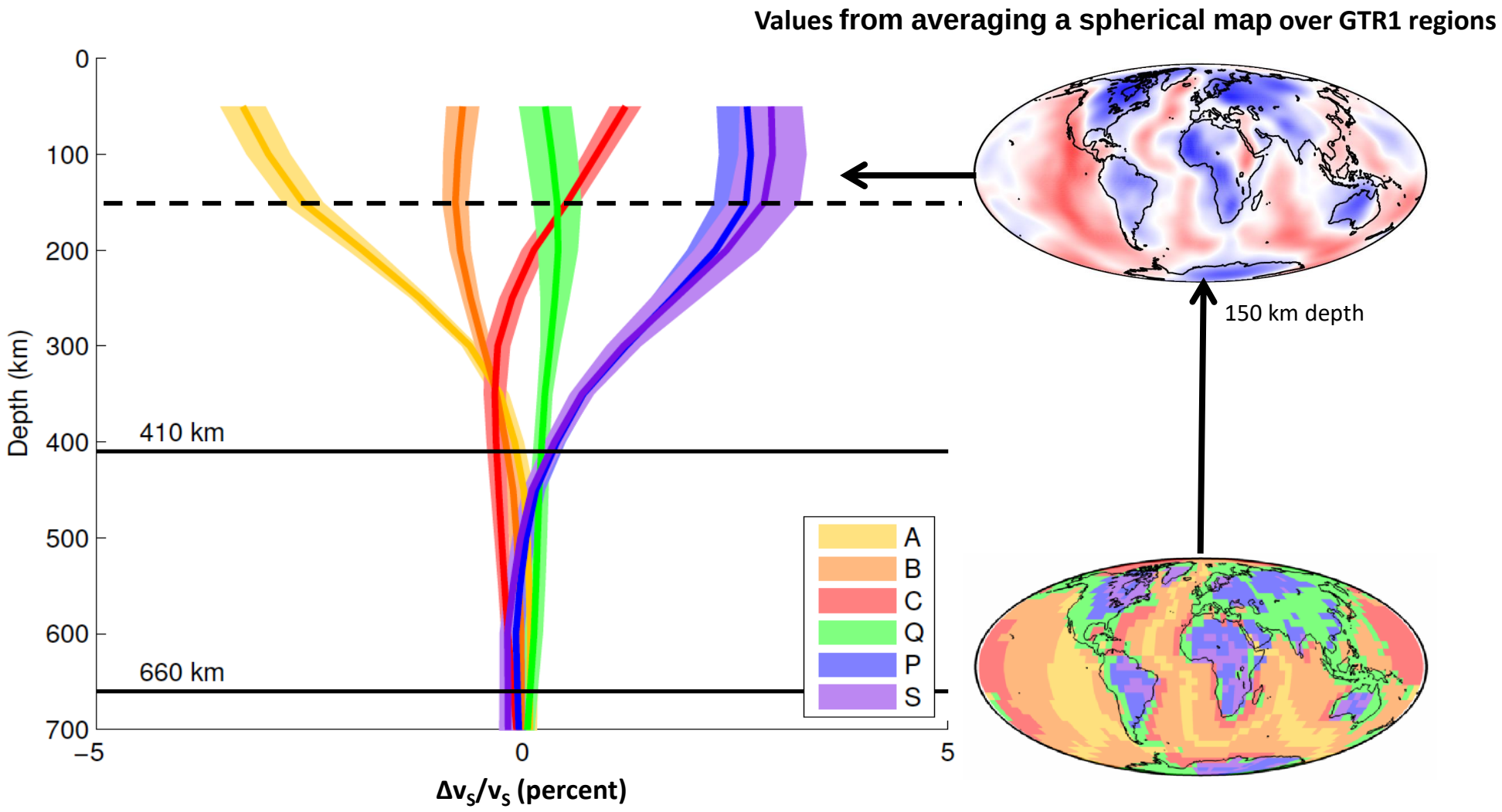

Model TX2008 (Simmons et al., 2009 *Geophys. J. Int.*, 177)

Global Tectonic Regionalization

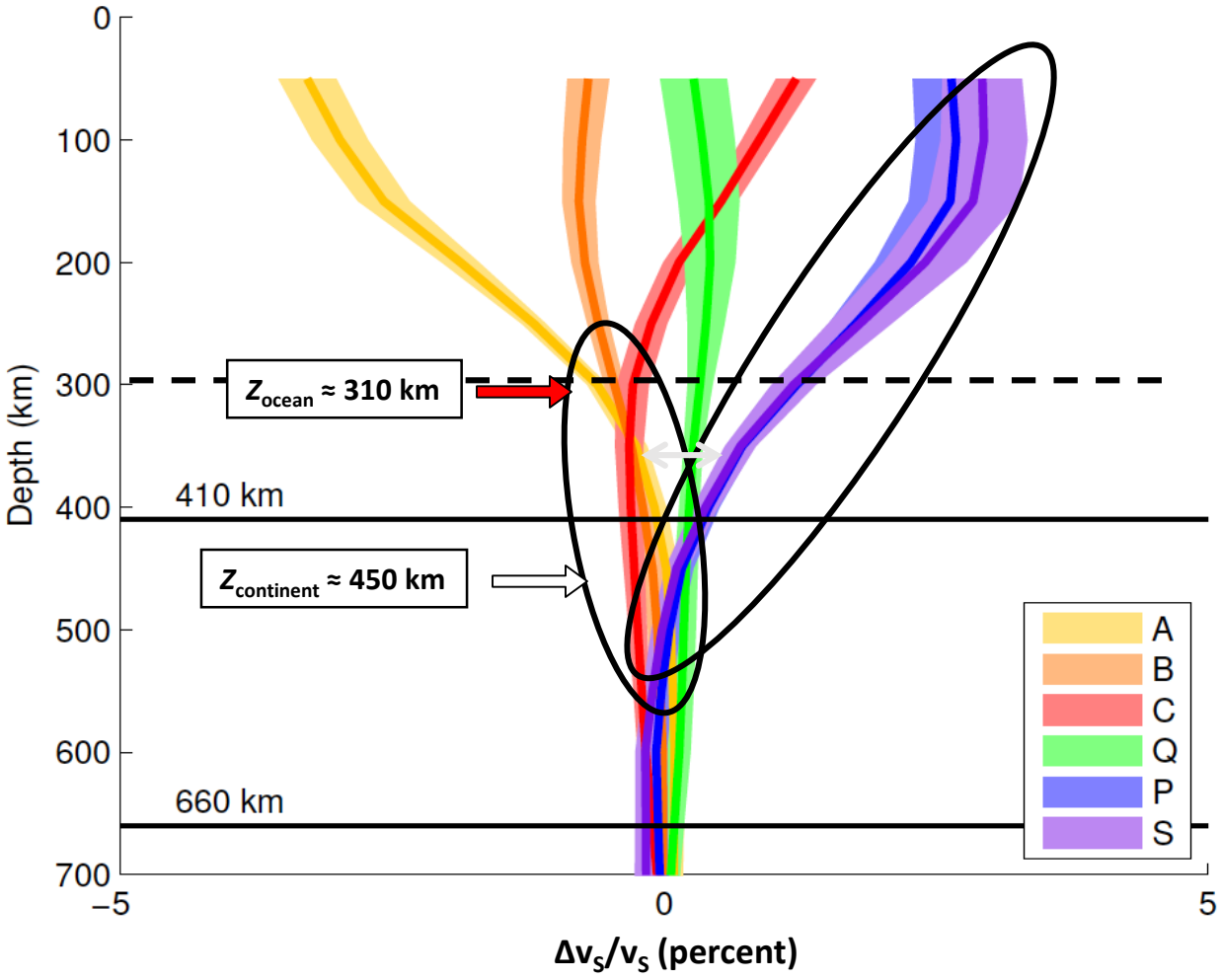

Common Features:

1. Platform and shield regions (P, S) show similar variations at all mantle depths
2. Ocean regions (A, B, C) show similar variations below 250-300 km
3. Differences between stable continents and oceans persist below 300 km

Model TX2008 (Simmons et al., 2009 *Geophys. J. Int.,* 177)

Upper mantle composition

	Archons (mean garnet SCLM)	Protons (mean garnet SCLM + massifs + xenoliths)	Tectons (mean garnet SCLM)	Tectons (mean Spinel peridotite)	Primitive Mantle, McDonough and Sun (1995)
SiO_2	45.7	44.6	44.5	44.4	45.0
TiO_2	0.04	0.07	0.14	0.09	0.20
Al_2O_3	0.99	1.9	3.5	2.6	4.5
Cr_2O_3	0.28	0.40	0.40	0.40	0.38
FeO	6.4	7.9	8.0	8.2	8.1
MnO	0.11	0.12	0.13	0.13	0.14
MgO	45.5	42.6	39.8	41.1	37.8
CaO	0.59	1.70	3.1	2.5	3.6
Na_2O	0.07	0.12	0.24	0.18	0.36
NiO	0.30	0.26	0.26	0.27	0.25
Zn	34	52	55	53	55
V	20	48	70	59	82
Co	93	107	110	110	105
Sc	7	10	14	12	16
Mg#	92.7	90.6	89.9	89.9	89.3
Mg/Si	1.49	1.43	1.33	1.38	1.25
Ca/Al	0.55	0.80	0.82	0.85	0.73
Cr/Cr+Al	0.16	0.12	0.07	0.09	0.05
Fe/Al	4.66	3.02	1.66	2.23	1.30
Olivine/orthopyroxene/ clinopyroxene/garnet	69/25/2/4	70/17/6/7	60/17/11/12	66/17/9/8	57/13/12/18
Density, g/cc	3.31	3.34	3.37	3.36	3.39
Vp, km/s (room temperature)	8.34	8.32	8.30	8.30	8.33
Vp, 100 km, 700 °C	8.18	8.05	7.85	7.85	
Vs, Km/s (room temperature)	4.88	4.84	4.82	4.82	4.81
Vs, 100 km, 700 °C	4.71	4.6	4.48	4.48	

Griffin et al., 2003, Precambrian Research 127

SCLM=Sublithospheric Continental Mantle

Chemical Boundary Layer

Partial Melting of Mantle Lherzolites

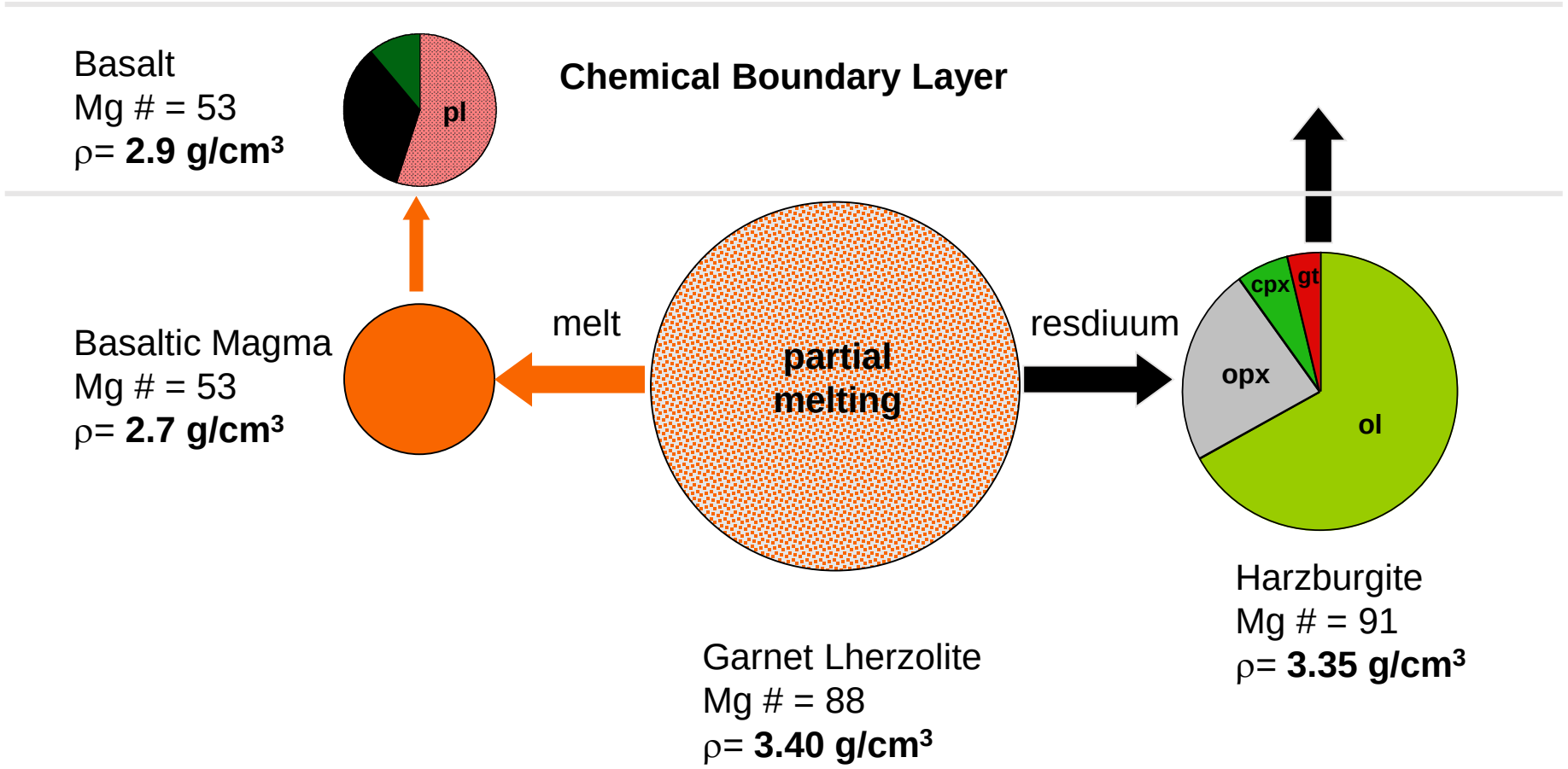

O'Hara (1975), Boyd & McCallister (1976), Jordan (1976, 1979)

Chemical Boundary Layer

Partial Melting of Mantle Lherzolites

Basalt
Mg # = 53
ρ= **2.9 g/cm³**

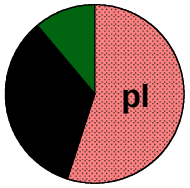

Chemical Boundary Layer

Eclogite
Mg # = 53
ρ= **3.60 g/cm³**

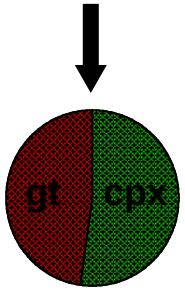

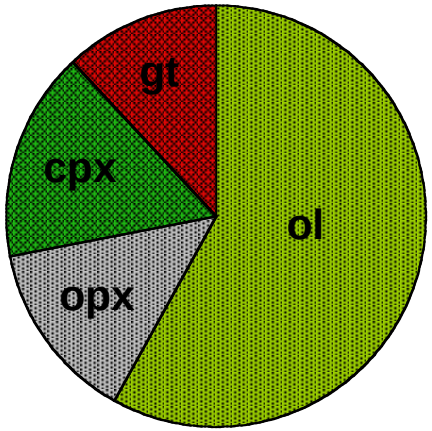

Garnet Lherzolite
Mg # = 88
ρ= **3.40 g/cm³**

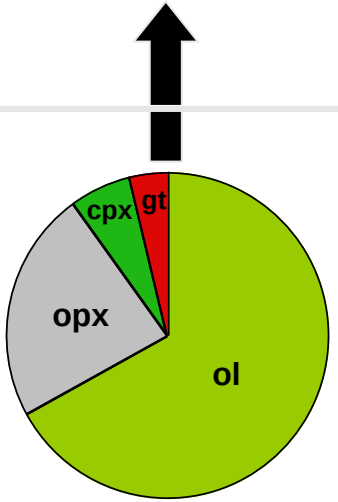

Harzburgite
Mg # = 91
ρ= **3.35 g/cm³**

O'Hara (1975), Boyd & McCallister (1976), Jordan (1976, 1979)

Compositional lithospheric variations in terms of olivine and Mg # (Mg/Mg+Fe)x 100

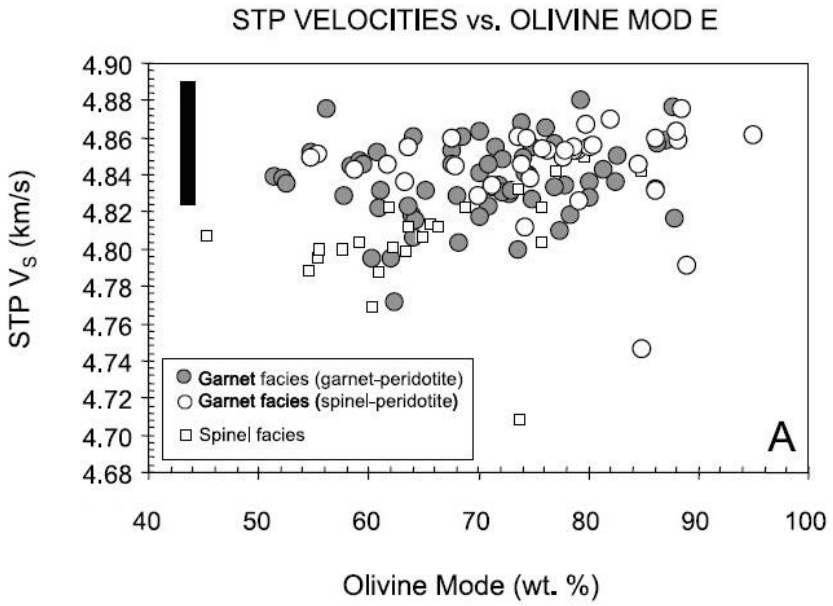

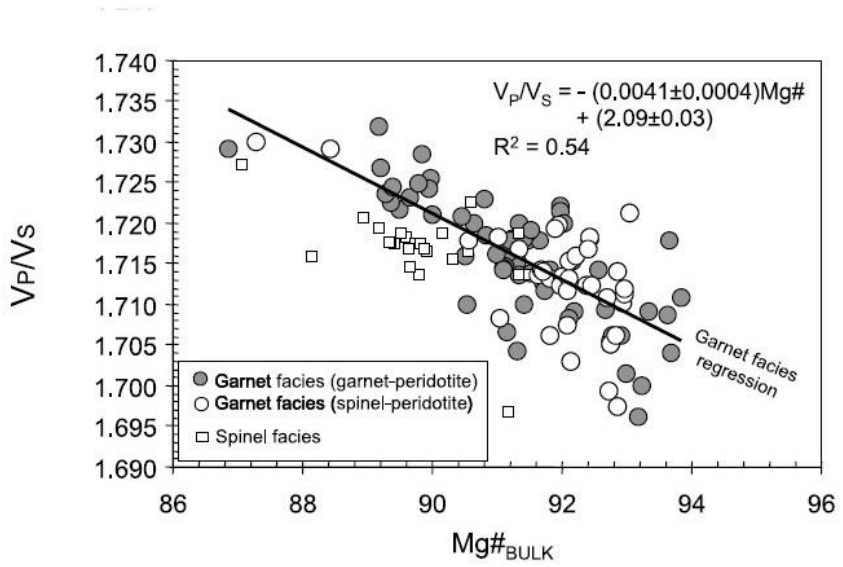

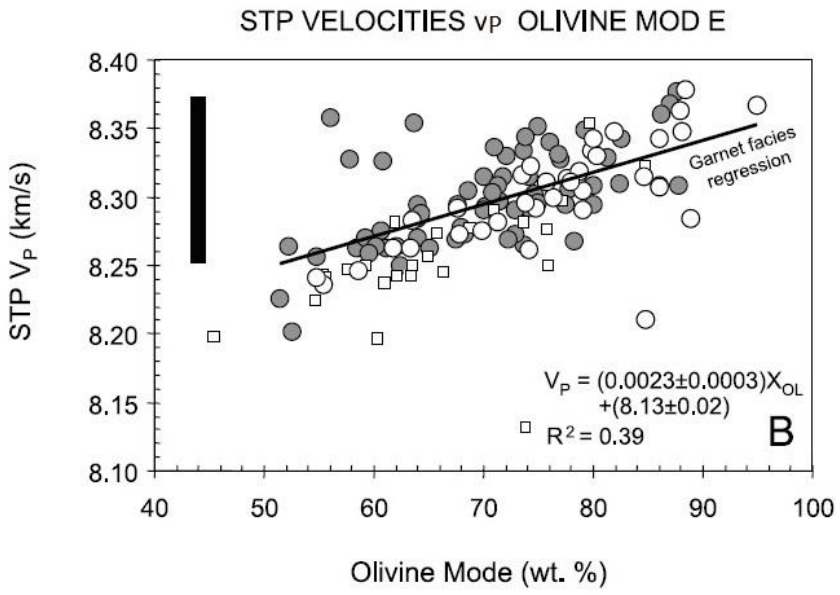

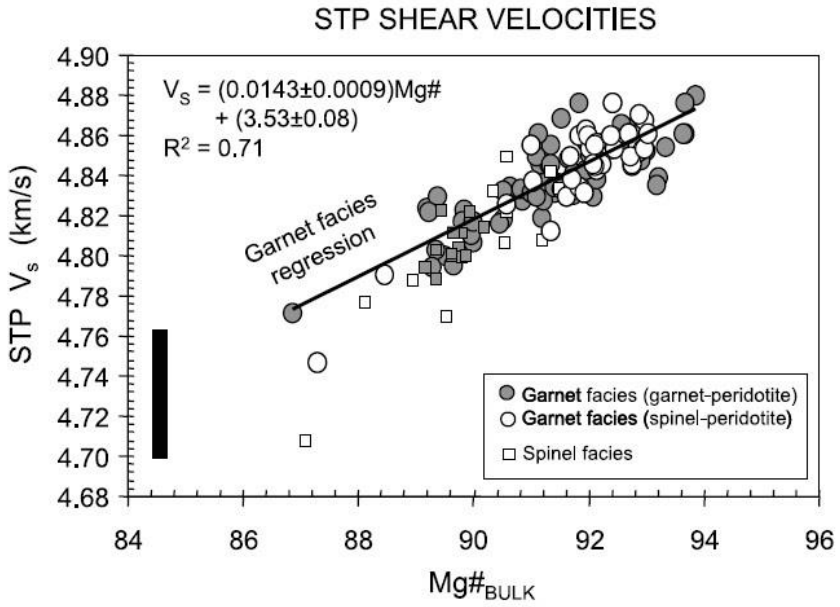

Lee, 2003, JGR, 108

Compositional lithospheric variations in terms of Mg# ((Mg/Mg+Fe)x 100)

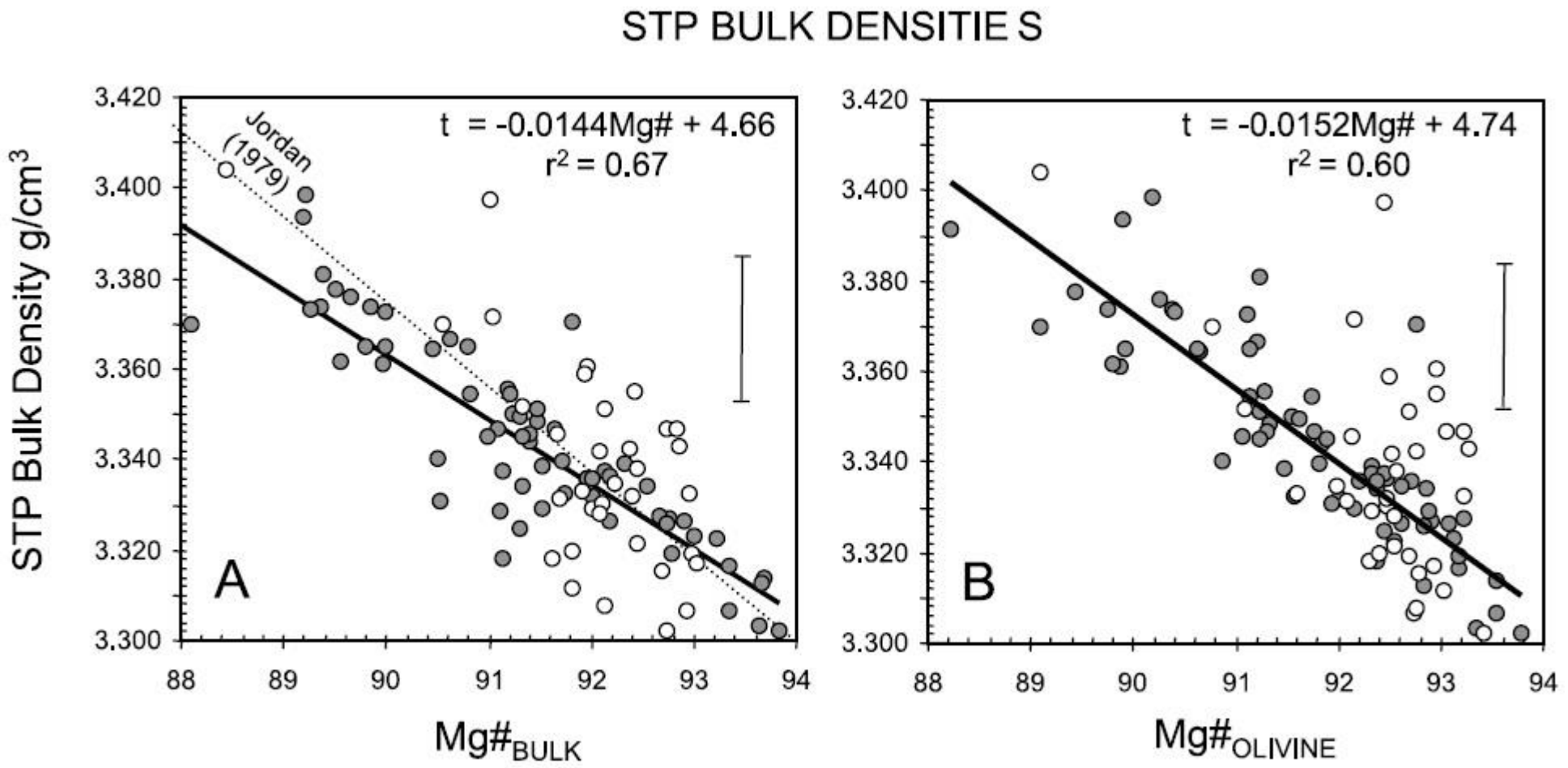

Lee, 2003, JGR, 108

Lithosphere-Asthenosphere Boundary (LAB)

The lithosphere-asthenosphere boundary (LAB) is a transtion zone over which a gradual change in physical and chemical characteristics occurs. It reflects the processes related to both global evolution and plate tectonics

Definition of the LAB depth depends on:

- Physical parameter variation with depth (e.g., temperature, seismic velocity, mechanical strength)
- Geophysical method used (e.g., seismic tomography, receiver functions, magnetotelluric)

Seismic lithosphere: It is the seismic high-velocity layer above the low-velocity zone (LVZ) caused by partial melting or by the effect of temperature (decrease of seismic velocity) prevailing on that of pressure (increase of seismic velocities).

- Large-scale tomography models (sensitive to velocity anomalies associated to convective mantle) identify the LAB depth as the top of a large-scale mantle convection (where thepositive velocity anomaly is redueced to 1%).
- The depth at which the axis of anisotropy changes orientation from fossil, frozen-in anisotropy (lithosheric mantle) to the present plate motions and mantle flow (asthenosphere).

Thermal lithosphere: It extends up to the depth of a costant isotherm (1250-1350 °C).
Lithospheric geotherms are costrained by: surface heat flow, from conversion of seismic velocities into temperatures, from pressure-temperature equilibrium conditions of mantle mineral pahses constrained by xenoliths.

Electrical lithosphere: It is the highly resistive upper layer above the higly conductive athenospehre. Its base corresponds to a sharp change in mantle conductivity, explained by the presence of 1-3% of melt fraction.

Elastic Lithosphere: It is the rheologically strong layer providing the isostatic response of the plate to topographic and/or subsurface loads, overlying a viscous mantle. It mechanically supports the elastic stresses induced by lithospheric bending (shallower than the other boundaries).

Seismic Lithospheric Thickness

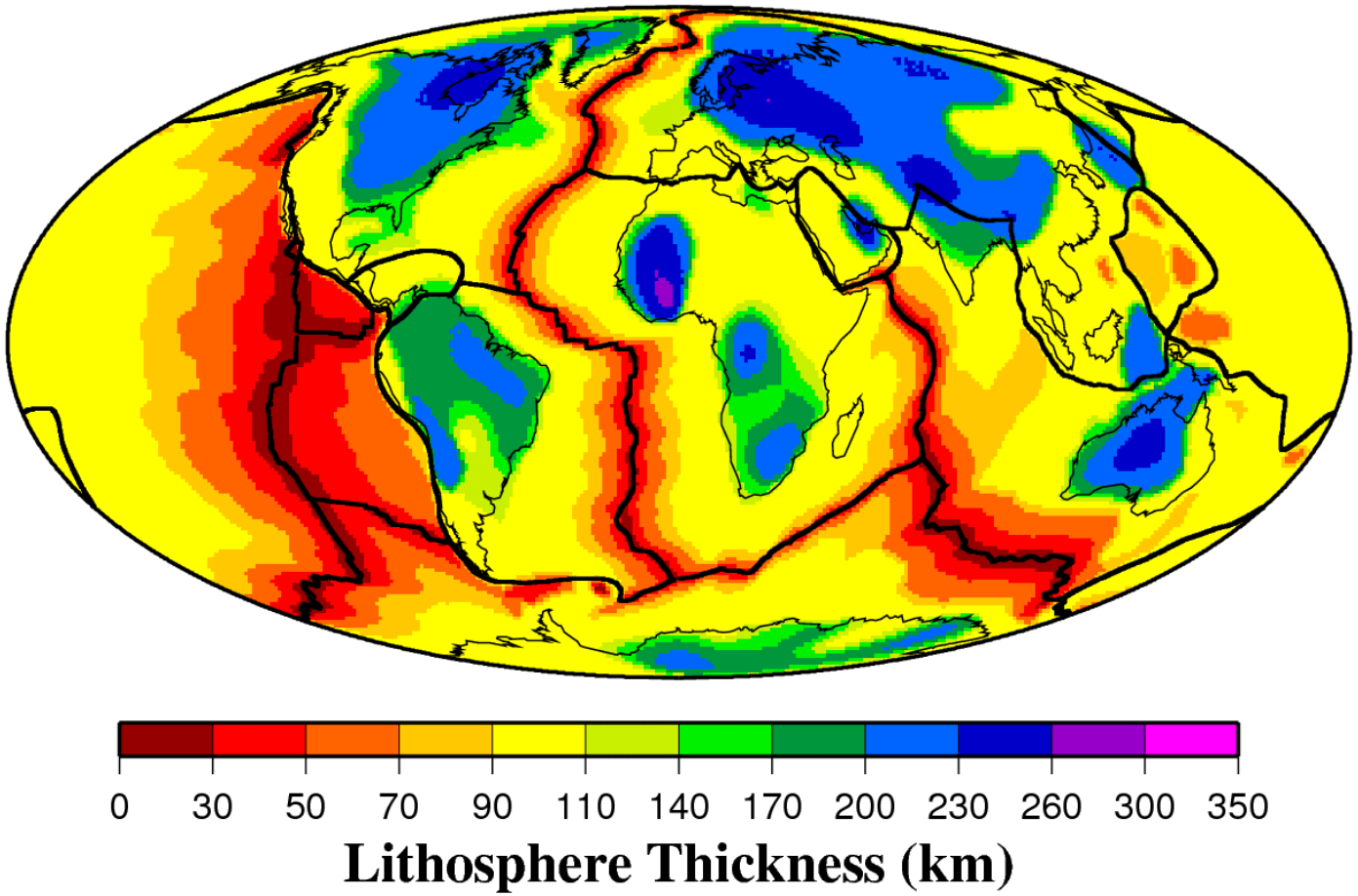

Estimated thickness of the lithosphere, determined using lithospheric age for oceanic areas and the thickness of positive seismic velocity anomalies for continental areas

Cratonic roots from seismic anisotropy

- Seismic anisotropy can be produced at the ***crystal scale*** by **lattice-preferred orientation (LPO)** due to alignment of anisotropic crystals such as olivine and OPX, at the ***rock scale*** by **rock fabric**, at the ***crustal scale***, caused by **rock foliation and layering**, and at ***large scale in the mantle***, by a **temperature difference between upgoing and downgoing flow in mantle convective cells**.
- **Three major types of anisotropy include intrinsic, azimuthal, and polarization (or radial) anisotropy:**

1. Intrinsic anisotropy refers to the material itself and depends on the difference between the maximum and minimum velocities in a medium.
2. Azimuthal anisotropy is the variation of wavespeed for a certain type of wave as a function of the azimuth of the propagation direction.
3. Polarization (or radial) anisotropy is the variation of wavespeed of phases with different polarization that travel along the same direction (e.g., Love and Rayleigh surface waves, since horizontally polarized Love waves travel faster than vertically polarized Rayleigh waves).

- Anisotropy in the upper mantle is most probably caused by lattice preferred orientation of anisotropic crystals and holds clues to dynamical processes responsible for past and present deformation.
- The top layer is thick (at ~150 km) under the Archaean core corresponds to the highly depleted iron layer inferred from thermo-barometric analysis of xenoliths. The LAB is relatively flat (from 180 to 240 km in depth), in agreement with the presence of a thermal conductive root that subsequently formed around the depleted chemical layer.

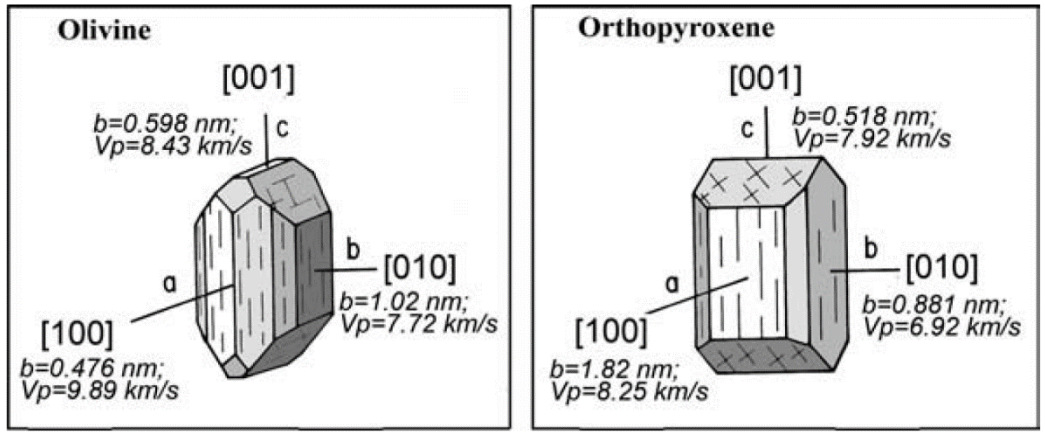

- The slip direction is characterized by the Burgers vector, which specifies the magnitude and direction of the lattice distortion in dislocations in a crystal lattice.
- The slip direction with the shortest Burgers vector is favored because of the lower strain energy associated with formation or motion of lattice dislocations.

Lithospheric stratification of NA continent

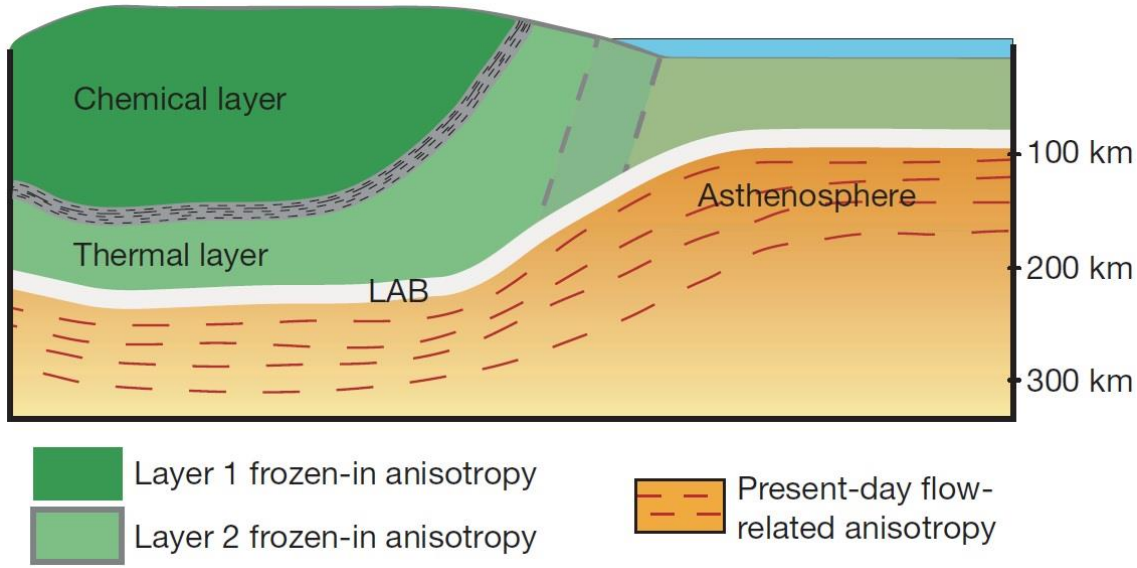

Cratonic roots from seismic anisotropy

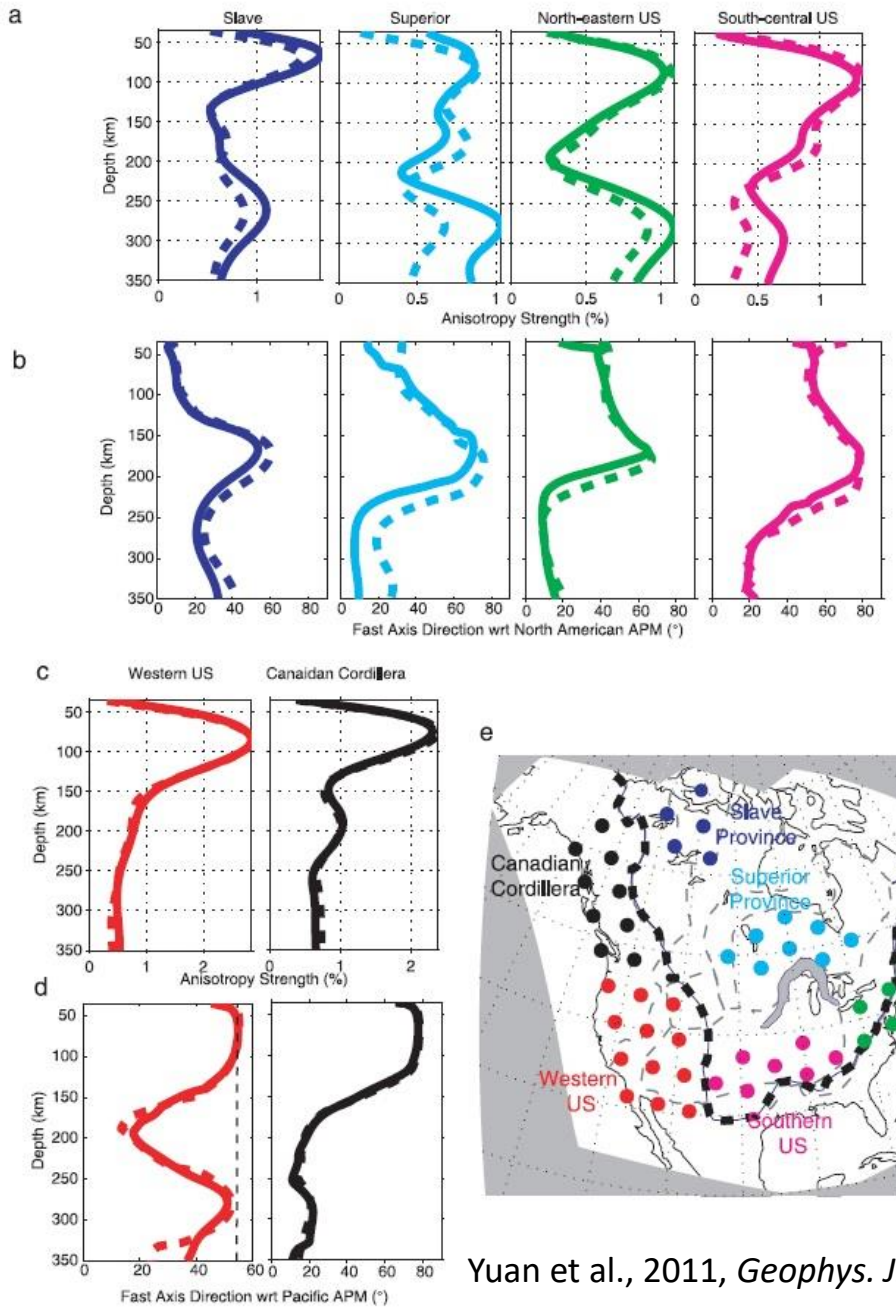

Yuan et al., 2011, *Geophys. J. Int., 184*

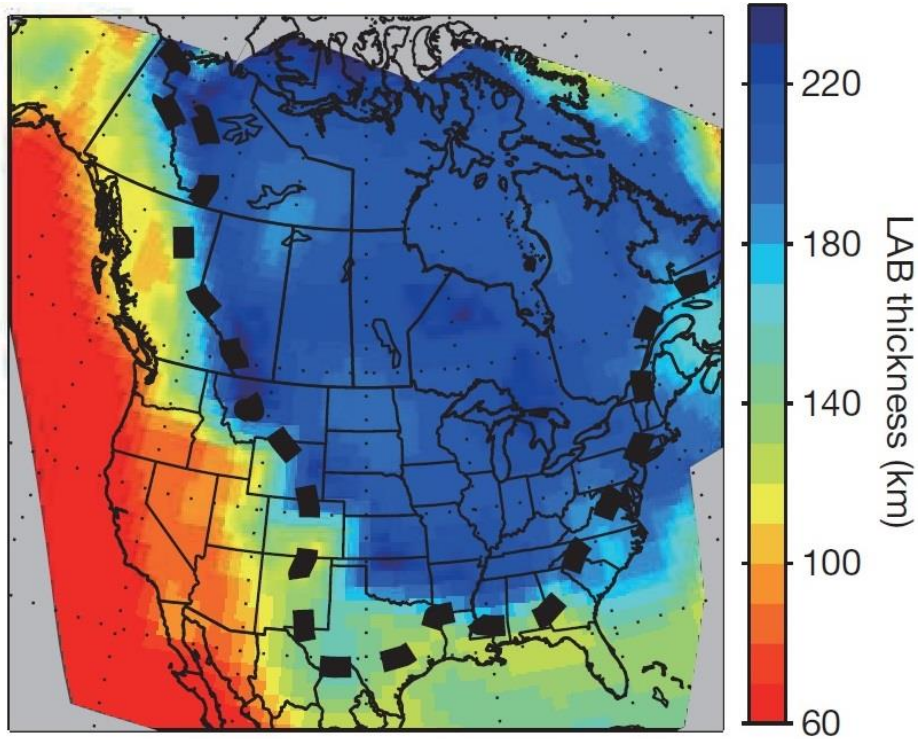

Yuan and Romanowicz, 2010, Nature, 466

- Average depth profiles of anisotropy strength (a and c) and fast axis direction (b and d) for six subregions of the North American continent.
- In (a) and (b) the anisotropy direction becomes subparallel to the North American Absolute Plate Motion (APM) below 200 km, with a maximum amplitude around 270 km.
- Large anisotropy strength is observed at 80–100 km depth in the western US (WUS) (c) and the Canadian Cordillera (d), which corresponds to sublithospheric depths. Subasthenospheric mantle is moving to the east with a velocity of ~5cm yr^{-1}.

European LAB depth

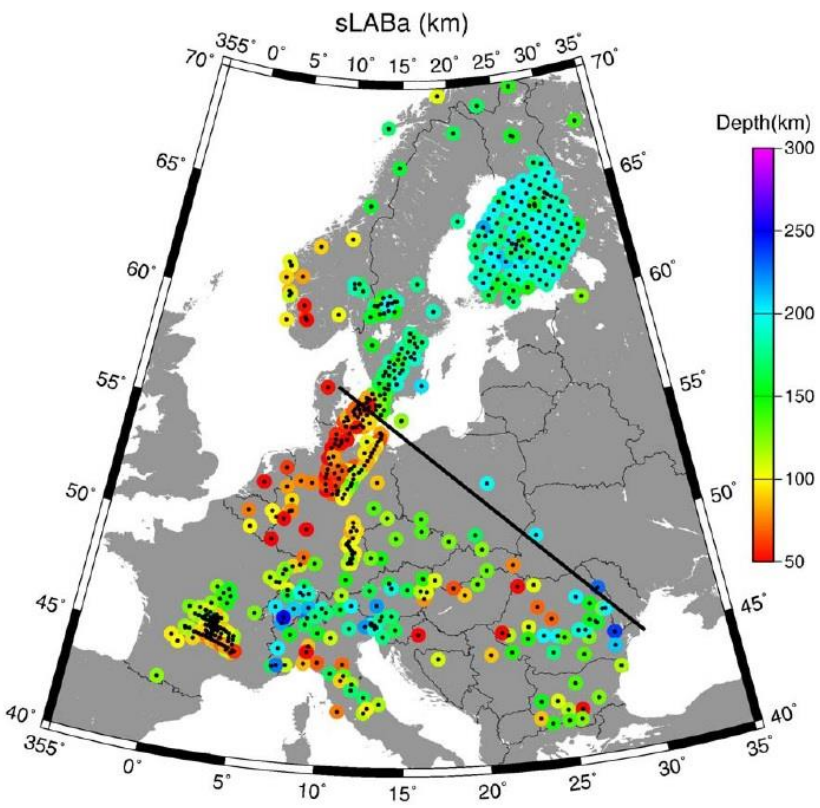

Seismic LAB (Anisotropy)

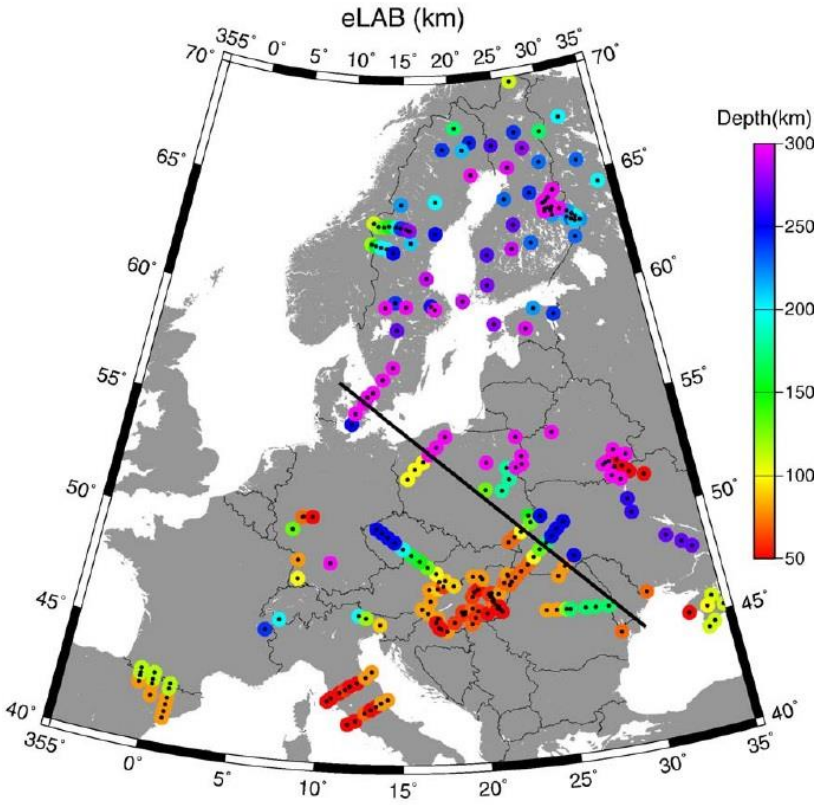

Electrical LAB

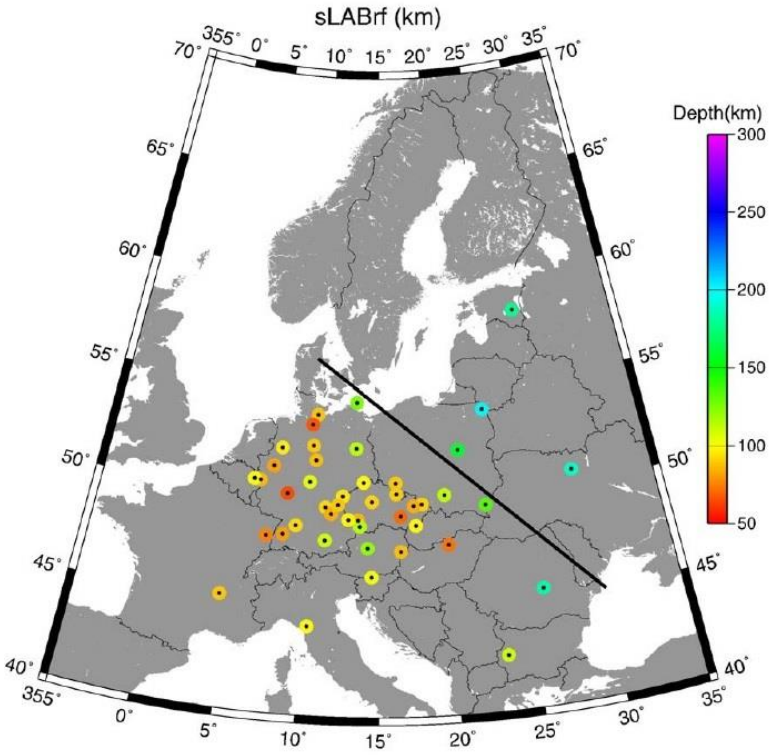

Seismic LAB (receiver functions)

Jones et al., 2010, Lithos, 120

European LAB depth

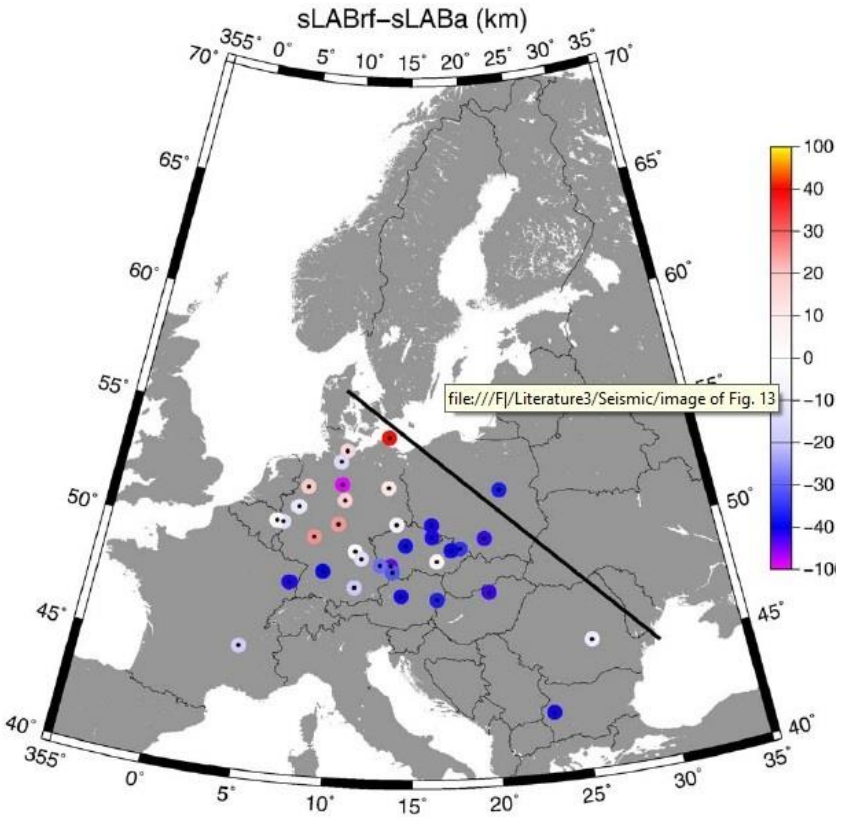

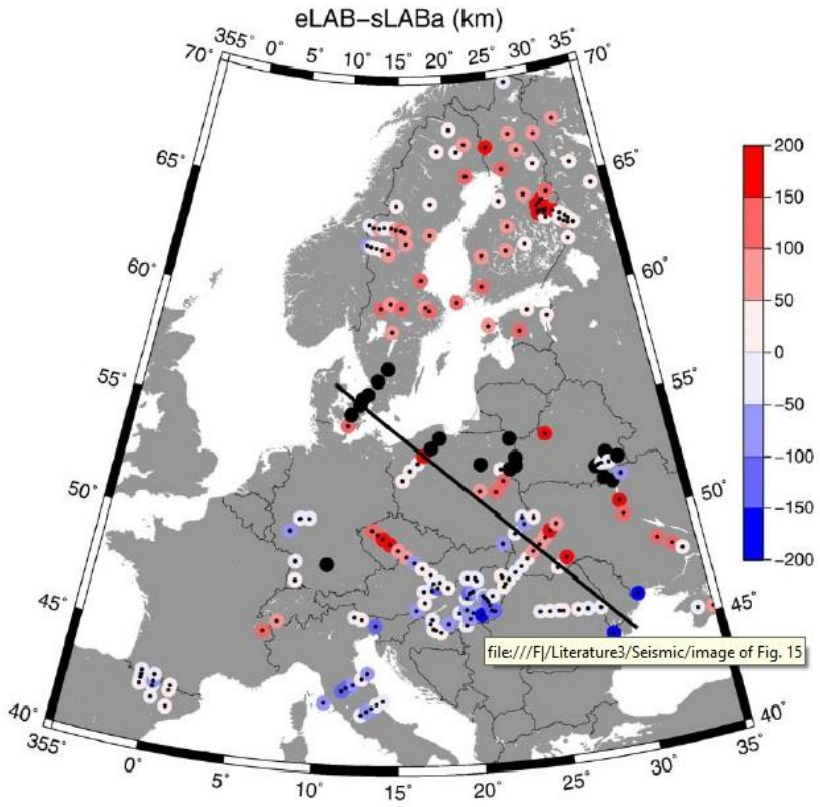

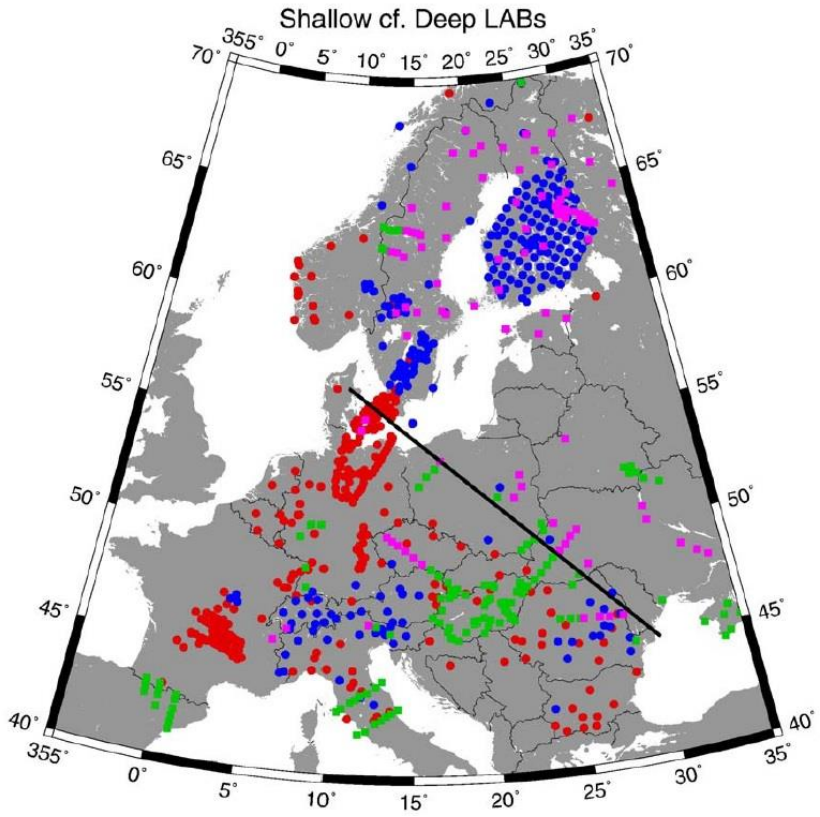

Jones et al., 2010, Lithos, 120

Shallow sLABa estimates (<150 km) dots in red, deep sLABa estimates (>150 km) in blue. Shallow eLAB estimates (<150 km) squares in green, deep eLAB estimates (>150 km) in purple.

The quantitative differences between the three types of LAB estimates reflect some aspect(s) of the physical transition from the lithosphere to the asthenosphere, which need not be the same for different parameters and for the different age of the provinces.

European LAB depth (Statistics)

Statistical estimates of the depth to the lithosphere–asthenosphere boundary from the different techniques and subsets.

	sLABa [km]	sLABrf [km]	eLAB [km]
All	137 ± 48	106 ± 34	170 ± 112
Within 95% of mean	138 ± 46	96 ± 18	153 ± 95
LABs<150 km	100 ± 27		78 ± 28
LABs>150 km	183 ± 19		250 ± 51
Phanerozoic[a]	118 ± 45	96 ± 17	98 ± 56
–Median smoothed[b]	133 ± 49		89 ± 49
Precambrian	169 ± 35	172 ± 26	237 ± 66
–Median smoothed	182 ± 13		253 ± 29

[a] Alps excluded.
[b] Northern Germany excluded.

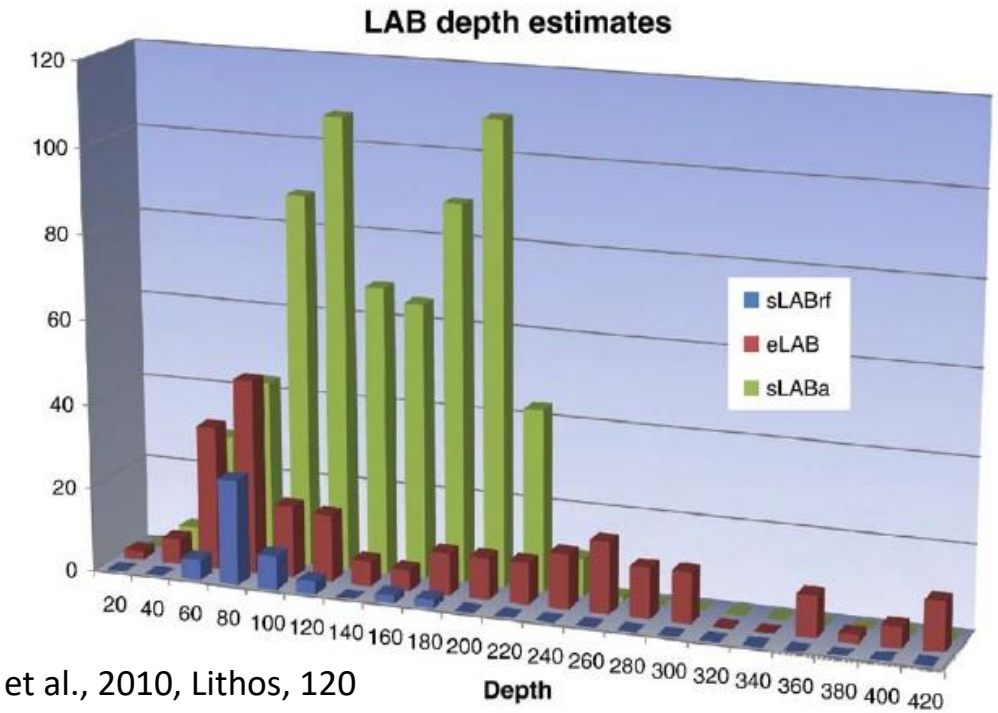

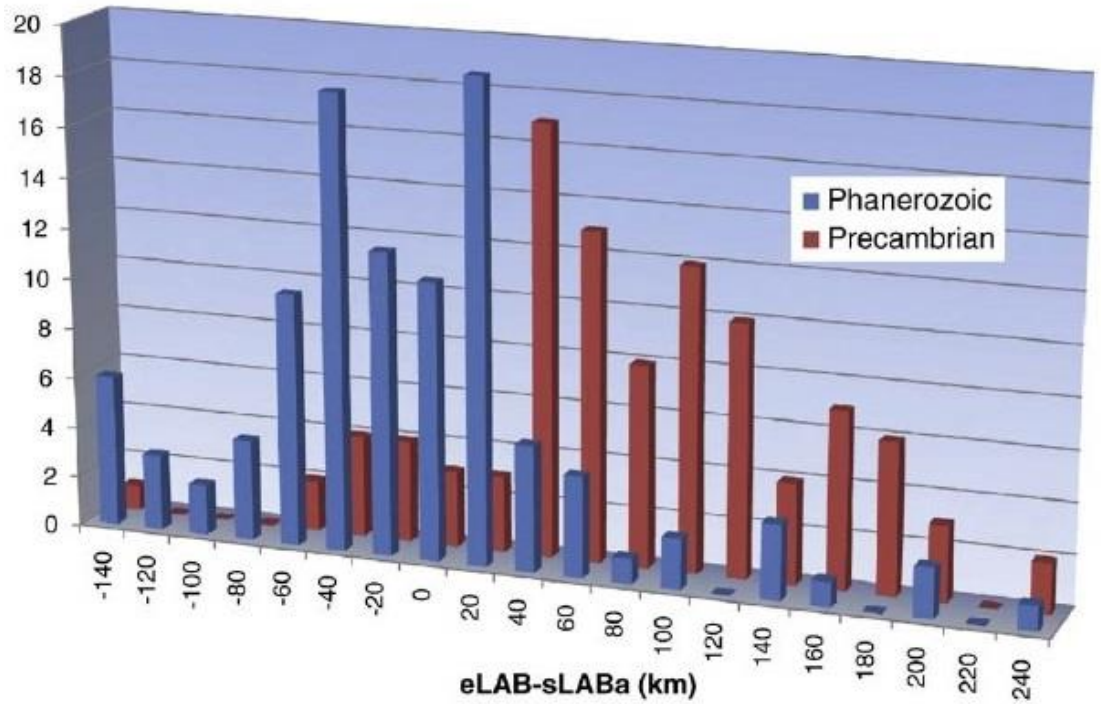

Jones et al., 2010, Lithos, 120

The Cratons

The cratons have usually a lithospheric roots of ~200–250 km and are characterized by high seismic velocities, low electrical conductivities and low surface heat flow.

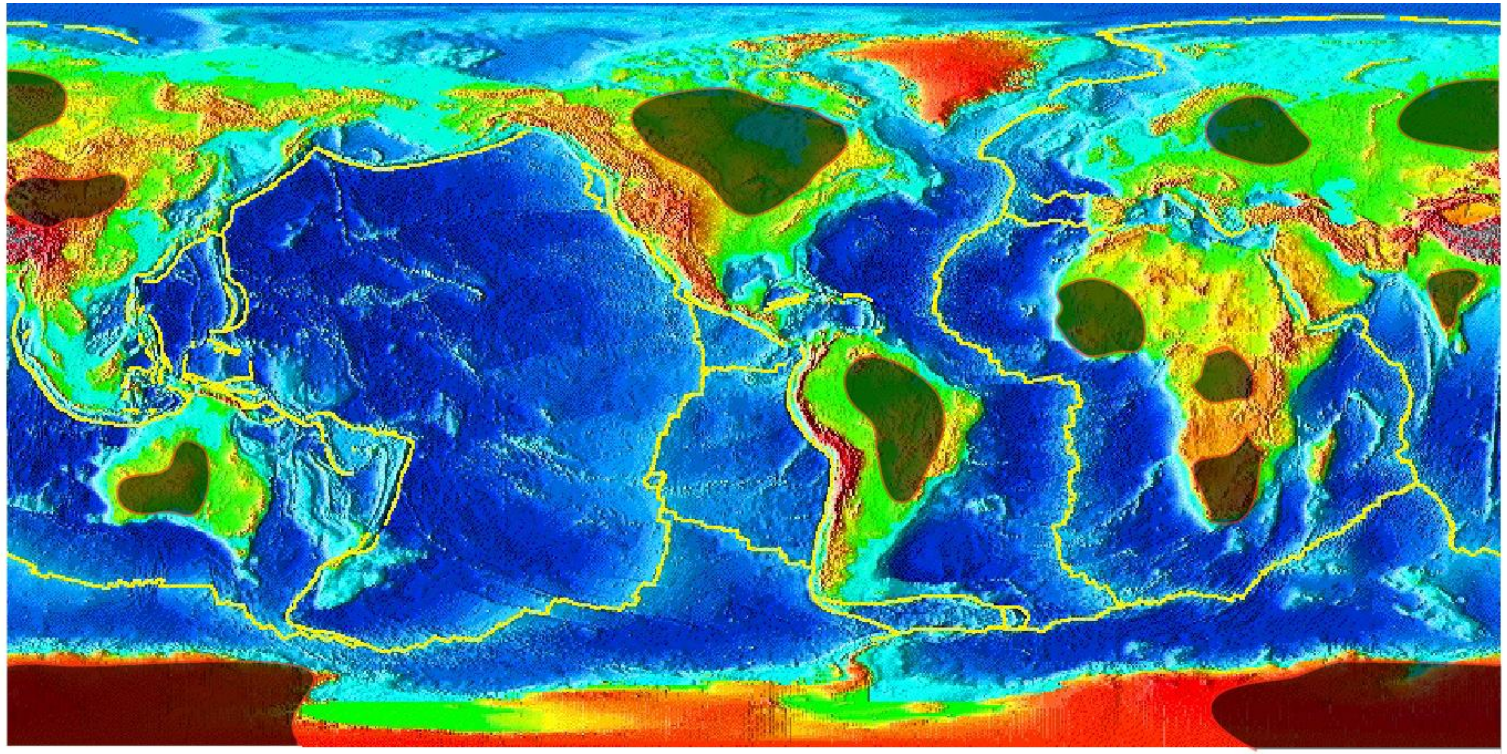

Why the cratonic lithosphere is so thick and stable? Isopycnic hypothesis:

The effect of composition and temperature on density cancel in cratonic roots making them neutrally buoyant

Higher densities due to lower temperatures are almost exactly balanced by lower densities due to lower ratios of Fe/Mg and Al/Mg (basalt depletion hypothesis)

Cratonic roots

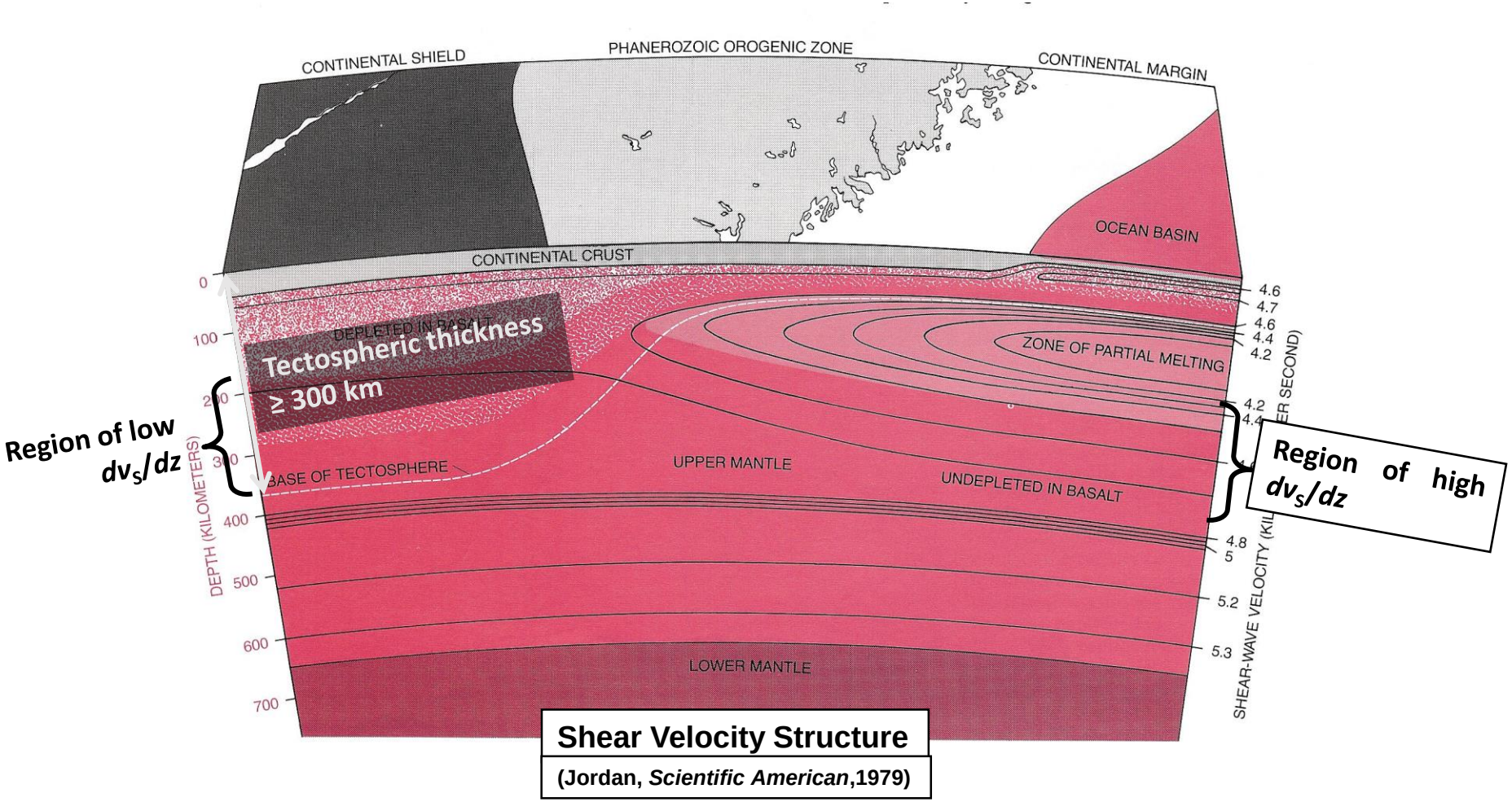

Shear Velocity Structure

(Jordan, *Scientific American*,1979)

The thermochemical boundary layer (tectosphere) beneath the continental cratons is much thicker than beneath old oceanic plates, and also much thicker than the continental mechanical boundary layer (lithosphere)

Models of cratonic roots formation

Mantle Plume

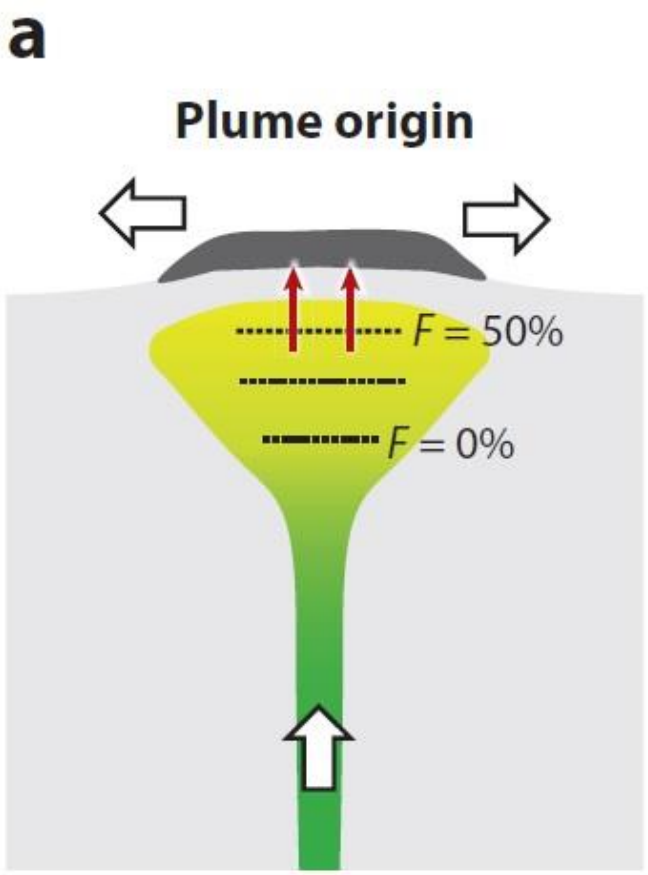

Slab Stacking

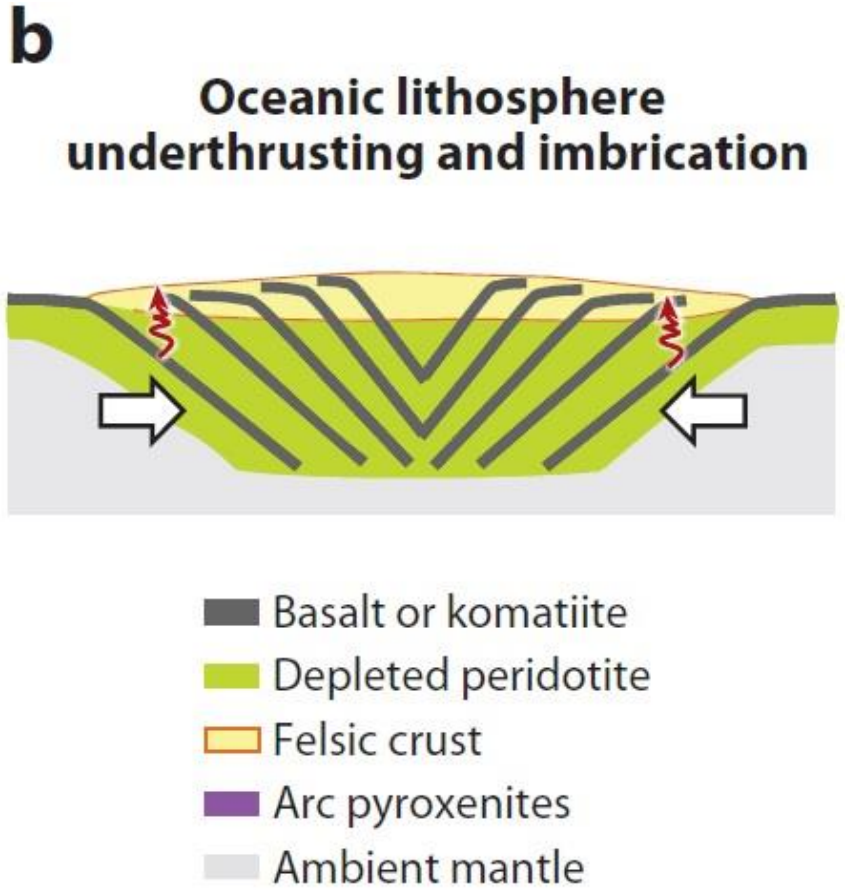

Advective Thickening

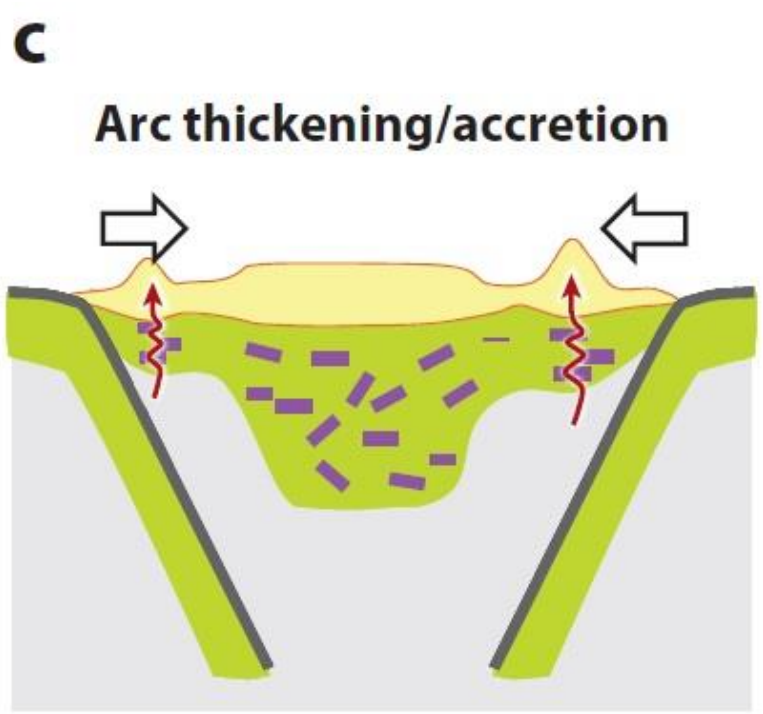

Lee et al., 2011, Annu. Rev. Earth Planet. Sci., 39

Models of cratonic roots formation

Three processes could have resulted in the mechanical segregation and accumulation of a layer of buoyant, viscous mantle during the Archean time:

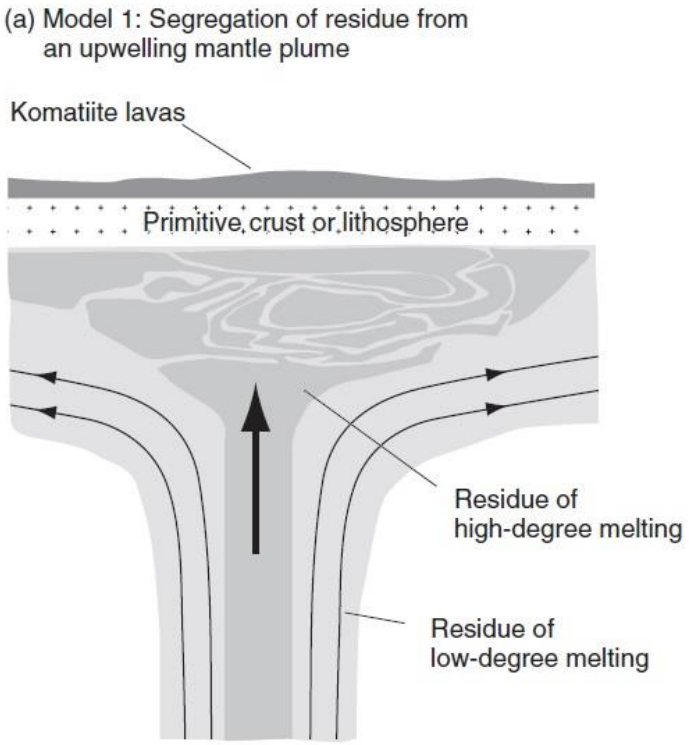

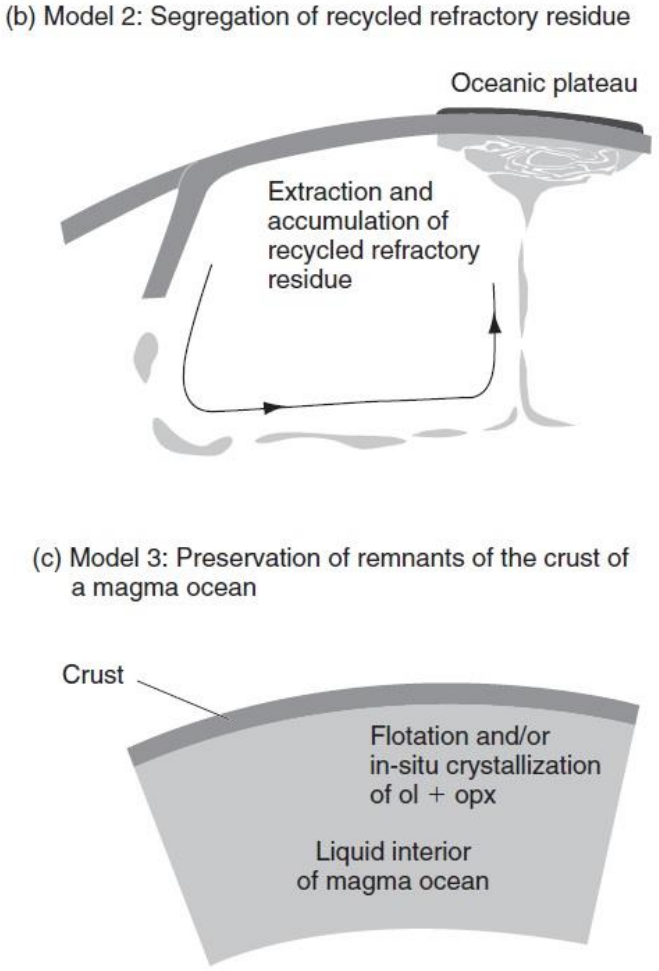

1. Upwelling buoyant residue in the core of a mantle plume could have separated from the cooler, denser exterior and accumulated during ascent.
2. Buoyant residue could have segregated slowly as material was transported down subduction zones and recycled through the mantle in convection cells.
3. Some subcontinental lithosphere could be the remnants of an initial crust that crystallized in an Archean magma ocean that formed during the final stages of Earth accretion.

Archean mantle roots probably resulted from more than one tectonic environment (no single setting is applicable)

Models of cratonic roots formation

1. **Plume Origin**: A highly melt-depleted, dehydrated, and low-density chemical boundary layer is an immediate product of very hot plume (> 1650 °C) melting, resulting in the formation of a craton from the outset.

- The plume model predicts a gradual stratification from highly melt-depleted (high Mg#) peridotite at shallow depths to fertile peridotites (low Mg#) at the base of the thermal boundary layer, but such stratification is not a general feature of cratons.
- This model predicts high-degree melting at a depth of ~200 km, but the 1700°C temperatures of melting recorded by cratonic peridotites are not high enough to generate extensive melting at these depths

2. **Underthrusting or imbrication of oceanic lithosphere (favored in the mid-Archean to the early Proterozoic):**

- It can explain the low-*P* and low-*T* components of cratonic peridotites, the general lack of systematic compositional stratification with depth, and the presence of subhorizontal and dipping discontinuities within the continental mantle.
- Partial melting of underthrusting oceanic crust could generate felsic magmas such that formation of evolved continental crust and thick continental mantle would be tectonically linked.
- This process is thought to be unlikely because negatively buoyant oceanic lithosphere should subduct instead of subcrete. In addition, the predicted amount of eclogite exceeds the present amount in the continents.

3. **Accretion and Orogenic Thickening of Arcs:**

- Young arcs are typically under extension, but as subduction zones mature, arcs often evolve into a compressional state as exemplified by the Cretaceous North American Cordilleran.
- Lithological similarities make this hypothesis attractive, but further data are needed.

Models of Komatiite generation

Influence of lithospheric thickness on the melting depth

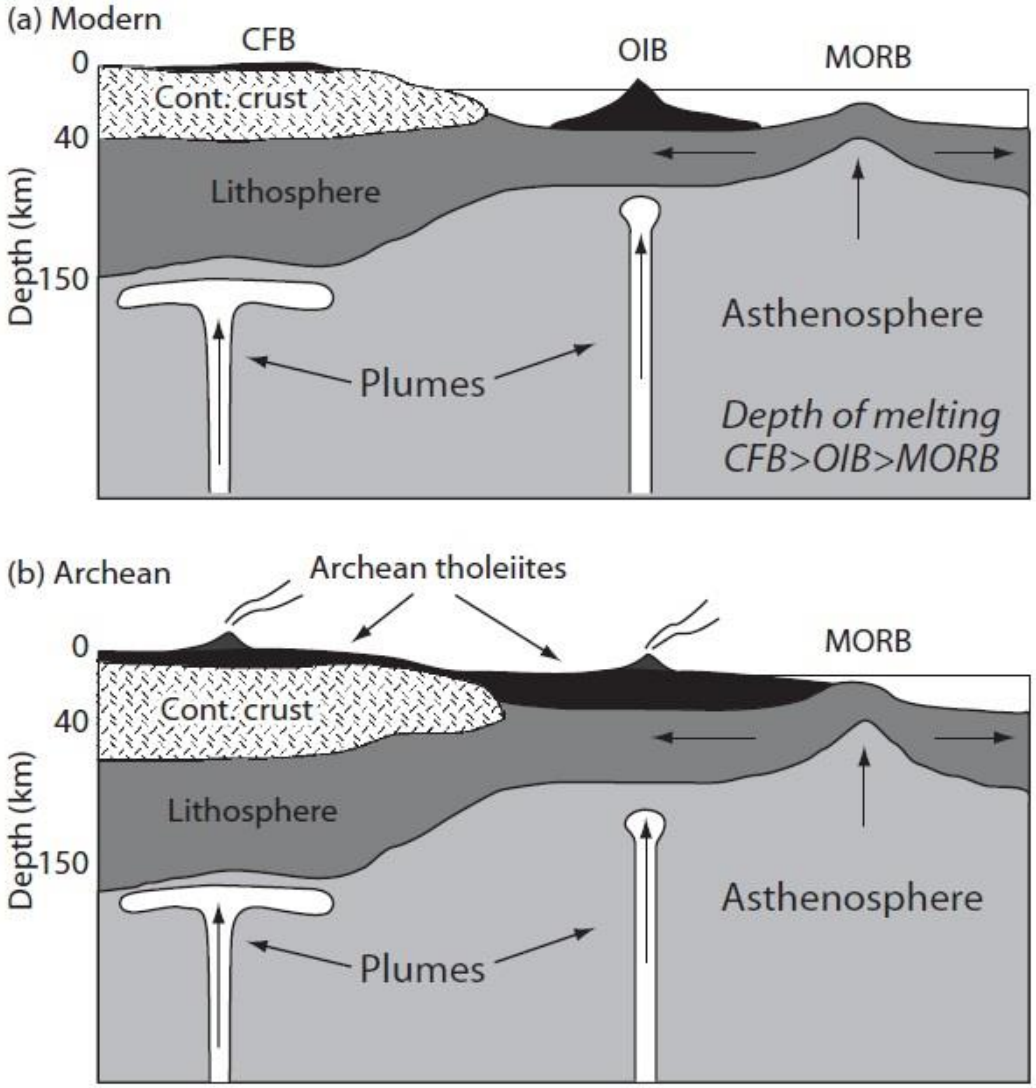

- If the source rocks of komatiites were dry then high ambient *T* in the Archean mantle would have caused melting to begin at larger depths, which would have produced large volumes of basalt (LIPs) and oceanic crust that was much thicker (20–40 km) than it is today.
- Source of the melting producing komatiites has important consequences for both the tectonic setting and the Earth's thermal evolution.

Mantle melt generation temperatures

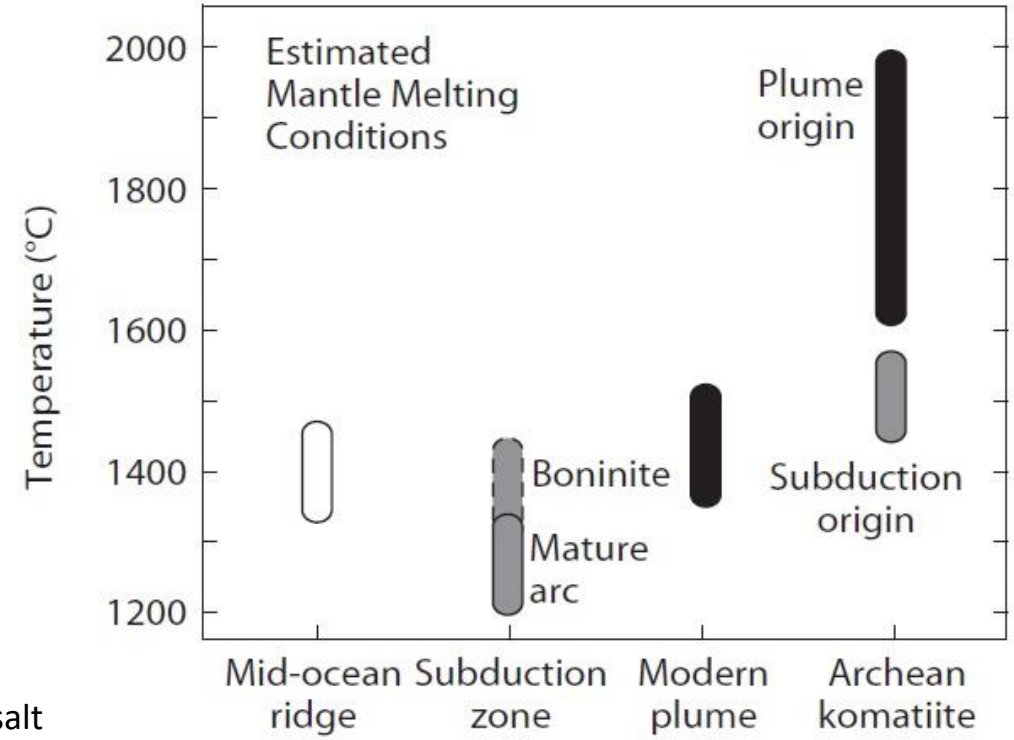

CFB=Continental Flood Basalt, OIB=Oceanic Island Basalt, MORB=mid-ocean ridge basalt

Models of Komatiite generation

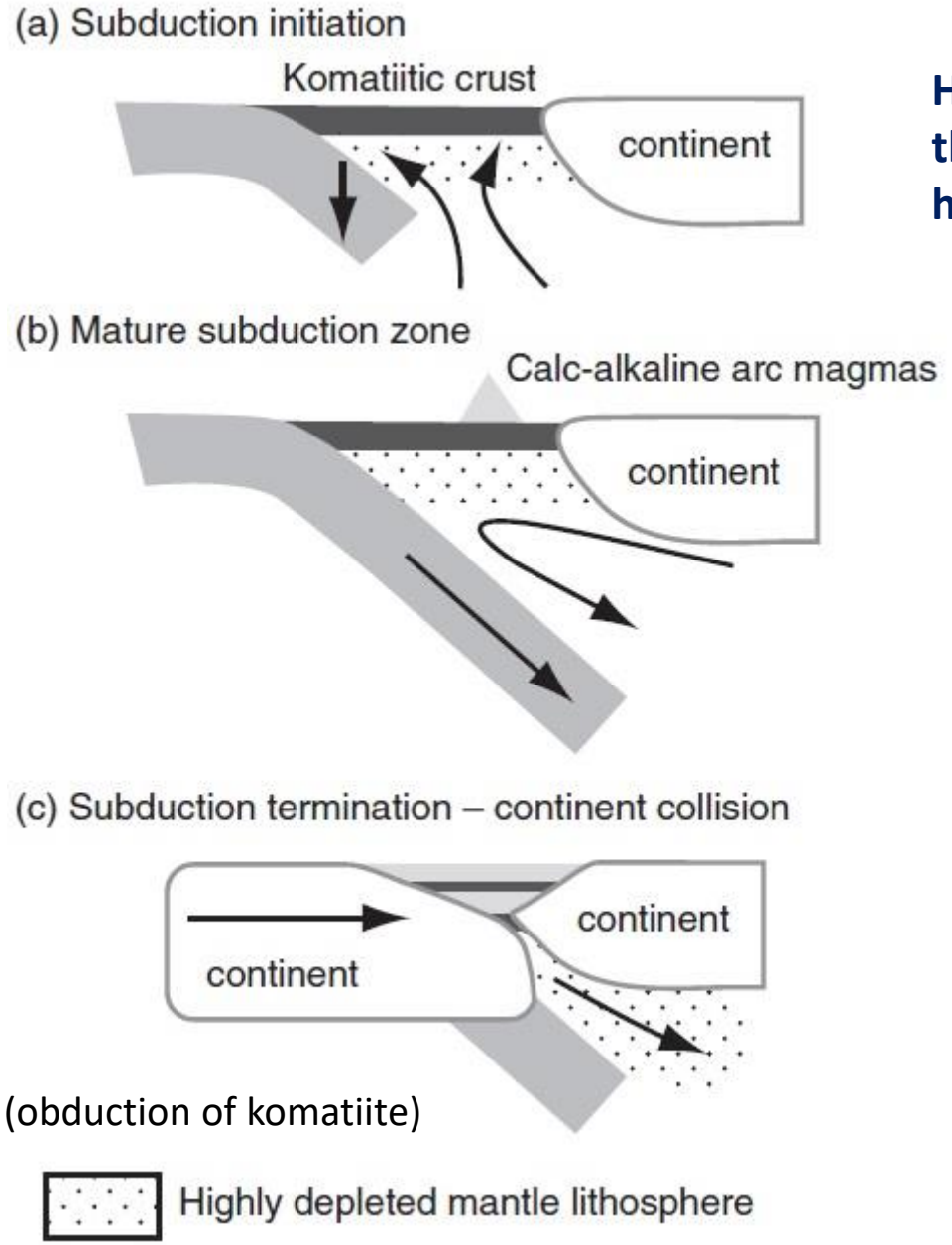

High magnesium contents and high degrees of melting associated with the formation of komatiites reflect melting *T* (1400–1600°C) that are higher than those of modern basaltic magmas.

- The komatiite may be the result of the melting of hydrous mantle in anomalously hot forearc regions above young subduction zones, like the boninites (high-Mg andesites) of in the Izu-Bonin-Marianna island arc.
- In this case, shallow melting and subduction result in the formation and thickening of highly depleted mantle lithosphere that some time later is incorporated into the cratonic mantle below a continent.

Evolution of the cratonic lithosphere

- In most of cratons, isotopic ages from mantle xenoliths and various crustal assemblages indicate that chemical depletion in the mantle lithosphere was coupled to accretionary processes in the overlying crust.
- This is a strong evidence that the crust and the underlying lithospheric mantle formed more or less contemporaneously and have remained mechanically coupled since at least the Late Archean.
- A progressive decrease in the degree of depletion in the lithospheric mantle since the Archean indicates that the Archean–Proterozoic boundary represents a major shift in the nature of lithosphere-forming processes, with more gradual changes occurring during the Phanerozoic.
- The main driving mechanism of this change is the secular cooling of the Earth and subsequently processes related to subduction, collision, terrane accretion, and magma addition.

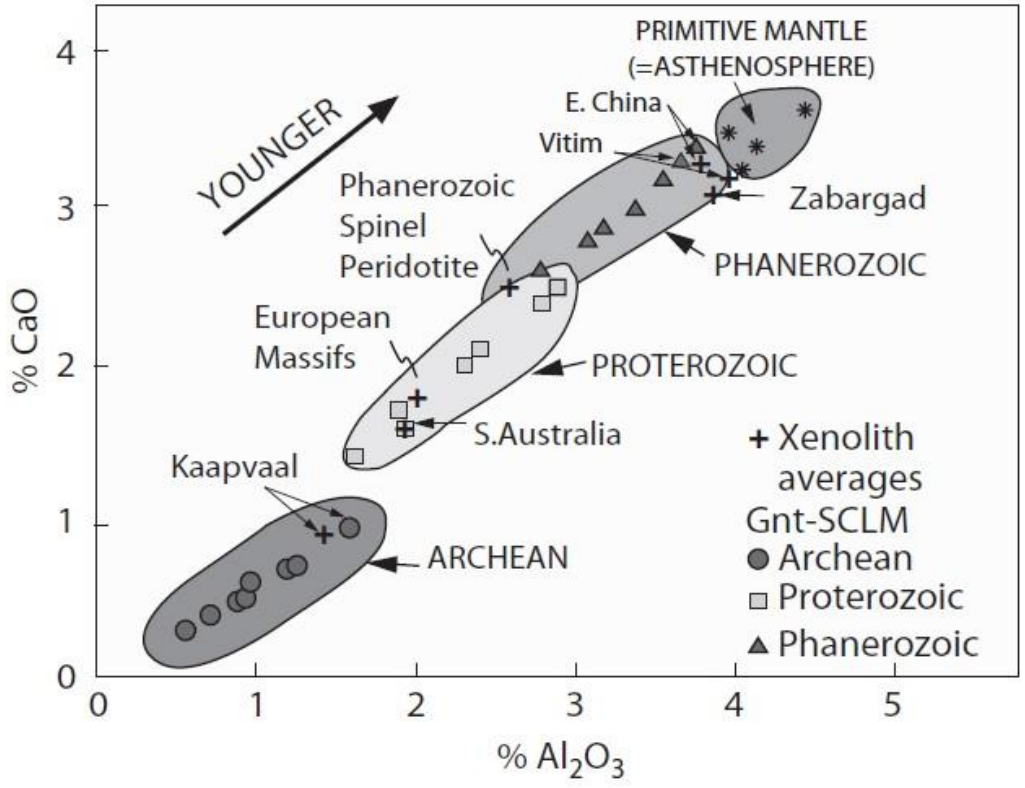

- *Range of subcontinental lithospheric mantle (SCLM) compositions for selected cratons that have been matched with ages of the youngest tectonothermal events in the overlying crust.*
- *Newly formed subcontinental lithospheric mantle has become progressively less depleted in Al and Ca contents from Archean through Proterozoic and Phanerozoic time.*

Precambrian Geodynamics

- Archean geodynamics was dominated by plume tectonics and the development of hot accretionary orogens with low topography.
- Due to the hot mantle temperature, slab break-off was more frequent in the Precambrian time and limited occurrence of ultrahigh-pressure (UHP) rocks. Mantle downwellings and slab break-off processes are likely to have played a key role in assembling and stabilizing the hot orogens.
- Both oceanic and continental lithospheres were rheologically weak due to the high temperatures.
- Numerical models suggest that the long-term stability of cratons sustaining multiple supercontinent cycles can be achieved if their viscosity and yield strength are sufficiently high and weak mobile belts are present along the boundaries of the cratons.
- Stable cratons facilitate subduction initiation of very young seafloor during continental growth and dispersal.
- Wide spread development of modern-style (cold) collision on Earth started during Neoproterozoic at 600–800 Myr. Cold collision created favorable conditions for the generation of UHP metamorphic complexes, which become widespread in Phanerozoic orogens.

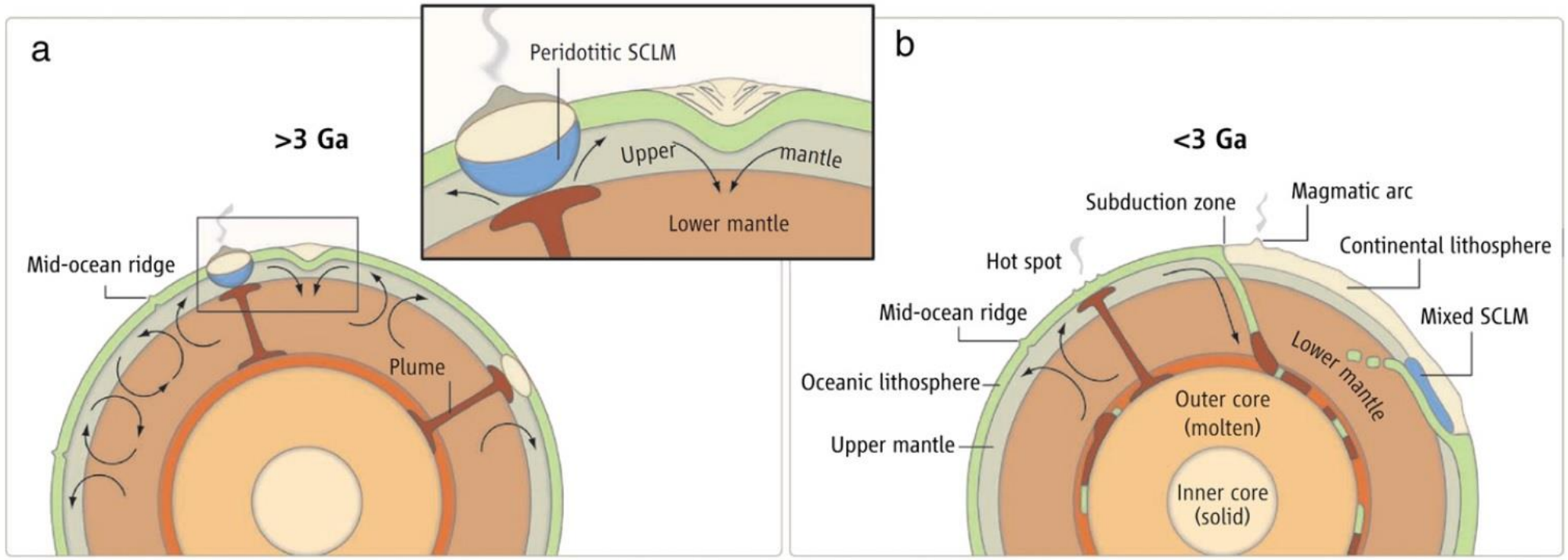

Gerya, 2014, Gondwana Research, 25

Implications of the Isopycnic Hypothesis for cratonic roots formation

- Mechanism must lead to an approximate isopycnic state by the time of large-scale tectonic stabilization
  - Single-stage models don't work (mantle plume)
  - Continuous growth models don't work (slab stacking)
- Plausible models must involve advective thickening of cool, depleted mantle
  - Primary depletion must precede thickening
- Process requires iteration
  - Large-scale instabilities lead to continental rifting and drift
  - Small-scale instabilities promote density-sorting and drive the tectosphere toward isopycnicity
  - Tectonic stabilization *precedes* magmatic stabilization

Implications of the Isopycnic Hypothesis for cratonic roots formation

- **Three progressive stages can be identified in the formation process**
  1. **Depletion of mantle material and incorporation into chemical boundary layer**
     - **May occur at spreading centers, plumes, and/or subduction zones**
  2. **Consolidation and cooling of the chemical boundary layer (CBL) during continental drift**
  3. **Advective thickening during continental collisions**
- **A fourth process, CBL metasomatism, may be distributed across these stages**

Advective thickening as a mechanims for tectospheric stabilization

Mantle is depleted by differentiation in mantle wedge above subduction zone:

A. Vulcanism along the active continental margins generates buoyant, refractory mantle resistant to convective recycling.

B. Accretion during continental drift consolidates and thickens the CBL.

C. Major advective thickening occurs in collisions during the formation of supercontinents.

- **A fourth process, CBL metasomatism, may be distributed across these s**

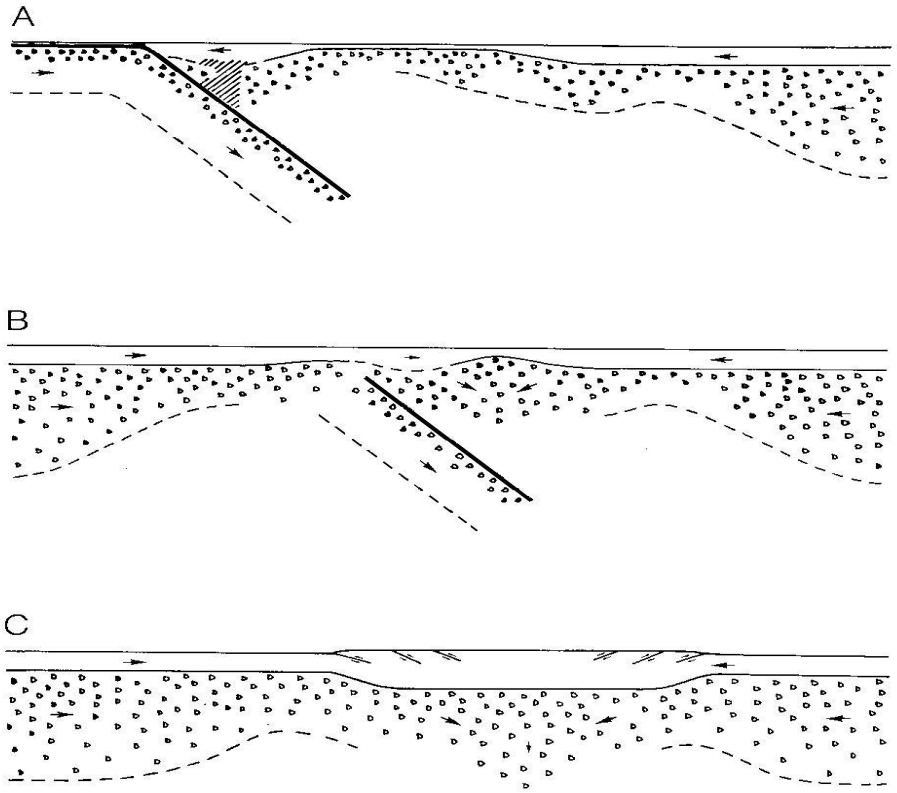

Jordan, 1988, J. Petrology

Crustal Structure of South African Craton

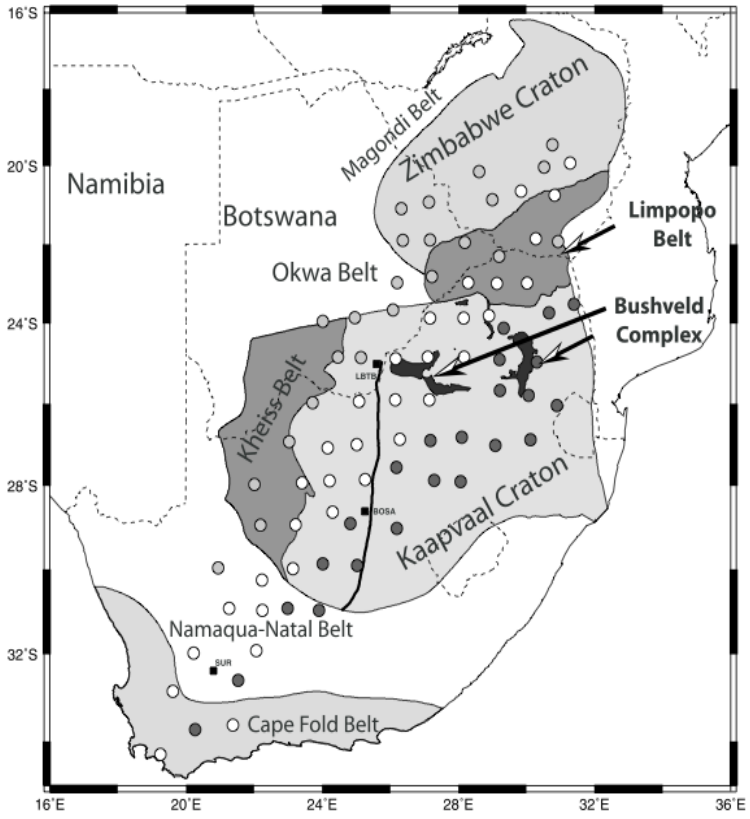

James et al, 2004, G3, 5

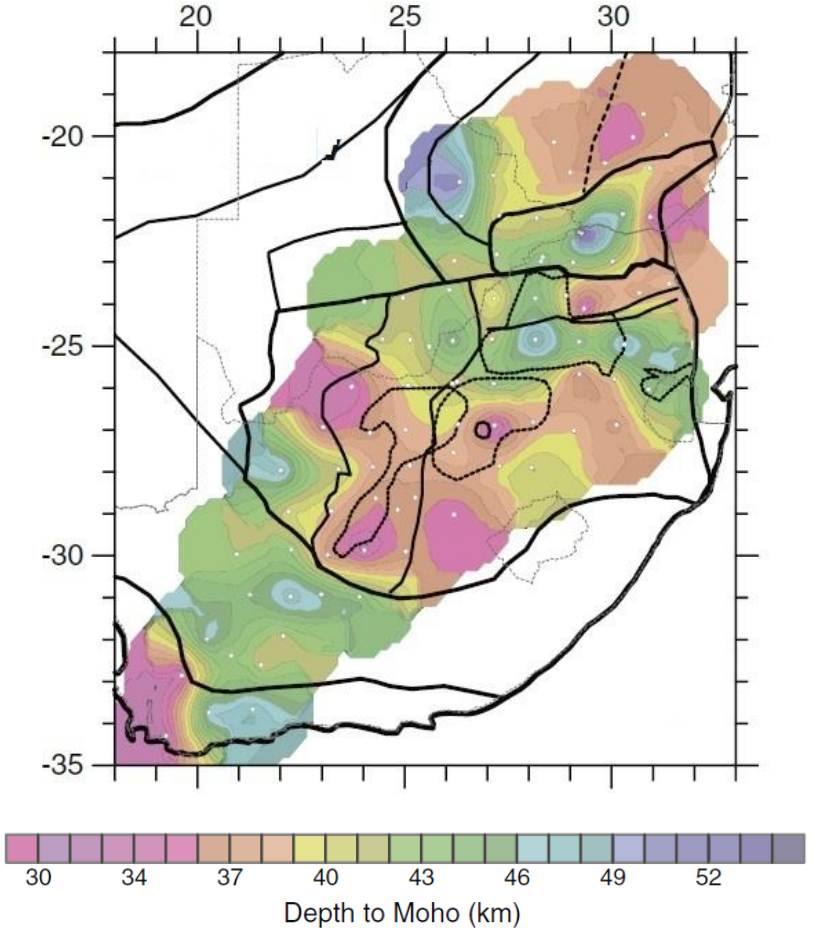

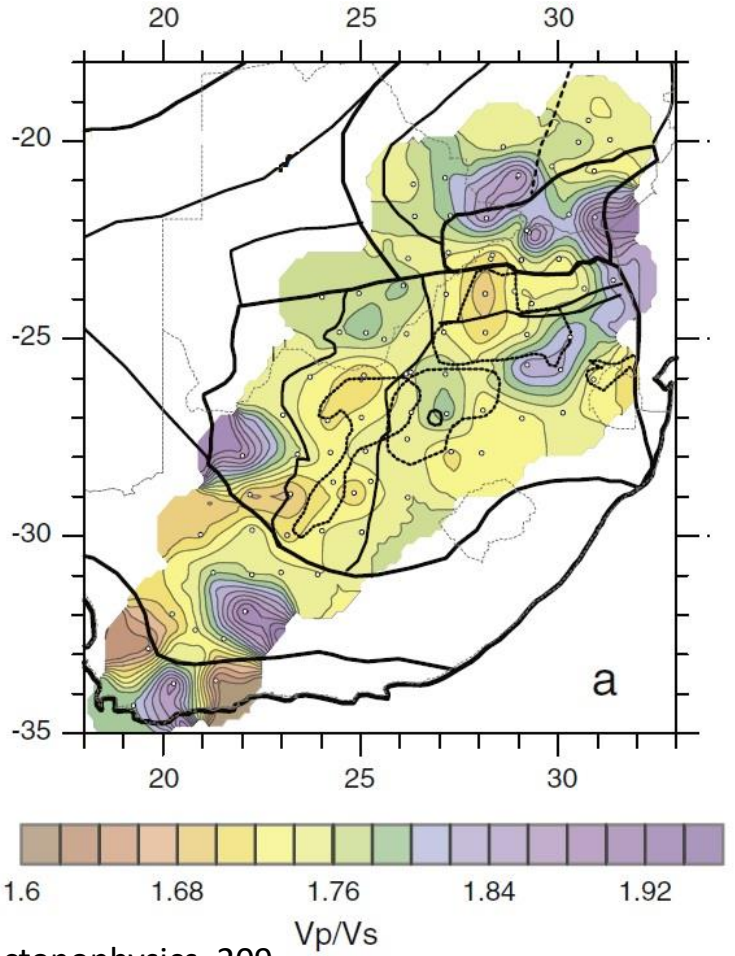

Youssof et al., 2013, Tectonophysics, 209

- Most of the Kaapvaal craton and Zimbawe craton have thin (35–40 km) crust and Vp/Vs ~1.74, which may indicate delamination of pre-existing lower crust, also supported by a very sharp Moho transition.
- Extreme values of 1.90–1.94 at the dyke swarms in eastern Limpopo, and 1.84 in the easternmost Bushveld Intrusion Complex (BIC) indicate voluminous magmatic intrusions in the whole crust.
- Highly heterogeneous crust, both in thickness and Vp/Vs-ratio is typical of the Namaqua–Natal and Cape Fold Belts.

Cratonic roots from Regional Tomography
South African Craton

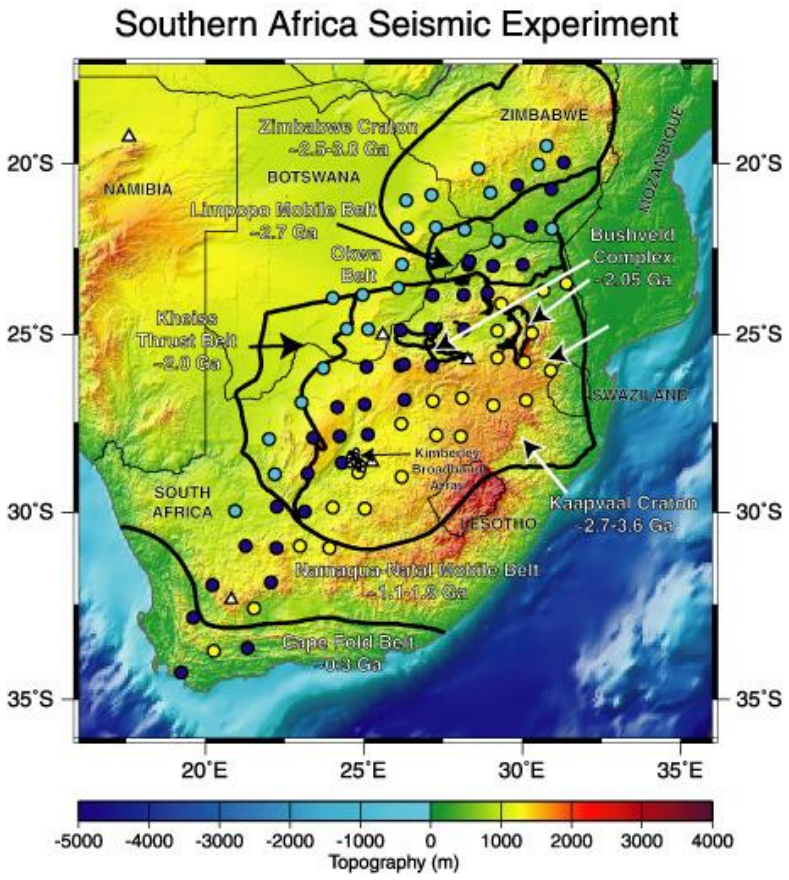

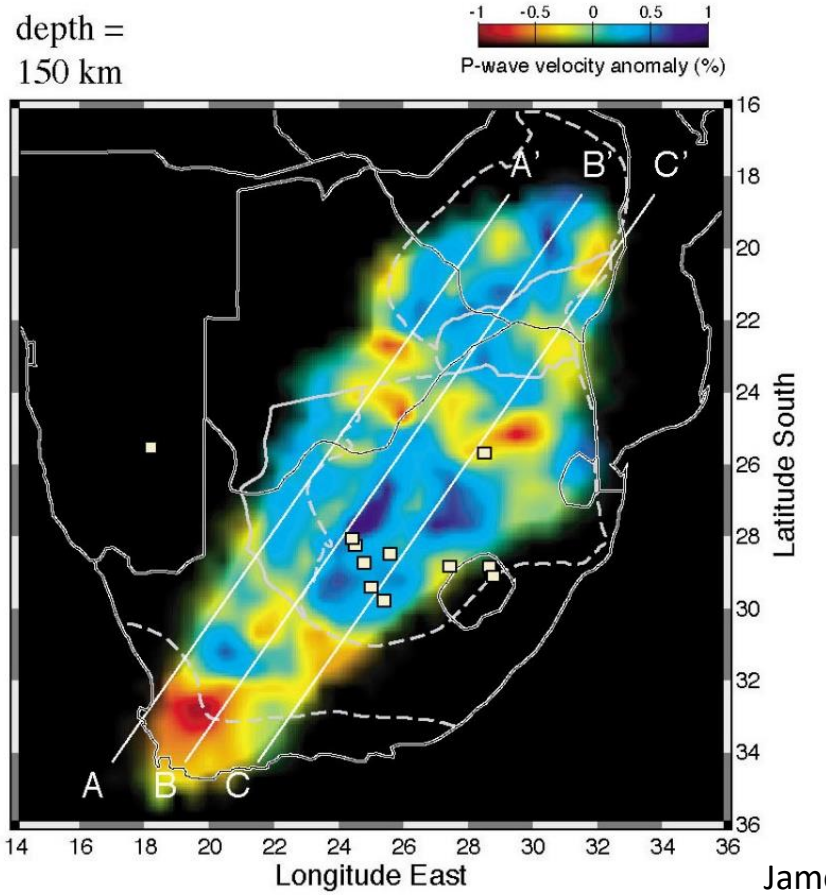

James et al. (2003)

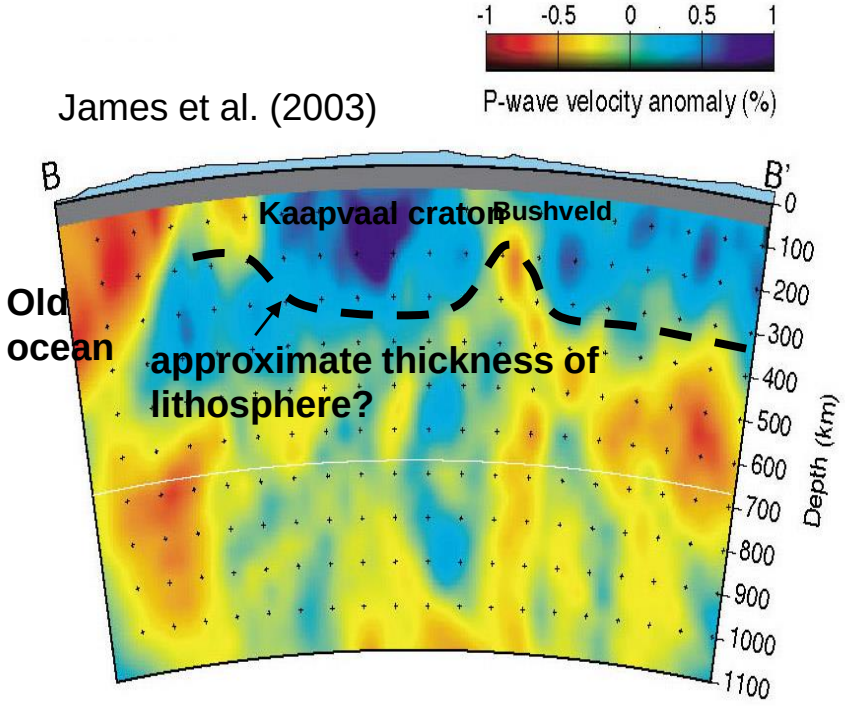

James et al, 2001, GRL, 28

James et al, 2004, G3, 5

- Cratonic root structures are irregular, reaching depths of at least 250-300 km in the southern part of the Kaapvaal craton and in regions of the Zimbabwe craton.
- The mantle beneath the Bushveld province exhibits anomalously low velocities suggesting refertilization of the cratonic mantle during the Bushveld magmatic event.
- There is a jump to low velocities at Cape Fold belt, intermediate beneath Proterozoic Namaqua-Natal belt.

Tectosphere Deformation Mapped in Southern Africa by S-Wave Splitting

Orientations of shear wave splitting fast polarization directions

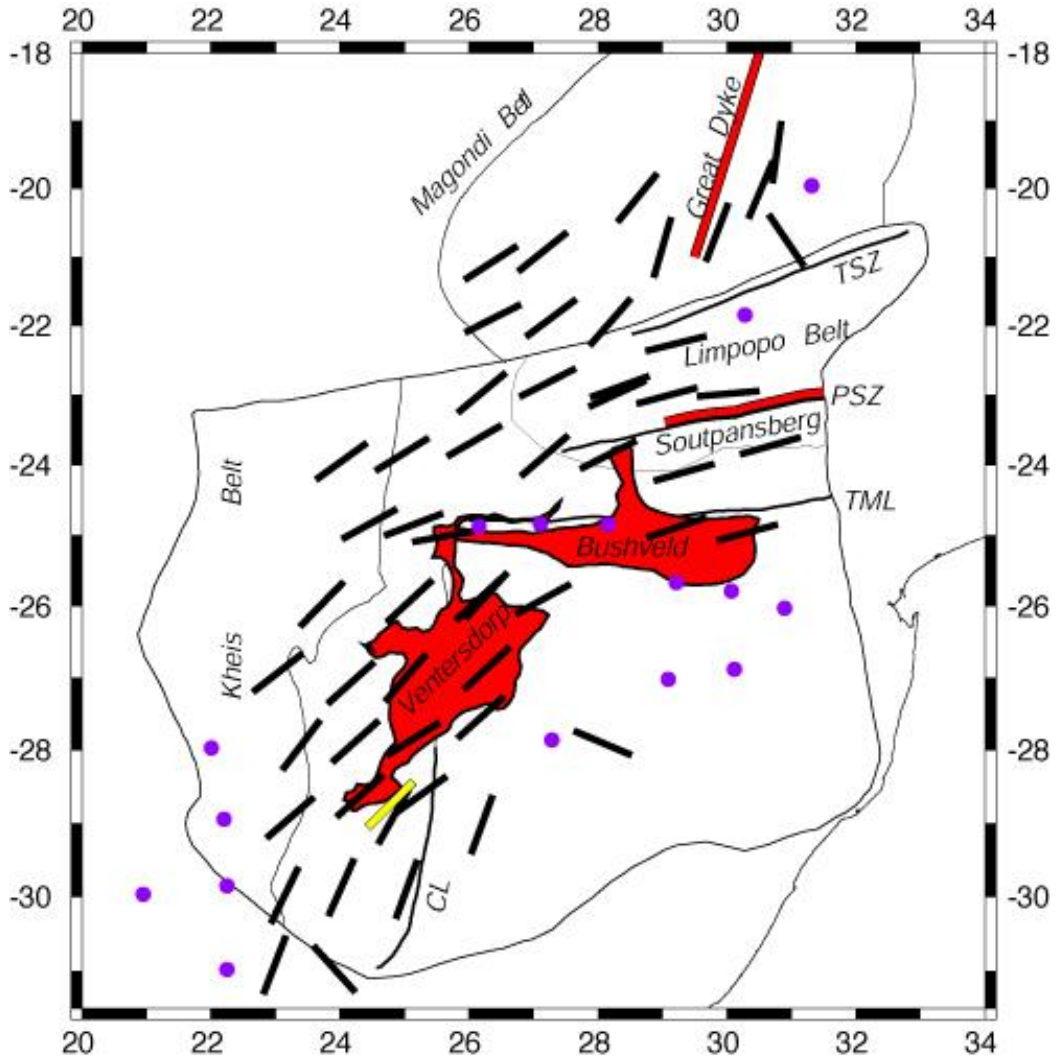

The values of lineation direction exhibit systematic spatial variations:

- In the southwestern Kaapvaal they are roughly north-northeast to south-southwest, rotate to northeast-southwest further north, and to nearly east-west in the northeastern part of the craton, including the Limpopo belt. Just north of the Limpopo, in the vicinity of the Great Dyke the values oriented north-northeast to south-southwest.
- Mantle anisotropy was produced by Archean deformation within the tectosphere, rather than present-day processes in the sublithospheric mantle
- Neo-Archean collisional orogenesis imparted a mechanical anisotropy to the tectosphere that controlled the subsequent magmatic history of cratonic southern Africa.

Silver et al., 2004, S. Afr. J. Geol., 107

Purple dots represent measurements with zero or near-zero splitting delay times. TML: Thabazimbi Murchison Lineament, CL: Colesberg Lineament, KGB: Kraaipan Greenstone Belts, SZ, shear zone

Interpretation of anisotropic structure of the mantle of cratonic Southern Africa

Tectonic stabilization by ~2800 Myr and subsequent magmatic history

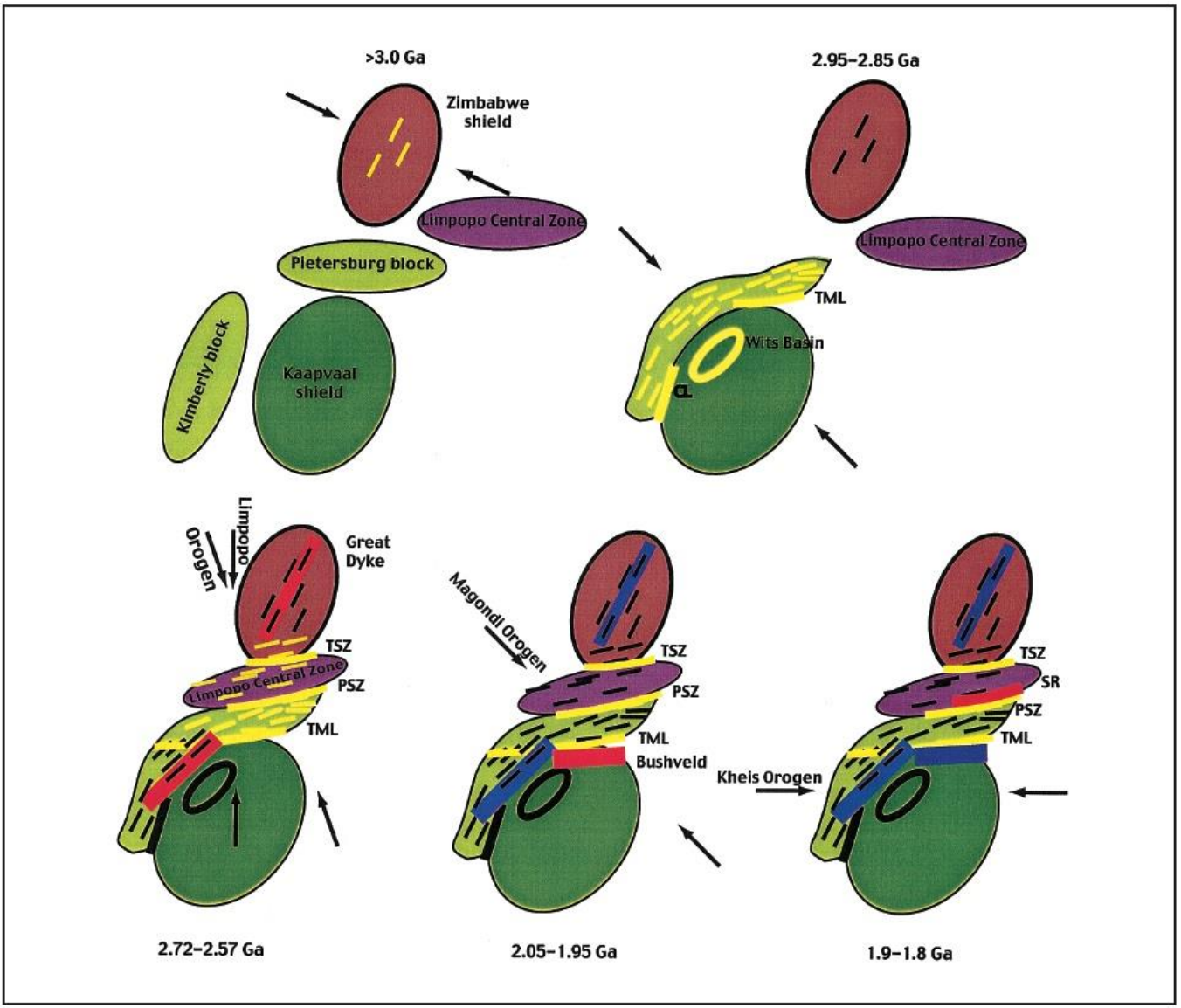

Silver et al., 2004, S. Afr. J. Geol., 107

Five major deformational phases control the history of the South African Craton:

i. An unknown pre-2.9 Gyr orogen that imparts a mantle fabric to the Zimbabwe craton;

ii. A collision at ~2.9 Gyr along the western and northern boundaries of the Kaapvaal Shield, imparting mantle fabric to the Kimberly and Pietersburg terranes;

iii. The Limpopo orogen, at ~2.6 to ~2.7 Ga, which imparts mantle fabric to the three Limpopo zones, and which produces collisional rifts to the north and south, namely the Great Dyke and Ventersdorp;

iv. The ~2.0 Ga Magondi orogen, both reactivating shear zones in the Limpopo and producing the Bushveld as another collisional rift;

v. The ~1.8 to 1.9 Gyr Kheis orogen, which produces the final collisional rift, namely the Soutpansberg trough.

In all of these cases, the rifts formed at an orientation that is parallel to preexisting mantle fabric, as inferred from mantle anisotropy.

Collisional Rifts form where the stress field associated with collision produces extension and rifting for orientations at a small angle to the direction of the collision.

Magamatic Activity after the cratonic roots stabilitation

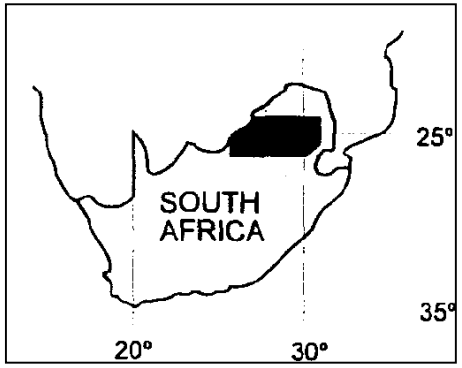

Bushveld Complex

Largest intrusion of layered mafic rocks

Rustenberg Layered Suite

Largest accumulation of siliceous volcanism

Rooiberg Group

Largest granite plutonism

Lebowa Granite Suite

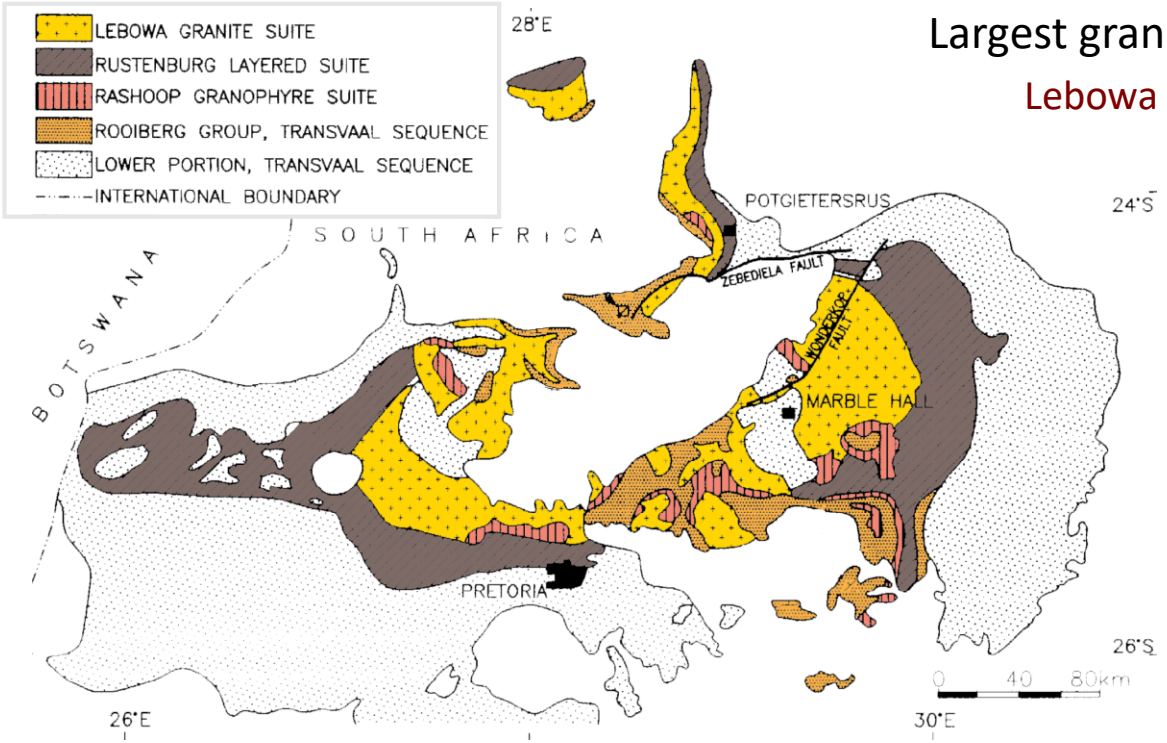

What explains the persistent magmatic activity after cratonic stabilization?

Proposed mechanisms:

Exogenous

- **Bolide impact**
- **Deep mantle plume**

Endogenous

- **Tectospheric instability (eclogite bodies formation)**
- **Higher mantle *T* at the base of the lithosphere**

- **Thick continental lithosphere has a thermal blanketing effect on the mantle below which result in higher mantle *T* up to the point that the geotherm could cross the solidus of fertile peridotite, while at the same time leaving the refractory depleted lithosphere intact.**

Chemical Limitations on Cratonic Growth

Why do older continental cratons have thicker tectosphere than younger continents?

Observations:

- Isopycnicity implies thick tectosphere stabilized by depleted peridotites
- Highly depleted, low-density peridotites (Mg # > 92) observed in the subcratonic mantle are primarily of Archean age
- Subsequent Proterozoic and Phanerozoic magmatism has not generated large volumes of such rocks

Implication:

- Proterozoic transition from thick to relatively thin tectosphere can plausibly be explained by the exhaustion of Archean mantle peridotitites with Mg # > 92

Can be cratonic lithosphere destroyed?

- A number of processes can erode or destroy cratonic lithosphere and, by lowering the viscosity and density contrast between cratonic root and convecting mantle, compromise its stability: Heating by impinging plumes, addition of water by dehydration of slabs beneath cratons, injection of wet melts at the LAB, or addition of *Fe*-rich melts during metasomatism.
- The consequences are: (1) partial melt of the litospheric roots (2) compositional changes (e.g., *Fe* enrichment) of the litospheric roots with densifications and rheological weakening of the lithosphere due to melt infiltration.

Example: North China Craton

Liu et al., GCA, 2011

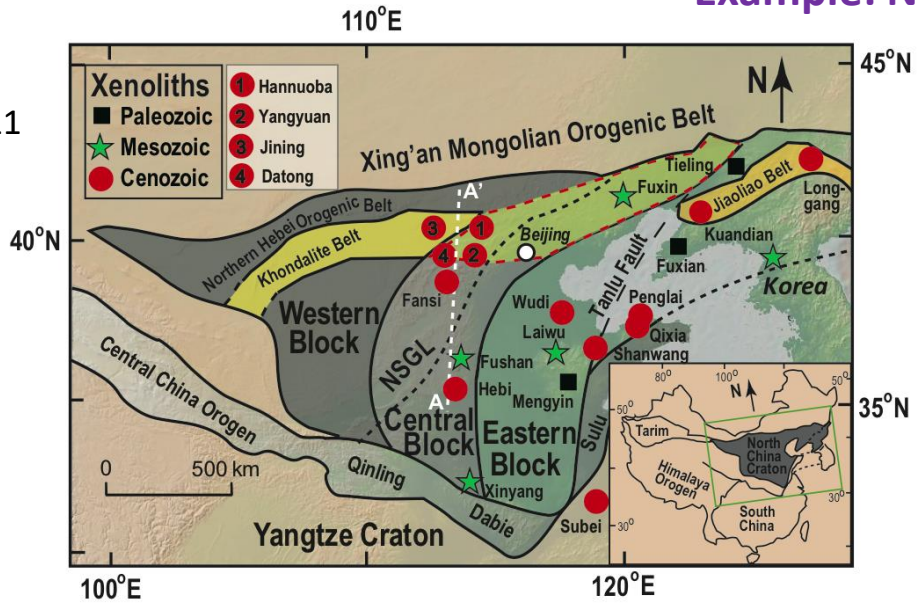

Obrebski et al., 2012, JGR, 117

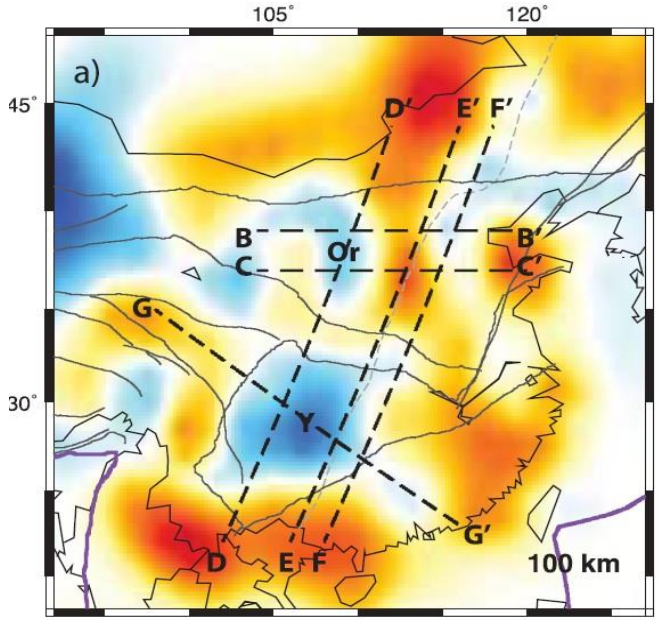

Ordos block (Or), Yangtze Craton (Y)

- High velocities only beneath western block, slower to the east beneath an area where the crust is still Archean, but the lithospheric mantle is Proterozoic to modern.
- Loss of the lithospheric root beneath the NCC is shown by the composition of mantle xenoliths present in early Palaeozoic and Mesozoic to Tertiary volcanic rocks.
- The subduction of the Pacific Plate started during the Mesozoic has extensively hydro-weakened the upper mantle beneath the NCC, causing its destabilization, thinning, and replacement.
- The tectonics of much of Asia changed from contractional to extensional at c. 130–120 Myr, at the same time of the subcontinental mantle root loss beneath the NCC.

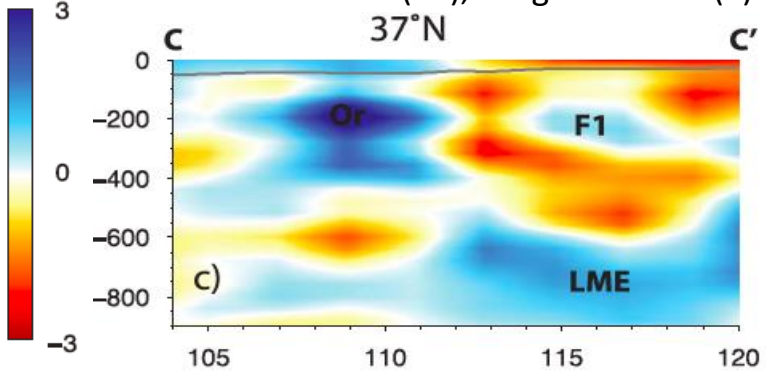

Evolution of the North China Craton

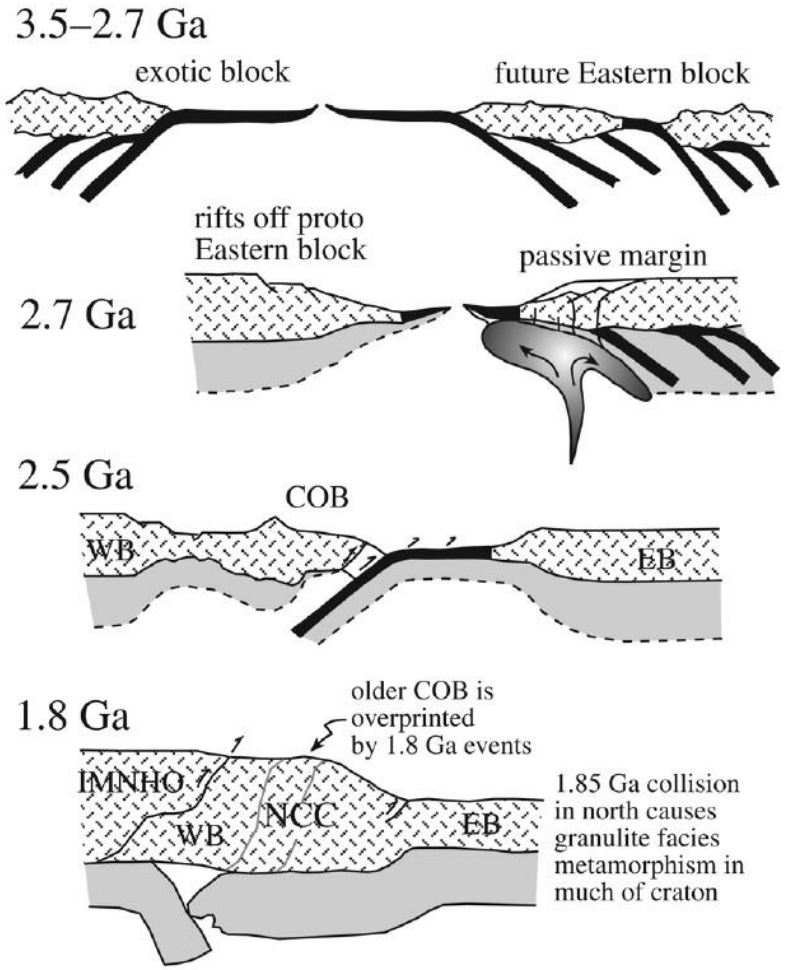

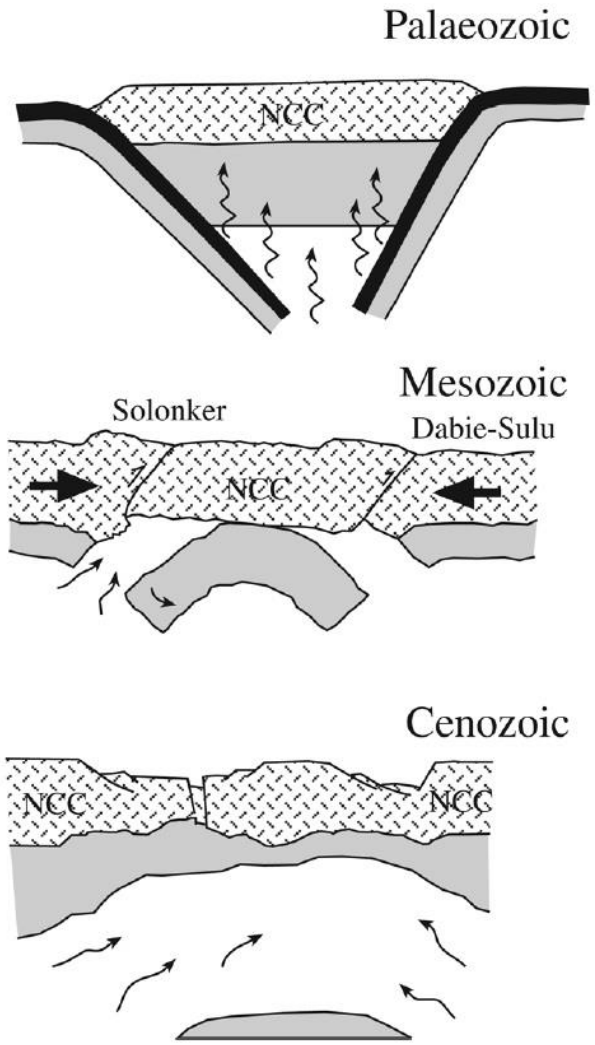

Kusky et al., 2018,Geol. Soc., London, 280

- Growth of the craton by subduction–accretion in arc settings probably involved the underplating of buoyant oceanic slabs (mantle root formation)
- Plume-influenced rifting at 2.7 Gyr broke apart the future Eastern Block and led to the development of a passive margin sequence on the western side of the Eastern block. This margin collided with a convergent margin at 2.5 Gyr, amalgamating the craton.
- At 1.85 Gyr the craton experienced a major collision event along its northern margin, which resulted in partial replacement of the mantle root and the formation of a collisional plateau and foreland basin.
- For much of the Palaeozoic the craton was relatively internally stable, but accommodated cumulative subduction along its northern, southern, and eastern margins.

- Subduction-related dehydration reactions in the slab released fluids that hydrated the mantle, which allowed the root to release a low-density melt phase during Mesozoic tectonism, become denser, and sink into the asthenosphere after being triggered by near-simultaneous collisions along its northern and southern margins.

Wyoming Craton

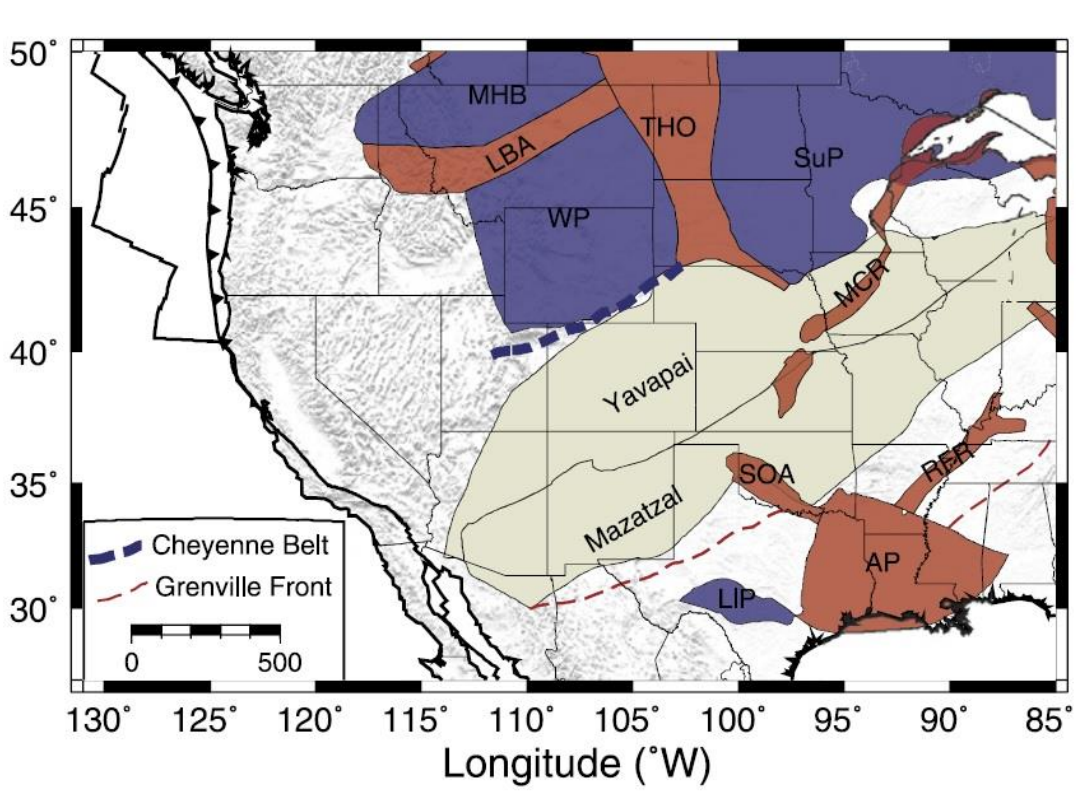

Porritt et al., 2014, EPSL, 402

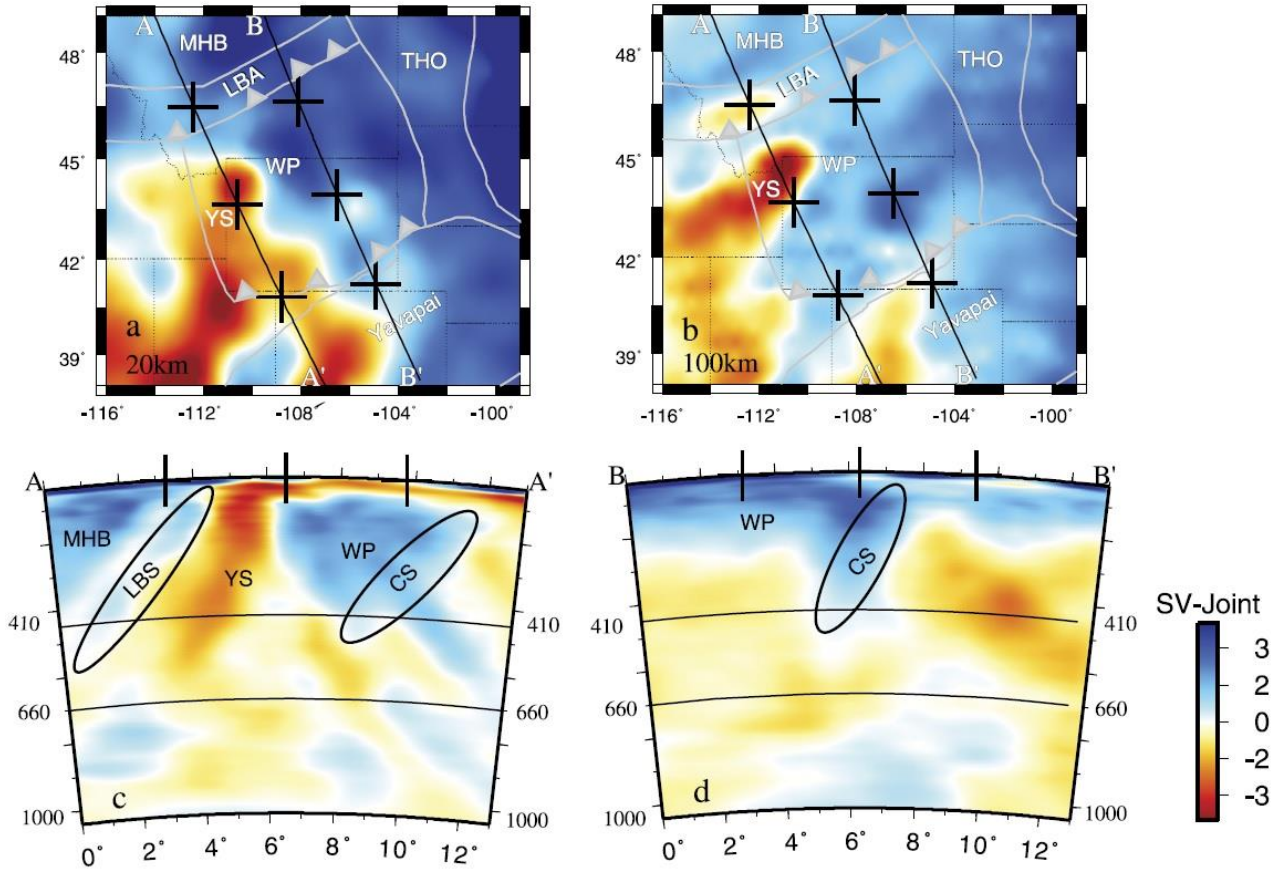

Gray triangles denote overriding plate in last collisional event. MedicineHatBlock (MHB), LittleBeltArc (LBA), LittleBeltSlab (LBS), Yellowstone (YS), WyomingProvince (WP), CheyenneSlab (CS), Trans-Hudson Orogen (THO), LaurentiaCraton (LC), Southern Oklahoma Aulacogen (SOA), Mid-Continent Rift (MCR), Reelfoot Rift (RFR), ArgentinePrecordillera (AP), and Llano Province(LlP).

- Low velocity anomalies are associated with the Little Belt Arc and the Yellowstone Plume.
- The Wyoming Province retains evidence of fossil slabs along its southern (Cheyenne) and northern (LittleBelt) boundaries. The Yellowstone plume is impinging on its western edge.
- The mantle lithosphere near the northern boundary of the Wyoming Craton has been more severely affected by post-Archean events occurring on the borders of the Craton (xenoliths show clear evidence of extensive interaction with incompatible-element-rich melts).

Causes of decratonization

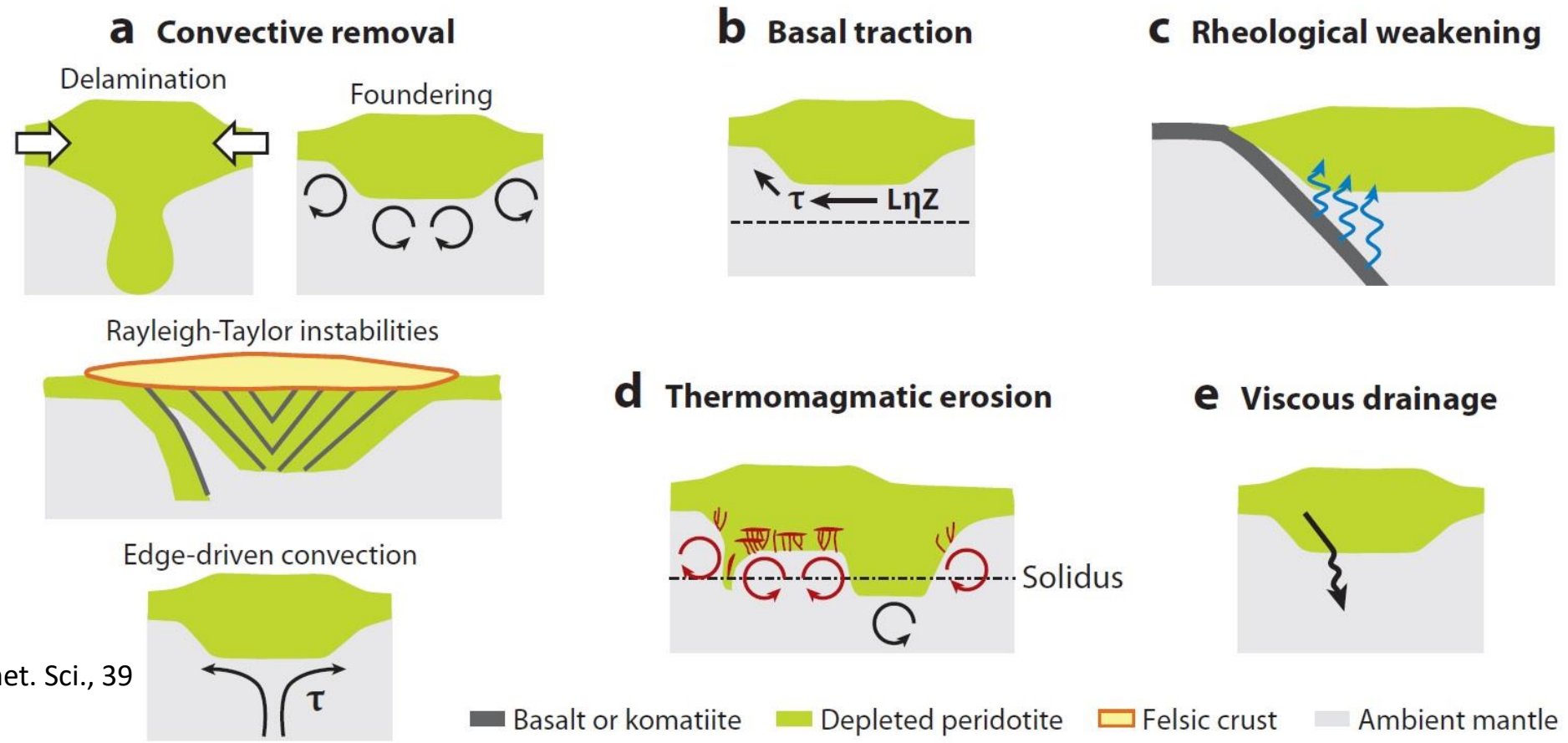

Lee et al., 2011,
Annu. Rev. Earth Planet. Sci., 39

a. Any lithospheric removal driven by thermal or chemical buoyancy forces (e.g., density-driven forces) is referred to as convective removal.
b. Erosion of continental lithosphere can be driven by basal shear stresses imposed by mantle flow in the asthenosphere (cratonic destruction is unlikely, since shear stresses decrease rapidly as craton thickness increases).
c. Weakening the rheology of continental mantle through fluids infiltration can facilitate convective removal.
d. Both plume impingement and small-scale convective instabilities are favorable environments for generating melts and cause a thermomagmatic erosion of the cratonic roots.
e. Inclined layers of garnet pyroxenite could “drain” back into the convecting mantle owing to their high densities and low viscosities compared with peridotite.

Middle Lithosphere Discontinuity (MLD)

- **Negative velocity gradients beneath cratons at ~170– 250 km depth are generally interpreted as the LAB, while seismic discontinuities, with a thickness of ~30–40 km, occurring around 80-120 km depth have been interpreted as MLDs.**
- **The MLD boundaries are characterised by both positive and negative seismic velocity anomalies (usually strong *S*-wave velocity drop), often accompanied by azimuthal and radial anisotropy.**

Origin of the MLDs

- Partial melting of mantle material in presence of volatile (e.g., Thybo and Perchuc, 1997, Science, 416).
- Changes in azimuthal (Sodoudi et al., 2013) or radial anisotropy (Rychert and Sherer, 2009, Science, 324), accompanied by seismic velocity reduction (Aulbach et al., 2017), may result from the accumulation of metasomes as layers at or as subvertical veins.
- Boundary between depleted and metasomatized lithosphere: lower lithosphere altered by metasomatic fluids resulting in crystallization of low-velocity minerals (e.g., amphibole: $x Si_8O_{22}(OH)_2$ or phlogopite: $KMg_3(AlSi_3O_{10})(F,OH)_2$) (Sodoudi et al., 2013, G3, 14).
- Grain boundary sliding (elastically accomodated) at a temperature of 900°C (Karato, 2012, EPSL, 321-322).

Models for craton thickening and associated development of fabric

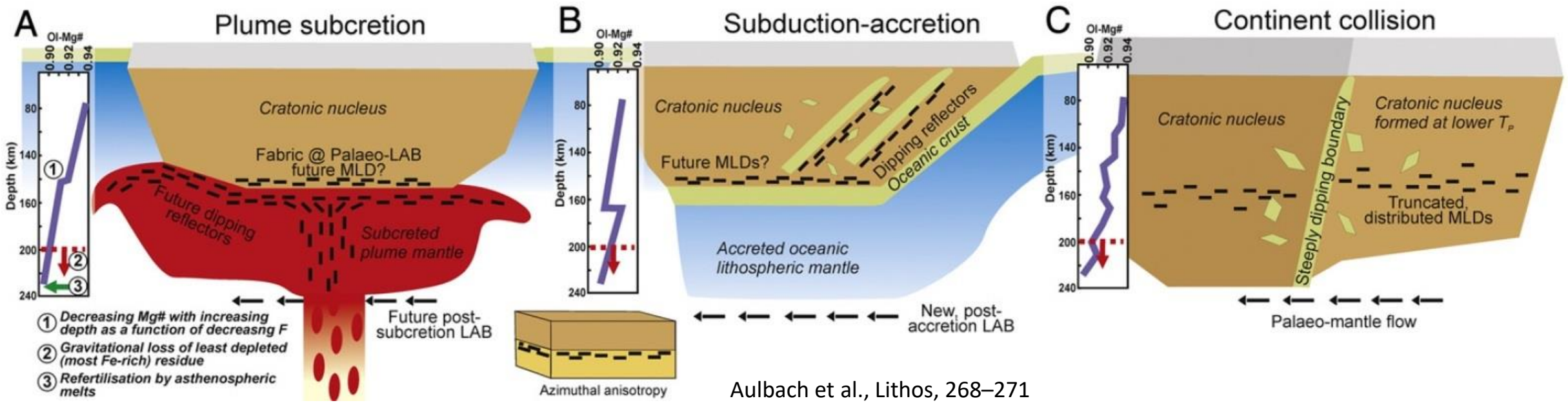

Aulbach et al., Lithos, 268–271

- Vertical lineation in the plume stem gives way to horizontal lineation when the plume impinges upon the LAB: Mg# decreases due to the effects of polybaricmelt extraction, while a discrete step forms when mantle packages formed at different T_P are juxtaposed.
- Imbrication of oceanic slabs leads to dipping lineations while horizontal lineations result from flat subduction: if the two packages formed at similar time by partial melting to low pressure, the Mg# profile of each lithosphere package would be identical.
- Collision of two cratonic nuclei subsequent to ocean closure, with different thicknesses at the time of collision due to formation at different T_P: near the boundary, Mg# with depth may show complexity.

Strong vs. weak or absent cratonic seismic LAB signals

The cratonic LAB is known to produce a much weaker seismic signature than the oceanic LAB, and is often characterized by a small and gradual velocity change with a weak and intermittent seismic signal:

- When present, seismically imaged discontinuities beneath cratons cannot be produced by thermal effects alone and instead require contrasts in composition, fabric, water content or the presence of partial melt or volatiles (e.g., in the cratonic lithosphere melt-related reworked and rejuvenated).
- Where discrete LABs are not detected in the cratonic lithosphere, the boundary is characterized by a velocity gradient and hence more accurately described as a transition zone that is spread out over a large depth interval (e.g., in the intact and undisturbed cratons).

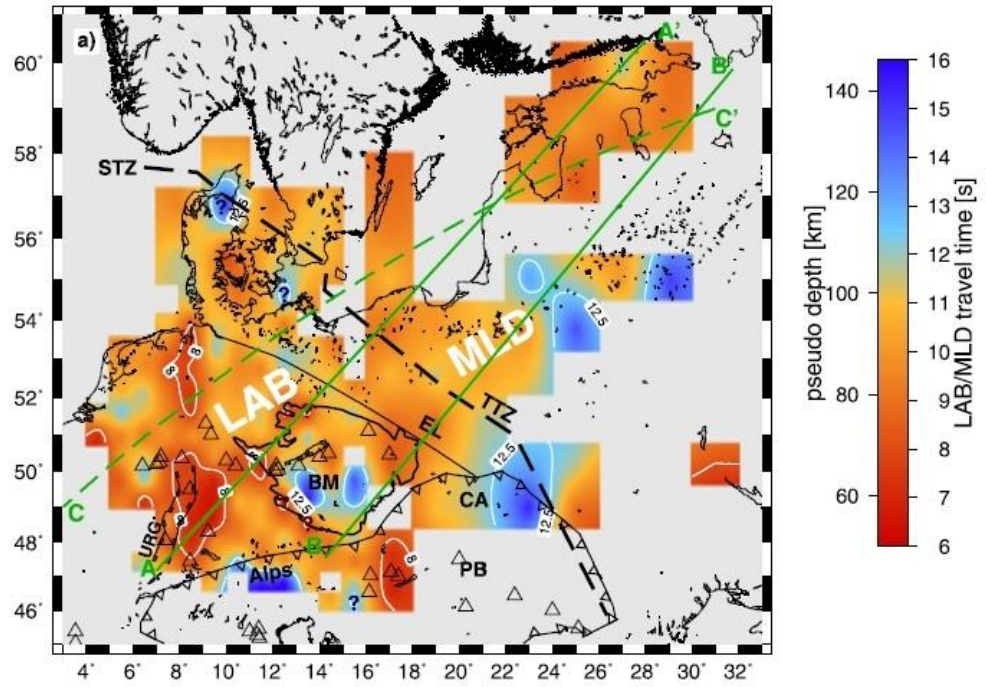

STZ: Sorgenfrei–Tornquist Zone, TTZ: Teisseyre–Tornquist Zone

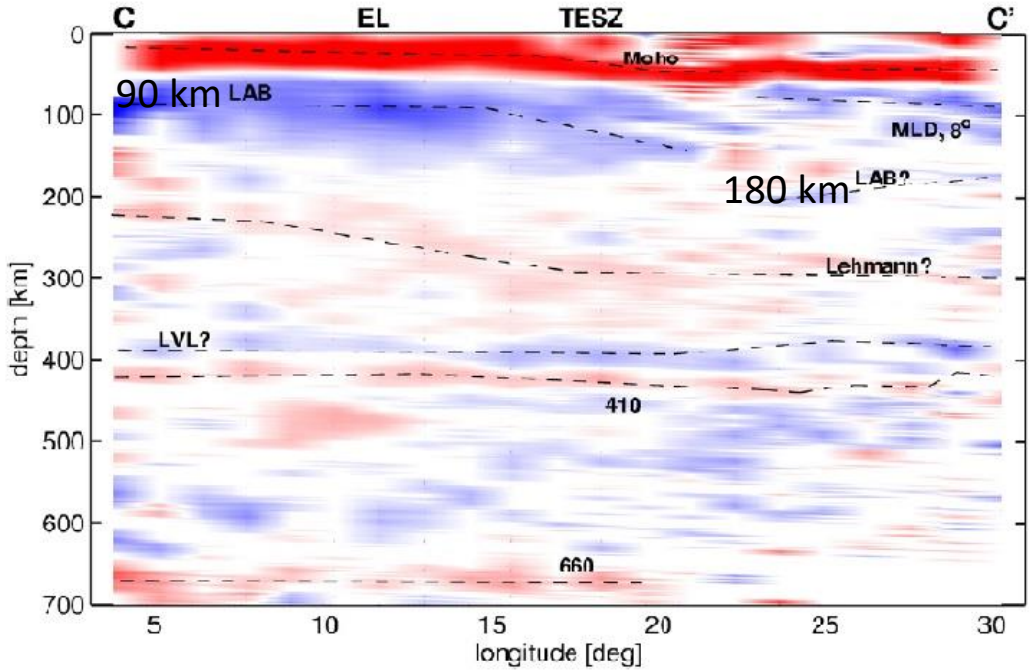

(Knapmeyer-Endrun et al., 2017, EPSL, 458)

LAB deeper, but weaker and less consistent in the EEC than in the Phanerozoic Europe

Thermal state of the lithosphere
(why do we want to know it?)

- Knowledge of the present thermal state of the Earth is crucial for models of crustal and mantle evolution, mantle dynamics, and processes of deep interior.

- Physical properties of crustal and mantle rocks are temperature dependant (density, seismic velocity, seismic attenuation, electrical conductivity, viscosity).

Temperature of the Earth is controlled by internal heat:

80% from the radiogenic heat production and 20 % comes from secular cooling of the Earth.

Heat is transferred to the surface of the Earth through three mechanisms: conduction (in the lithosphere), convection (below the lithosphere), and advection (hydrothermal circluation in sediments).

Knowledge of the thermal state of the lithosphere from more than 20000 heat flux measurements at the Earth's surface

Global Surface Heat Flux

- Oceanic heat flux follows a decreasing trend as a function of age, average: 67 mWm^2 (only due to conduction), 101 mWm^{-2} (including heat loss form hot fluids).
- Oceanic lithosphere is in a transient thermal state
- Over 96% of heat flow from oceanic lithosphere originates from beneath the crust, poor of ^{238}U, ^{235}U ^{40}K, and ^{232}Th.
- In the continents there is not a clear trend of heat flux with age (due to their longer evolution and complicated structure), average: 65 mWm^{-2}.
- Old continental lithosphere is close to thermal steady state .
- A large percentage of the heat flow is generated in the upper crust (10-20 km), rich of ^{238}U, ^{235}U ^{40}K, and ^{232}Th.
- Mantle thermal anomalies cause surface heat flow perturbation with wavelength of several hundred km.

- **Global average: 87 mWm^{-2}. Most common Q_0 and geothermal gradient values: 20-125mWm^{-2} 10-80°C/km (largest values in the tectonically active regions and lowest where mafic crust is present)**

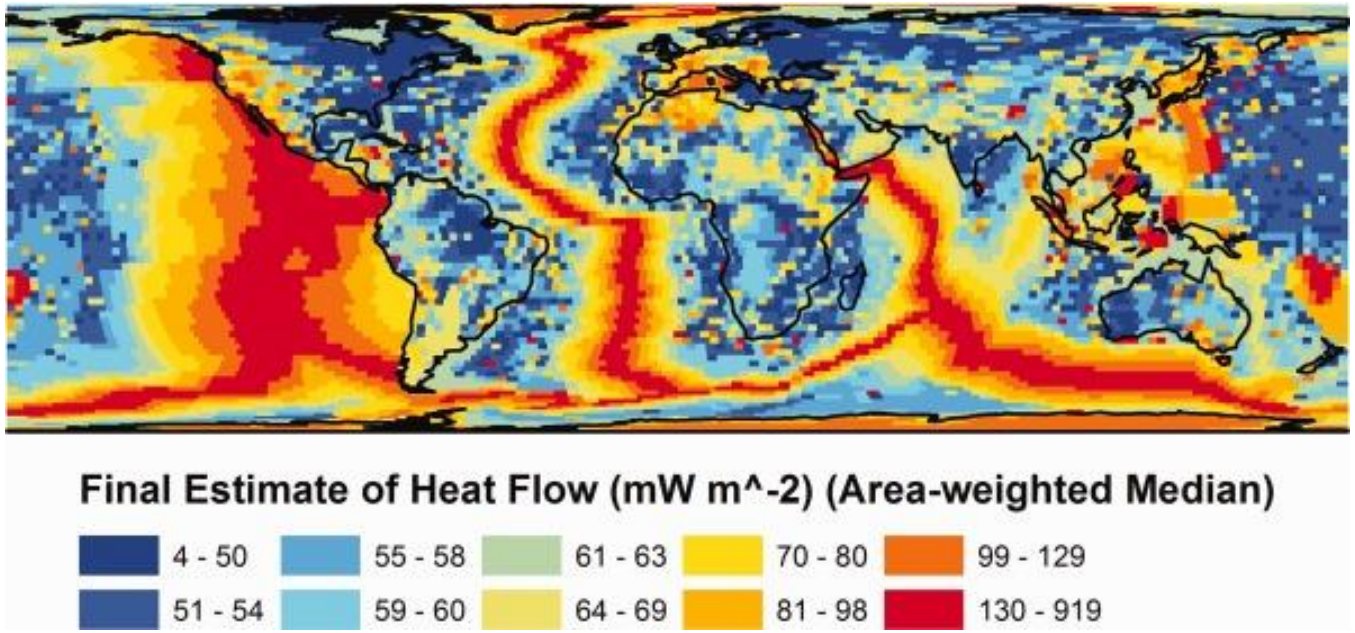

Thermal state of the continental lithosphere

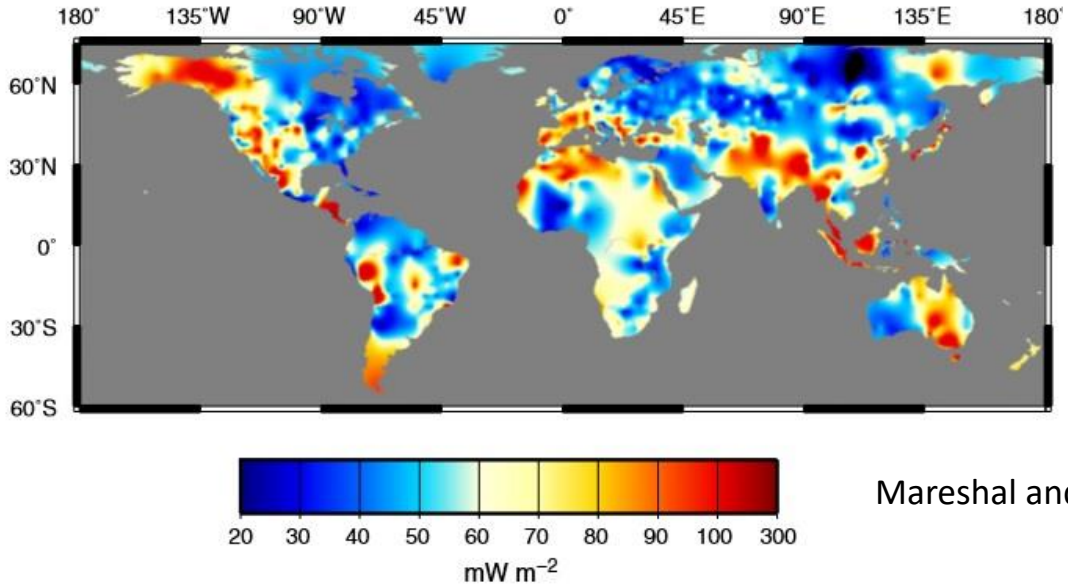

Mareshal and Jaupart, 2013, Tectonophiscis, 609

Heat flow density (HFD) determines the amount of heat per unit of area and per unit of time which is transmitted by heat conduction from the Earth's interior.

Fourier Law states that the rate of flow of heat is proportional to the temperature gradient:

$$\mathbf{q} = -\lambda \,\mathrm{grad}\, T = -\lambda \nabla T.$$

For 1D: $q = -\lambda \frac{\partial T}{\partial x}$

- minus sign shows that heat flows from points with high *T* to points with lower *T*
- λ *or K*= thermal conductivity (rocks dependent), for an isotropic and homogeneous layer has only one value
- Most of heat loss derives from heat production (*A*) due to the decay of ^{238}U, ^{235}U, ^{232}Th, and ^{40}K in ^{206}Pb, ^{207}Pb, ^{208}Pb, and ^{40}Ar or ^{40}Ca, respectively, which contributes 18-38 mWm^{-2} to the observed heat flow:

$$q = -\lambda \frac{\partial T}{\partial x} + A$$

- The Archean mantle was 100-300 °C hotter. Heat production was higher because of large amounts of long and short half-life (e.g., ^{36}Cl and ^{26}Al) unstable isotopes.

Thermal Conductivity

Thermal conductivity or the thermal conductivity coefficient (λ) of a material defines its ability to transfer heat

There are two main mechanisms which contribute to thermal conductivity: (i) the diffusion of heat by phonon propagation (**lattice conductivity k_l**), (ii) the transfer of heat through emission and absorption of photons (**radiative conductivity k_r**).

λ (m^{-1} s^{-1} K^{-1} or W m^{-1} K^{-1}) of rocks is dependent on *T*, *P*, porosity (ϕ), composition, and properties of pore-filling fluids and gases.

Material	Wm^{-1} K^{-1}	Source
Earth's crust	2.0–2.5	Mean value, Kappelmeyer and Hänel (1974)
Rocks	1.2–5.9	Sass et al. (1971)
Sandstone	2.5	Clark (1966)
Shale	1.1–2.1	Clark (1966), Blackwell and Steele (1989)
Limestone	2.5–3	Clark (1966), Robertson (1979)
Water	0.6 at 20 °C	Birch et al. (1942)
Oil	0.15 at 20 °C	Birch et al. (1942)
Ice	2.1	Gretener (1981)
Air	0.025	CRC (1974) Handbook
Methane	0.033	CRC (1974) Handbook

Rock	From published data[a]		After Sharma (2002)
	No. of samples	Average heat conductivity	Average heat conductivity
Sand	1,149	1.79	1.1–2.1
Siltstone	476	1.58	–
Argillite, clay schist	783	1.67	2.09
Clay	660	1.43	0.8–1.5
Marl	217	1.78	–
Limestone	781	2.37	3.44
Chock	21	1.63	
Granite	383	2.68	3.07
Granodiorite	83	2.79	2.63
Porphyrite	137	1.74	–
Diorite	78	2.10	2.5
Andesites, andesite-basalt	81	1.87	2.26
Basalt	98	2.11	1.69
Diabase	67	2.50	2.2
Gabbro	116	2.47	2.57
Schist	181	2.55	–
Gneiss	88	2.41	2.7–3.1
Amphibolite	47	2.39	3.33
Gneiss-granite	35	2.04	–
Quartzite	–	5.00	5.03
Anhydrite	–	–	5.43
Harzburgite	106	2.69	–
Dunites	23	2.77	–
Olivine gabbro	55	2.65	–
Gabbro-norite	36	2.22	–

Heat Flow data

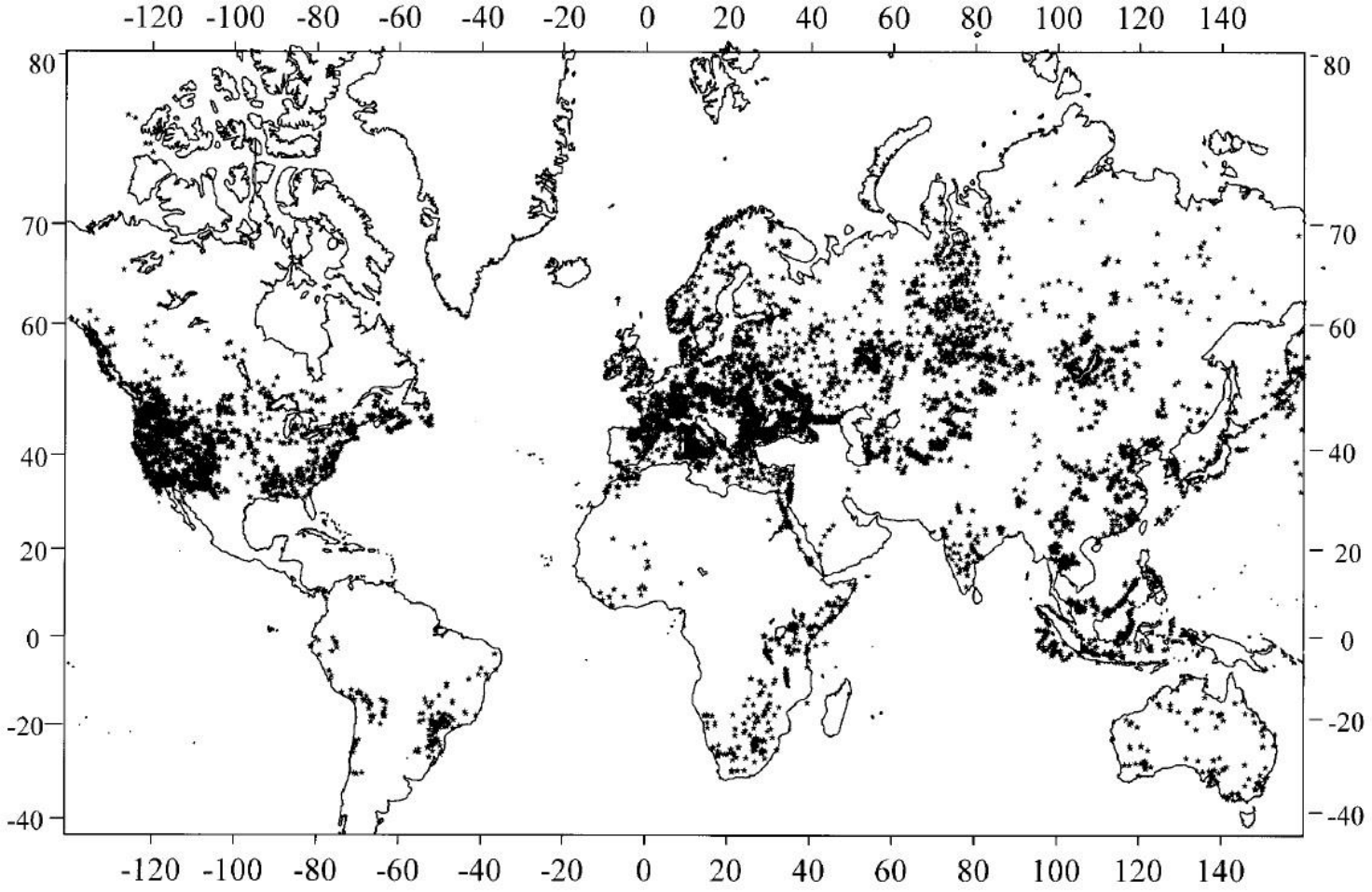

Artemieva and Mooney, 2001, JGR, 106

Country or region	HFD range (mW m^{-2})	References
Austria	43–127	Čermák (1984)
Bulgaria	8–132	Čermák (1984)
Cyprus	41–185	Čermák (1984)
France	45–176	Čermák (1984)
Eastern Germany	26–172	Čermák (1984)
Western Germany	21–168	Čermák (1984)
Greece	30–105	Čermák (1984)
Hungary	52–139	Čermák (1984)
Iceland	63–281	Čermák (1984)
Israel	7–93	Čermák (1984)
Italy	17–143	Čermák (1984)
Romania	19–118	Čermák (1984)
Spain	29–189	Čermák (1984)
USSR (European part)	19–142	Čermák (1984)
Greenland and Norwegian Seas	14–268	Čermák (1984)
Reykyjanes range	2–343	Čermák (1984)
Ranges of the Atlantics	0–282	Čermák (1984)
Other regions of the Atlantics	11–90	Čermák (1984)
Mediterranean near Spain	55–155	Čermák (1984)
Mediterranean West of Sardinia	33–132	Čermák (1984)
Tyrrhenian Sea, Mediterranean	30–173	Čermák (1984)
Adriatic Sea, Mediterranean	36–104	Čermák (1984)
Aegean Sea, Mediterranean	47–114	Čermák (1984)
Ionic and Eastern Mediterranean Seas	10–74	Čermák (1984)
Black Sea	8–91	Čermák (1984)
Caspian Sea	40–99	Čermák (1984)
Alaskan interior	42–130	Williams et al. (2006)
Egypt	42–175	Morgan and Swanberg (1978)
Marmara Sea	35–115	Pfister et al. (1998)
Baltic Shield	25–70	Kukkonen et al. (1998)
Kura Depression, Azerbaijan	12–105	Pilchin (1983)
Cordillera, South America	25 to >160	Hamza and Muñoz (1996)
Brazilian platform	30 to >100	Hamza and Muñoz (1996)
Altiplano, Cordillera	50–180	Springer and Förster (1998)
Oregon Cascade Range, USA	40–100	Blackwell et al. (1980)
Pannonian basin	50–130	Lenkey et al. (2002)
Deccan basalt province, India	33–73	Kumar et al. (2007a)
Mesozoic Luangwa and Zambezi rifts	44–110	Nyblade et al. (1990)

Heat flux and age: is there any trend?

Archean

Regional variations of the heat flow in some Archean Cratons

Province, Craton	HFD range (mW m^{-2})	References
Superior Province	22–48	Mareschal and Jaupart (2006)
Australian Cratons	34–54	Mareschal and Jaupart (2006)
Baltic Shield	15–39	Mareschal and Jaupart (2006)
Siberian Shields	18–46	Mareschal and Jaupart (2006)
Anabar Shield	15–25	Duchkov (1991)
Ukrainian Shield	30–50	Galushkin et al. (1991)
Karelia, Baltic Shield	35–40	Slagstad et al. (2009)
Dharwar Craton, India	25–51	Roy and Rao (2000)
eastern Dharwar Craton, India	33–73	Kumar et al. (2007a)
Karelian and Belomorian prov., Baltic Shield	20–30	Shwartsman (2001)
Belomorian Belt, Baltic Shield	20–30	Čermák et al. (1993)
Karelia and Kola Peninsula, Baltic Shield	<20–35	Čermák et al. (1993)
Laponian supracrustals	20–30	Čermák et al. (1993)

Paleozoic

Regional mean heat flows in different Paleozoic regions

Region	Average HFD (mW m^{-2})	References
The Appalachians	57	Jaupart and Mareschal (1999)
Mainland United Kingdom	54	Lee et al. (1987)
Dnieper aulacogen, the Ukraine	45	Čermák (1993)
Pripyat Depression, Belorussia	66	Čermák (1993)
Russian Platform	68	Čermák (1993)
Caledonian	~50	Čermák et al. (1993)
Hercynian	~70	Čermák et al. (1993)
Altay-Ergula Belt (China)	60	Hu et al. (2000)
Junggar-Higgan Belt (China)	47	Hu et al. (2000)
The Urals	30	Kukkonen et al. (1997)
Ural Foredeep[a]	29	Kukkonen et al. (1997)
West Ural Folded Zone[a]	28	Kukkonen et al. (1997)
Central Ural Uplift[a]	24	Kukkonen et al. (1997)
Tagil-Magnitogorsk Zone[a]	14	Kukkonen et al. (1997)
East Ural Uplift[a]	18	Kukkonen et al. (1997)
East Ural Depression[a]	27	Kukkonen et al. (1997)
Trans-Ural Uplift[a]	20	Kukkonen et al. (1997)
Tyumen-Kustanay Depression[a]	26	Kukkonen et al. (1997)

[a] Different regions of the Urals

Range of Heat Flux:

Archean: 36–50mWm^{-2}

Proterozoic: 36–94mWm^{-2}

Paleozoic: 30–57 mWm^{-2}

Regional variability of heat flux

	Minimum	Maximum
	(mW m^{-2})	
Superior Province	22	48
Trans-Hudson Orogen	22	50
Australia	34	54
Baltic Shield	15	39
Siberian Shield	18	46

Minimum and maximum values obtained by averaging over 200 km × 200 km windows.

Thermal history of the Earth

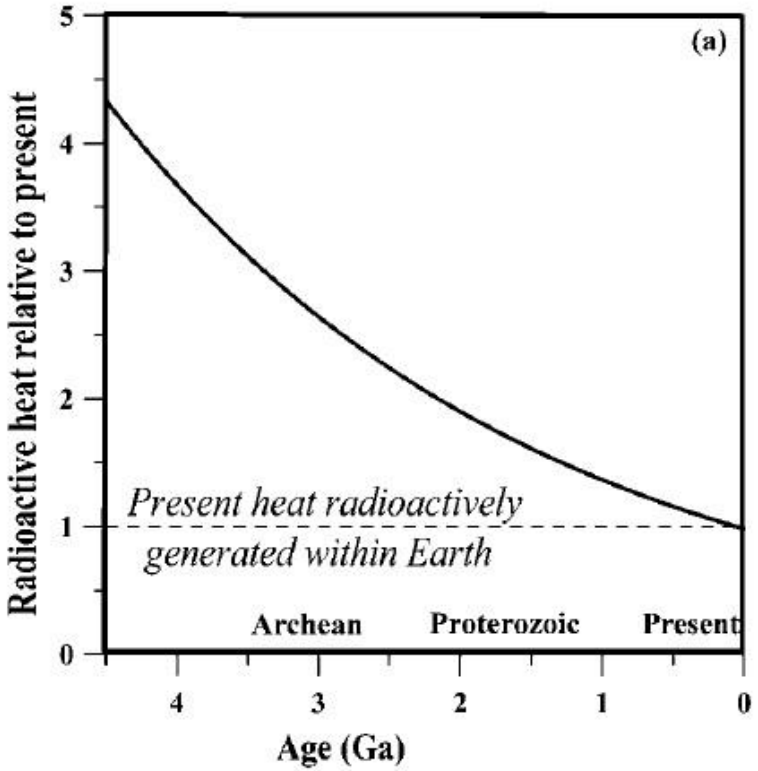

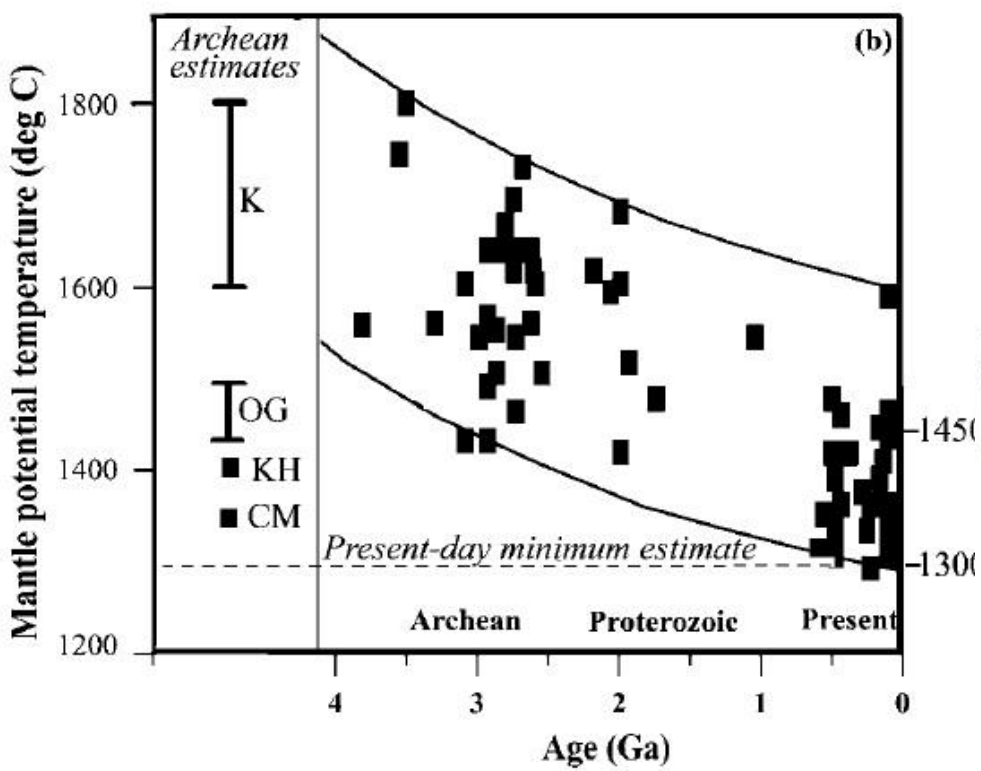

Present T conditions

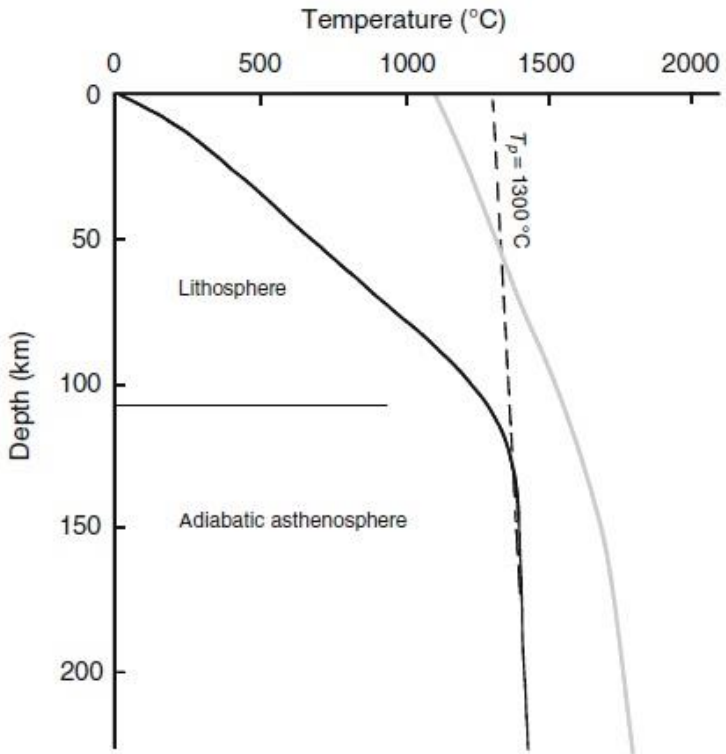

Garnet Peridotite Solidus

K=Komatiite
KH=Hydrous Komatiites
OG=Ophiolites and Greenstone belts
CM=Mantle convection models

Radiogenic Heat Generation

$$A = \rho \sum P A_s c$$

ρ is the rock density, P the abundance and A_s the rate of heat generation per *kg* of isotope and c the concentration.

$$c_t = c \exp(t \ln 2/\tau)$$

$$A = \rho \left[\begin{array}{r} 0.993\, c_U A_{U^{238}} \exp(t\ln 2/\tau_{U^{238}}) + 0.0071\, c_U A_{U^{235}} \exp(t\ln 2/\tau_{U^{235}}) \\ + c_{Th} A_{Th^{232}} \exp(t\ln 2/\tau_{Th^{232}}) + 0.00012\, c_K A_{K^{40}} \exp(\ln 2/\tau_{K^{40}}) \end{array} \right]$$

c_t = concentration of an isotope at time t
$\tau = \ln 2/\lambda$ = half life with λ decay costant

$^{238}U \longrightarrow {}^{206}Pb$

$^{235}U \longrightarrow {}^{207}Pb$

$^{232}Th \longrightarrow {}^{208}Pb$

$^{40}K \rightarrow {}^{40}Ca$ (89%)
$^{40}K \rightarrow {}^{40}Ar$ (11%)

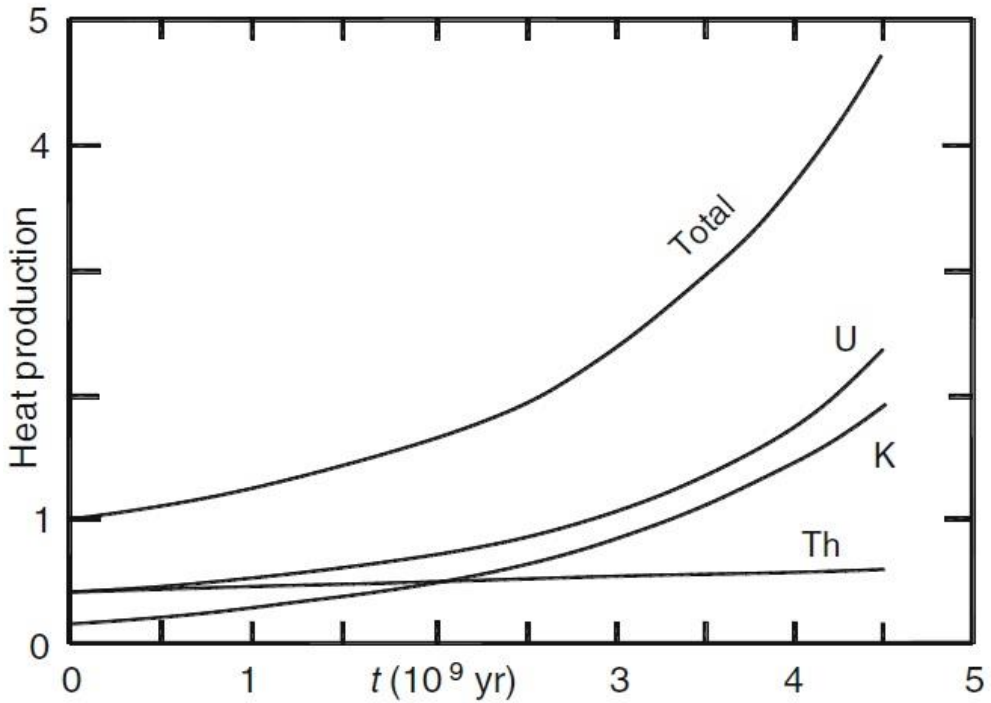

t is in 10^9 years

Radiogenic Heat Generation in Depth

$$A(z) = A_o \exp\left(-\frac{z}{D}\right) \qquad q_o = q_a + A_o D$$

The linear relationship supposes an exponential variation of *A*

A_0 (in μW m^{-3}) = radiogenic heat at the surface and D (km) = thickness of layer enriched by heat producing elements (5-15 km), q_0 = heat flowing out from the Earth' surface, and q_a is the component of heat flow from the mantle.

If the thickness of *D*-layer is much smaller than the scale of horizontal fluctuation in radioactivity, the effect of lateral heat production variation on *Q* is negligible.

***A* = 2.5 mW/m^3 through a depth of 10 km produce a surface heat flux of 25 mWm^{-2} (about half of typical continetnal heat fluxes)**

For magmatic and metamorphic rocks A=2.5–3.5 μW m^{-3}

Measurements in boreholes have shown that *A* does not systematically decrease with depth, since tectonics can modify the distribution

Compositional model of the Variscan crust as inferred from the $v_P(z)$ structure and the corresponding radiogenic heat *A* deduced from petrographical data (after Verdoya et al. 1998b)

Depth range (km)	Lithotype	Percentage of rock type	*A* (μW m^{-3})
Upper crust			
0–12	Granite-granodiorite	100	3.0
12–18	Granitic gneiss	55	
	Granite-granodiorite	20	1.6
	Tonalitic gneiss	25	
Lower crust			
18–22	Amphibolite	60	0.4
	Mafic granulite	40	
22–30	Mafic garnet granulite	65	0.3
	Amphibolite	35	
30–32	Mafic garnet granulite	100	0.2

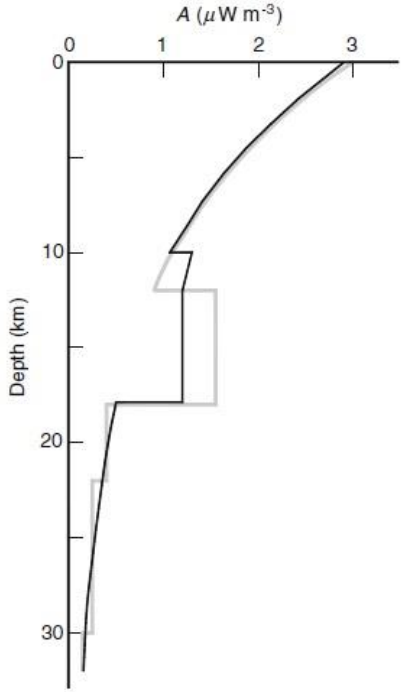

For the lower crust, xenolith lead to a global average of 0.28 mWm^{-3}

Radiogenic Heat Generation of igneous rocks

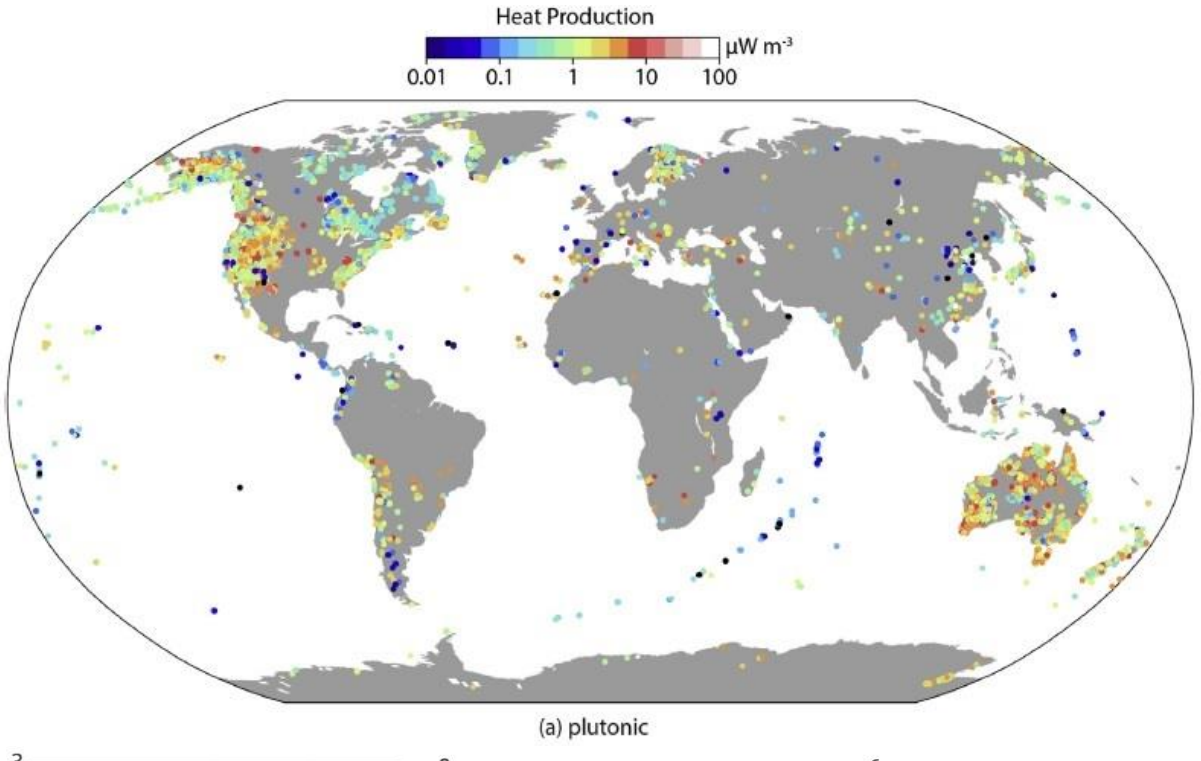

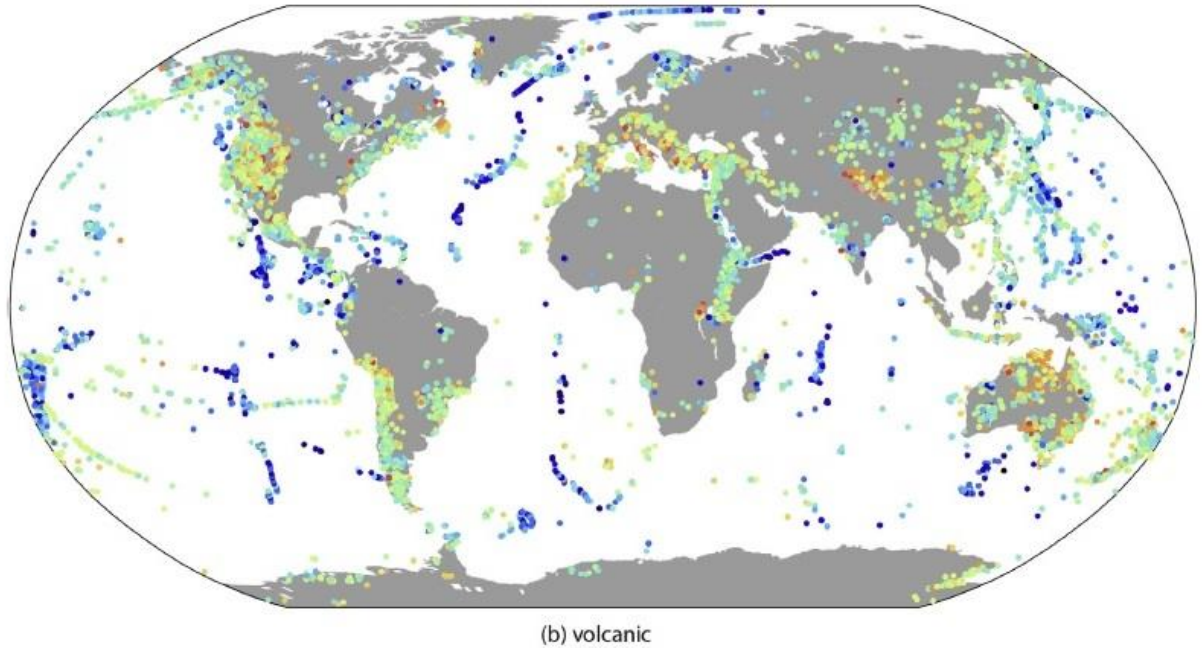

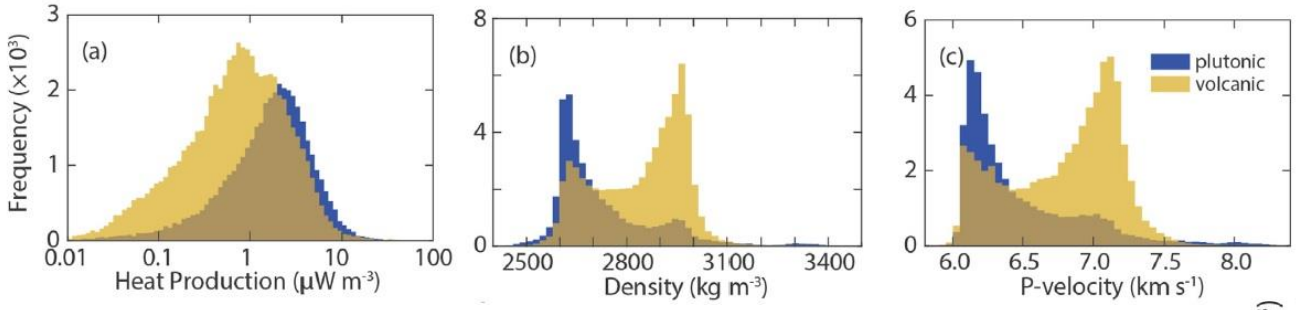

Hasterok and Webb, 2017, Geoscience Frontiers, 8

Heat production estimates range from a maximum of 14,000 mWm^3 to a minimum of 0.001 mWm^3, but the vast majority of the data fall between 0.01 and 30 mWm^3.

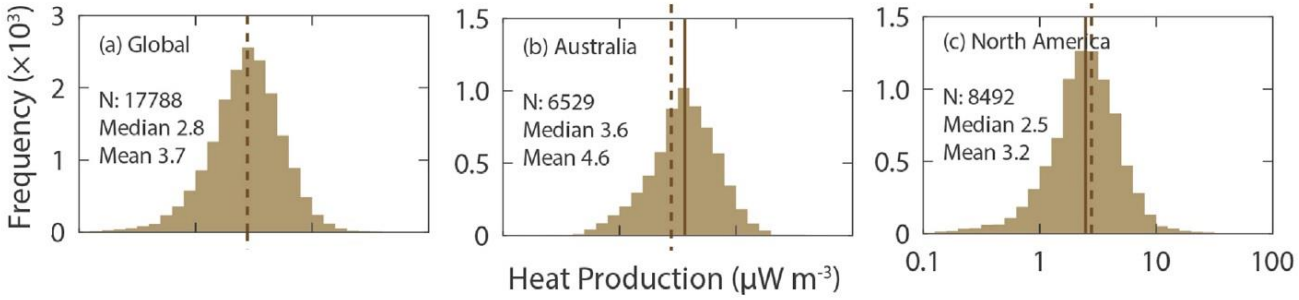

Radiogenic Heat Generation, density, and *P*-wave velocity: dependency on SIO_2 (first order compositional variations)

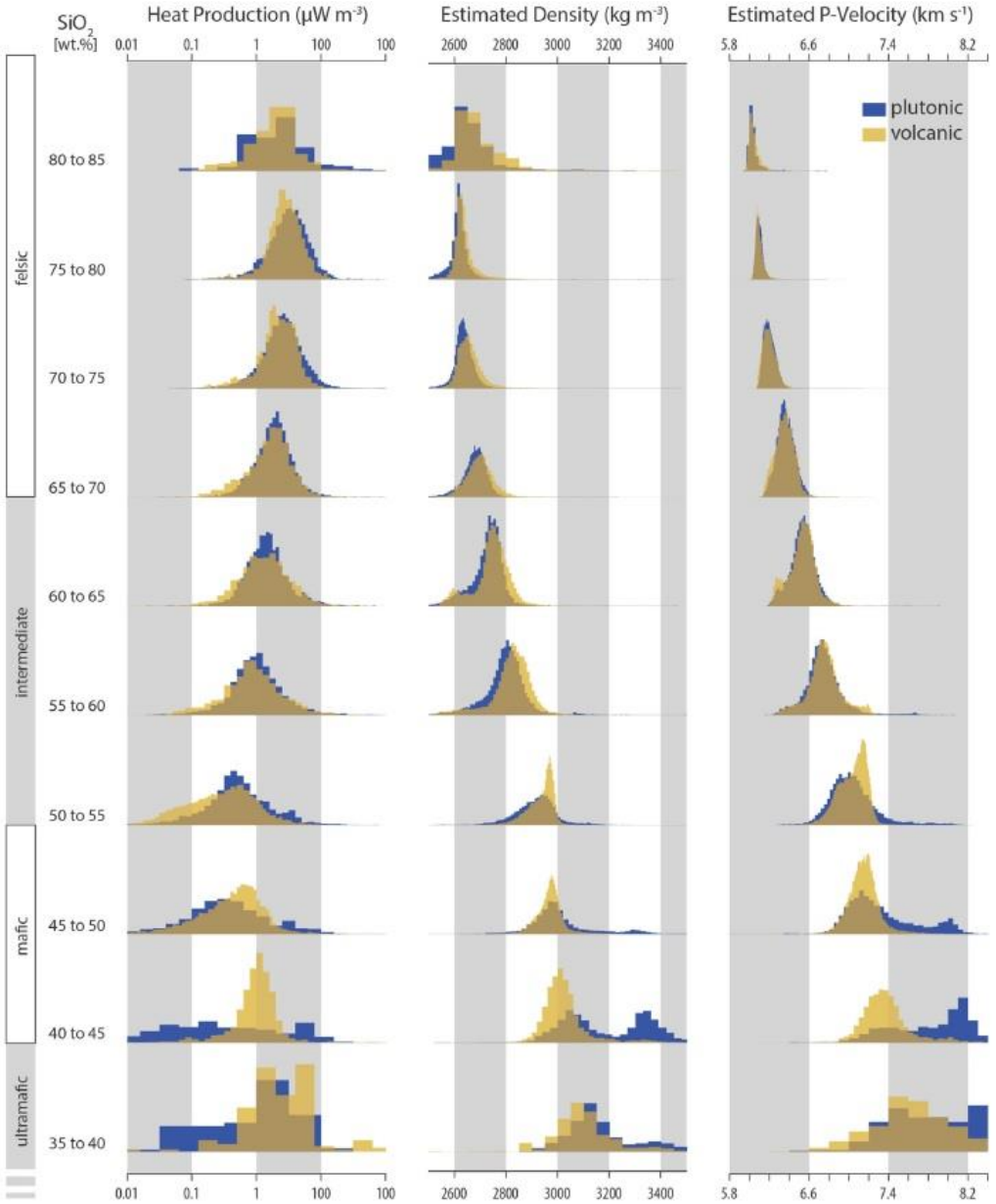

- Density and seismic velocity generally increase as composition ranges from felsic to mafic, while heat production decreases from felsic to mafic compositions.
- Density and seismic velocity distributions show a more complex behaviour for SIO_2 <65 wt.%, while heat production distribution for SiO_2 <55 wt.%, due to the presence of other oxides in the rocks.

Hasterok and Webb, 2017, Geoscience Frontiers, 8

Radiogenic Heat Generation and Surface Heat flow

Radiogenic heat production and surface heat flow values from a range of geological provinces. Data from Roy *et al.* (1968).

Locality	*A* Radiogenic heat production 10^{-13} cal cm^{-3} s^{-1} (μW m^{-3})	Q_0 Surface heat flow 10^{-6} cal cm^{-2} s^{-1} (mW m^{-2})
New England		
1	20.7 (8.7)	2.27 (95.0)
2	21.2 (8.8)	2.15 (90.0)
3	17.6 (7.4)	1.89 (79.1)
4	12.9 (5.4)	1.80 (75.3)
5	11.6 (4.9)	1.63 (68.2)
6	9.6 (4.0)	1.63 (68.2)
7	7.8 (3.3)	1.34 (56.1)
8	3.8 (1.6)	1.08 (45.2)
Central Stable region		
9	7.6 (3.2)	1.46 (61.1)
10	5.8 (2.4)	1.22 (51.0)
11	5.5 (2.3)	1.17 (49.0)
12	1.4 (0.59)	0.82 (34.3)
13	<0.4 (0.17)	0.81 (33.9)
14	<0.4 (0.17)	0.79 (33.1)
15	<0.4 (0.17)	0.81 (33.9)
Sierra Nevada		
16	8.8 (3.7)	1.30 (54.4)
17	4.0 (1.7)	1.25 (52.3)
18	9.6 (4.0)	1.25 (52.3)
19	6.4 (2.7)	1.06 (44.4)
20	4.7 (2.0)	0.83 (34.7)
21	3.2 (1.3)	0.73 (30.5)
22	1.8 (0.75)	0.62 (25.9)
23	2.2 (0.92)	0.60 (25.1)
Basin and Range province		
24	10.7 (4.5)	2.40 (100.4)
25	6.0 (2.5)	3.40 (142.3)
26	7.9 (3.3)	2.30 (96.2)
27	10.3 (4.3)	2.22 (92.9)
28	7.1 (3.0)	2.20 (92.0)
29	6.7 (2.8)	2.20 (92.0)
30	2.0 (0.84)	2.14 (89.6)
31	7.7 (3.2)	2.00 (83.7)
32	5.7 (2.4)	1.90 (79.5)
33	5.3 (2.2)	1.88 (78.7)
34	7.7 (3.2)	1.82 (76.1)
35	3.8 (1.6)	1.78 (74.5)
36	3.1 (1.3)	1.65 (69.0)
37	6.6 (2.8)	1.64 (68.6)
38	3.1 (1.3)	1.60 (66.9)

$$q_0 = q_a + A_0 D$$

Reduced heat flows	Depth constant
Sierra Nevada 22 mW m^{-2}	8.4 km
Basin and Range 72 mW m^{-2}	5.8 km
Stable interior 31 mW m^{-2}	8.6 km
New England 38 mW m^{-2}	6.2 km

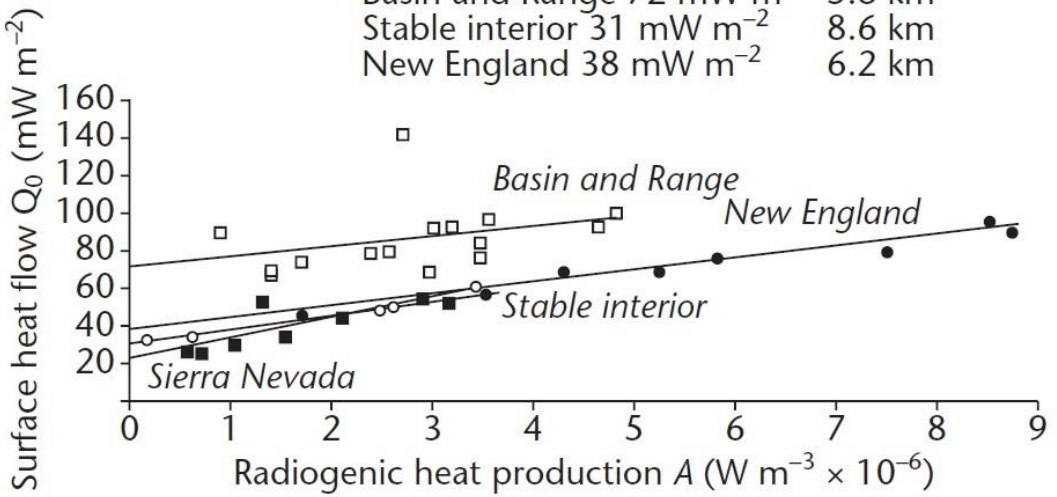

- Surface heat flow reflect the amont of radiogenic heat production in the shallow crust (e.g., New England), as well as the contribution of deeper sources, such as a shallow hot upper mantle (Basin and Range)

Heat

EXAMPLE 1.

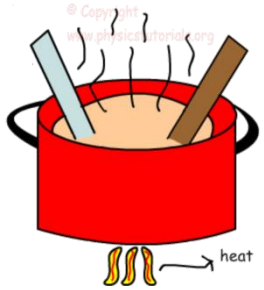

MORE HEAT = HIGHER TEMPERATURE

$$Q = T$$

EXAMPLE 2.

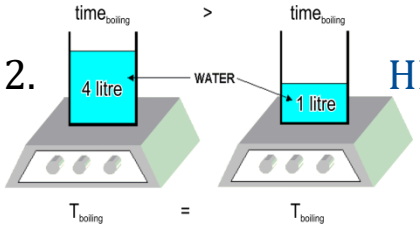

HEAT depends on the MASS, TEMPERATURE NO

$$Q = m\,T$$

EXAMPLE 3.

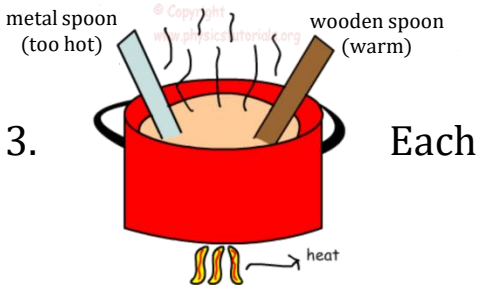

Each material has its own characteristic to absorb HEAT

$$Q = m\,c_p\,T$$

Conductive Heat Transfer

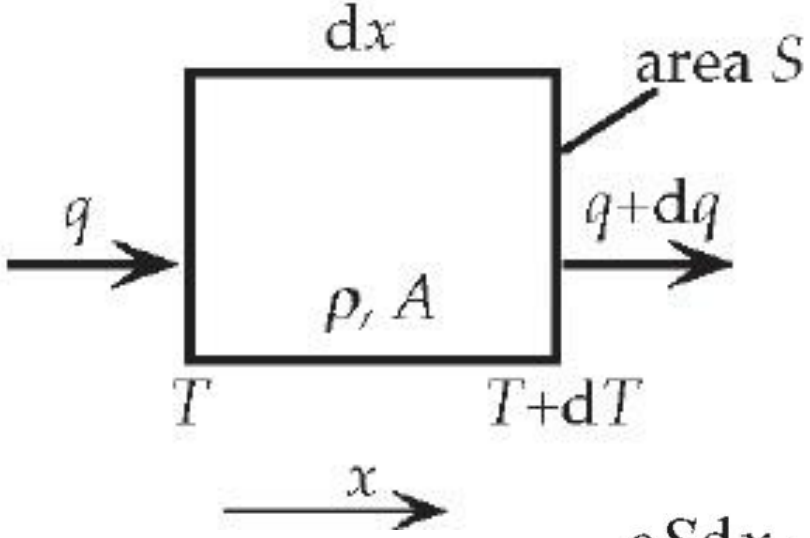

The change in heat content of the block during a time interval will be equal to the heat conducted in minus the heat conducted out plus the heat generated internally (*A*).

$$dH = \rho S dx \cdot C_P \cdot dT$$

$$\rho S dx \cdot C_P \cdot dT = qS\,dt - (q + dq)S\,dt + A \cdot S dx \cdot dt$$

$$\rho C_P \frac{\partial T}{\partial t} = -\frac{\partial q}{\partial x} + A$$

H = heat content, ρ = density, *S* = area of the end surfaces of the block (ρSdx = mass of the block), and C_P = specific heat at constant pressure, which measures the capacity of a material to hold heat, and for mantle minerals it has a value of the order of 1000 J/kg K.

$$q = -\lambda \frac{\partial T}{\partial x}$$

λ=K

$$\partial T/\partial t = 0$$

Poisson Equation

$$\frac{\partial T}{\partial t} = \kappa \frac{\partial^2 T}{\partial x^2} + a$$

κ=K/ρC_p and a=A/ρC_p

$$\frac{\partial^2 T}{\partial z^2} = -\frac{A}{K}$$

Change of the vertical geothermal gradient with depth

κ = **thermal diffusivity** (physical property that controls the rate at which heat dissipates through a material)

Temperature variations with depth (steady state conditions)

If A=0 $T_0' = -q_0/K \approx 20\,^{\circ}\mathrm{C/km}$

For a constant gradient, at 60 km depth the temperature would be 1200 °C (it would approach the melting point)

$\frac{\partial^2 T}{\partial y^2} = -\frac{A}{K}$ First integration gives $\frac{\partial T}{\partial y} = -\frac{A}{K}y + c_1$

For $T=T_0$ at y=0:

Second integration

$\partial T/\partial y = Q_0/K$ at $y = 0$ $T = -\frac{A}{2K}y^2 + \frac{Q_0}{K}y + c_2$

since $T=T_0$ at y=0, $c_2=T_0$ $T = T_0 + \frac{Q_0}{K}y - \frac{A}{2K}y^2$

Temperature variations with depth (steady state conditions)

Heat Generation changes exponentially with depth
If q_0 varies linearly with q_a:

$$q_o = q_a + A_o D \qquad A(z) = A_o \exp\left(-\frac{z}{D}\right)$$

q_a=mantle heat flow

$$\partial T/\partial t = 0$$

$$\frac{\partial^2 T}{\partial z^2} = -\frac{A}{K}$$

First Integration

$$k\frac{d^2T}{dz^2} + A_o \exp\left(-\frac{z}{D}\right) = 0 \qquad k\frac{dT}{dz} - D\,A_o \exp\left(-\frac{z}{D}\right) = c_1$$

c_1 is the heat flow from the mantle q_a

$$q = -q_a - D\,A_o \exp\left(-\frac{z}{D}\right)$$

Second Integration

$$k\,T + D^2 A_o \exp\left(-\frac{z}{D}\right) - q_a\, z = c_2$$

$$T = T_o \text{ at } z = 0 \qquad c_2 = k\,T_o + D^2\,A_o$$

$$T = T_o + \frac{D^2\,A_o}{k}\left[1 - \exp\left(-\frac{z}{D}\right)\right] + \frac{q_a}{k}\,z$$

If A_0 is unknown we can substitute DA_0 with Q_0-Q_a, since $q_0=q_a+A_0D$

Temperature variations with radiogenic heat production

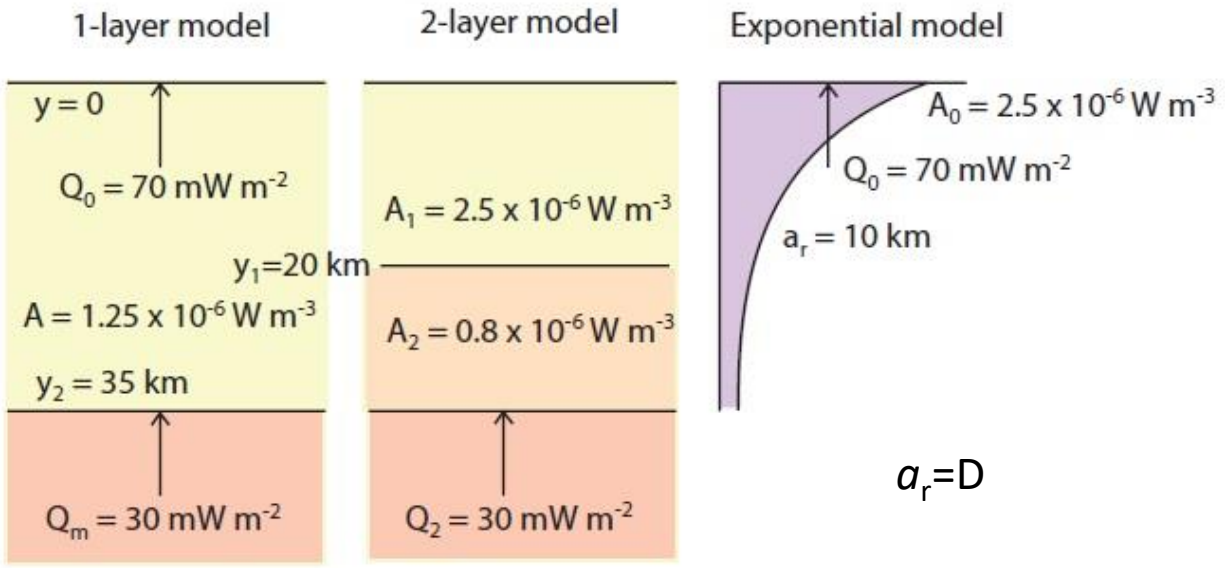

a_r=D

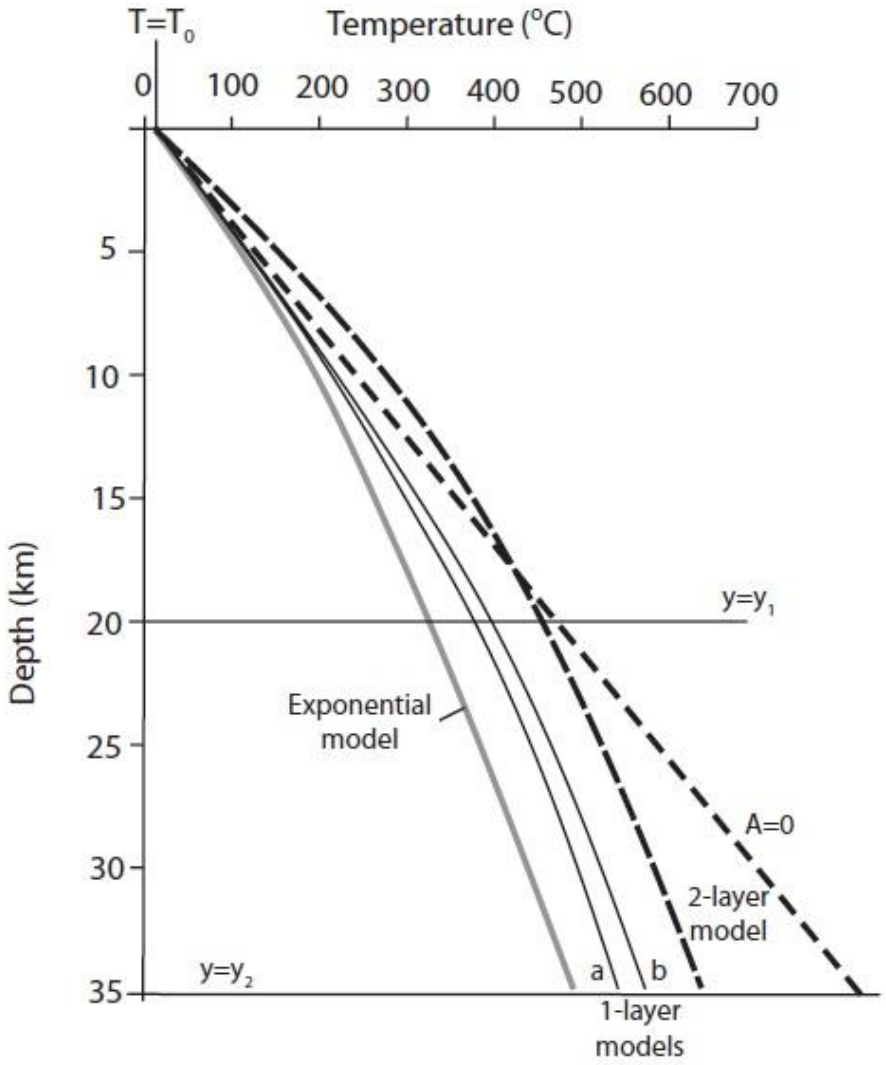

Relationship between local heat flow and heat production values ?
Test : Trans Hudson Orogen

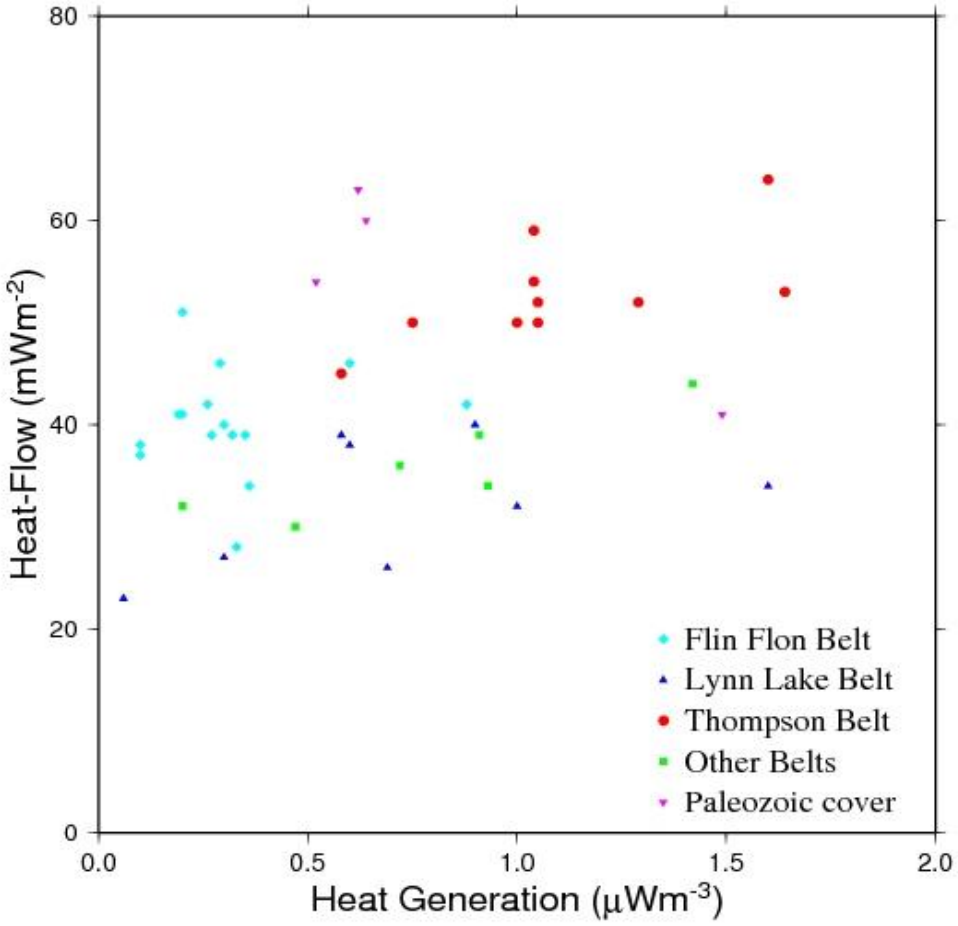

- No clear heat flow – heat production relationship for the entire THO nor for its individual belts.

- No meaningful relationship for any province of the Canadian Shield.

Radiogenic Heat Generation lateral variability

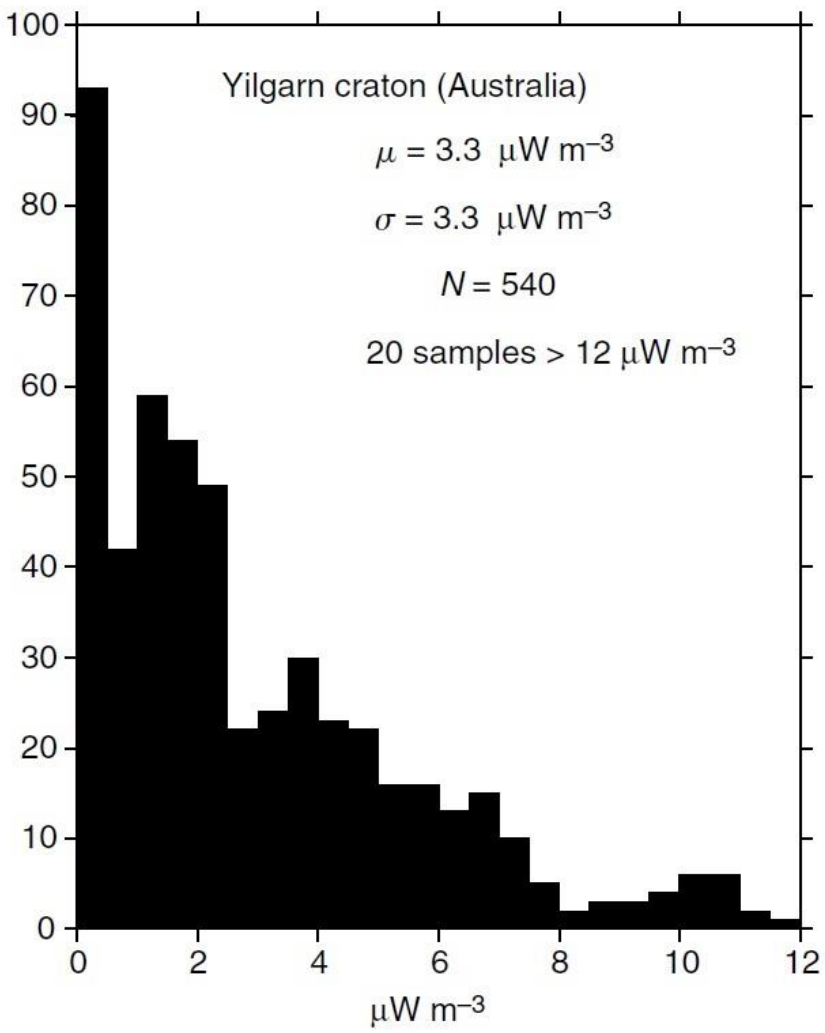

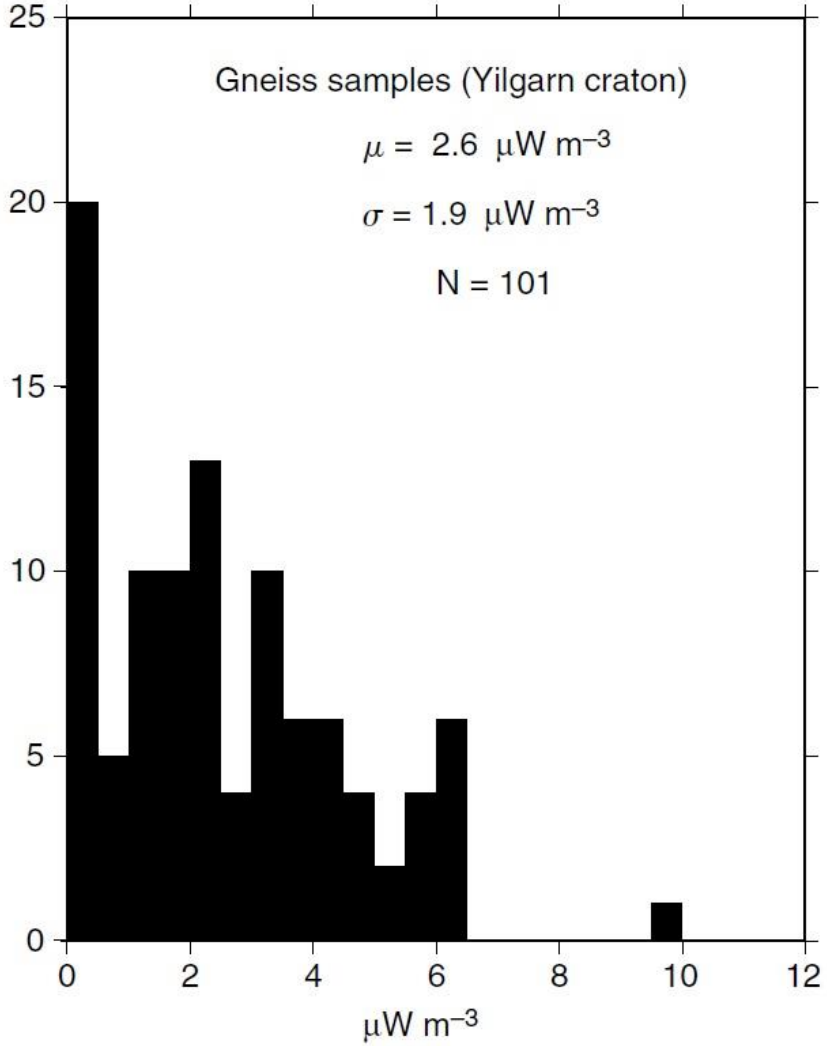

- Heat Generation may vary by a factor of 5 over horizontal distances of few tens of meters, due to rocks heterogeneity, fluid migration, and phase changes.

Scale for a representative heat production model

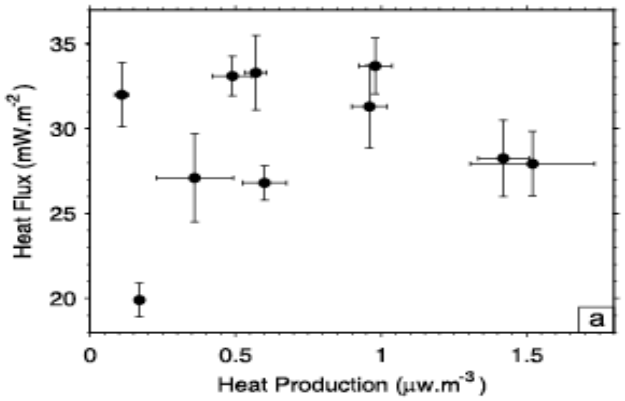

Individual measurements

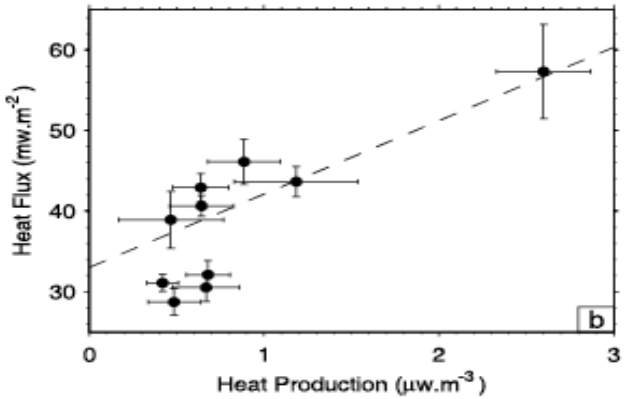

≈ 200x200 km windows

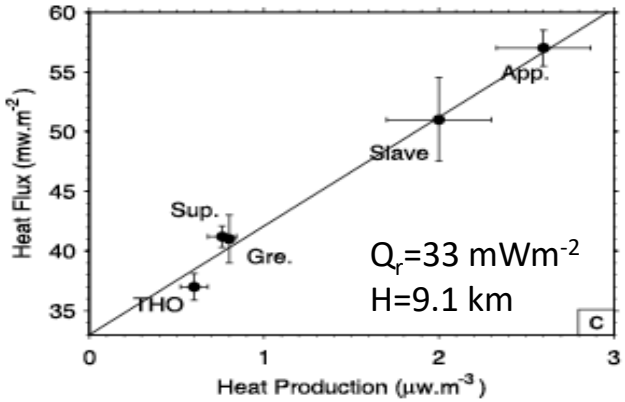

≈ 500x500 km windows

- **On a large scale there is a relationship between heat flux and heat production when they are averaged on a province.**
- **Variations in surface heat flux between geological province occur on a short distance (< 50 km, due to variations of surface heat flow in the crust)**

On a large scale, three key control variables on lithospheric temperatures are correlated:

- **average surface heat flux,**
- **average crustal heat production,**
- **vertical variation of heat production.**
- **Variations in the basal heat flux are small (3 mWm^2).**

Estimating the degree of enrichment in the upper crust (Differentiation Index)

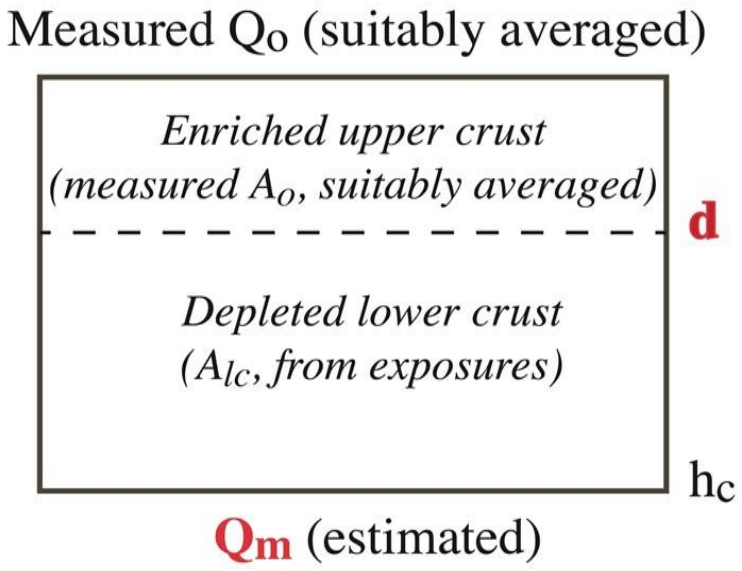

$$q_o = q_a + A_o D$$

$q_a = Q_m$ $A_0 = A_c$ $D = z_m$

$$D_i = \frac{A_s}{A_c} = \frac{A_s z_m}{Q_0 - Q_m}$$

A_s = average surface heat production
A_c = average crustal heat production
$A_c = (Q_0 - Q_m) / Z_m$
z_m = Moho depth

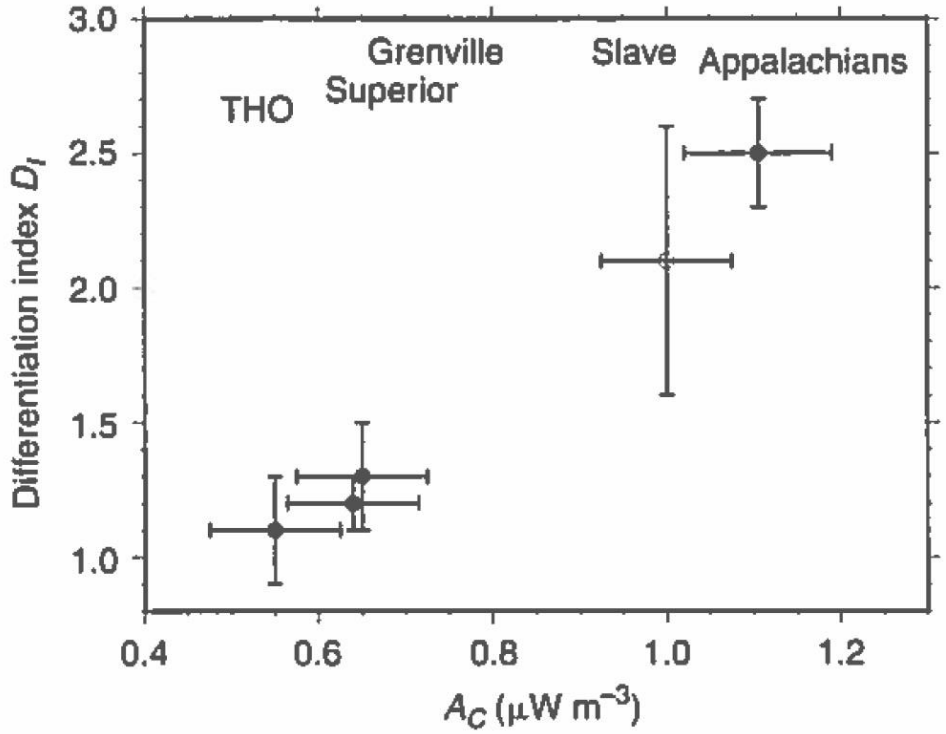

- Usually $D_i > 1$ (e.g., D_i ~3 for Phanerozoic Appalachian and D_i ~ 1 for Proterozoic Greenville).
- D_i=0.4 at Kola peninsula (Baltic Shield), since Proterozoic rocks were tectonically transported over Archean basement (more radiogenic).
- Moho temperature increases with increasing A_c and decreases with increasing D_i.

Heat Flux and Crustal Thickness

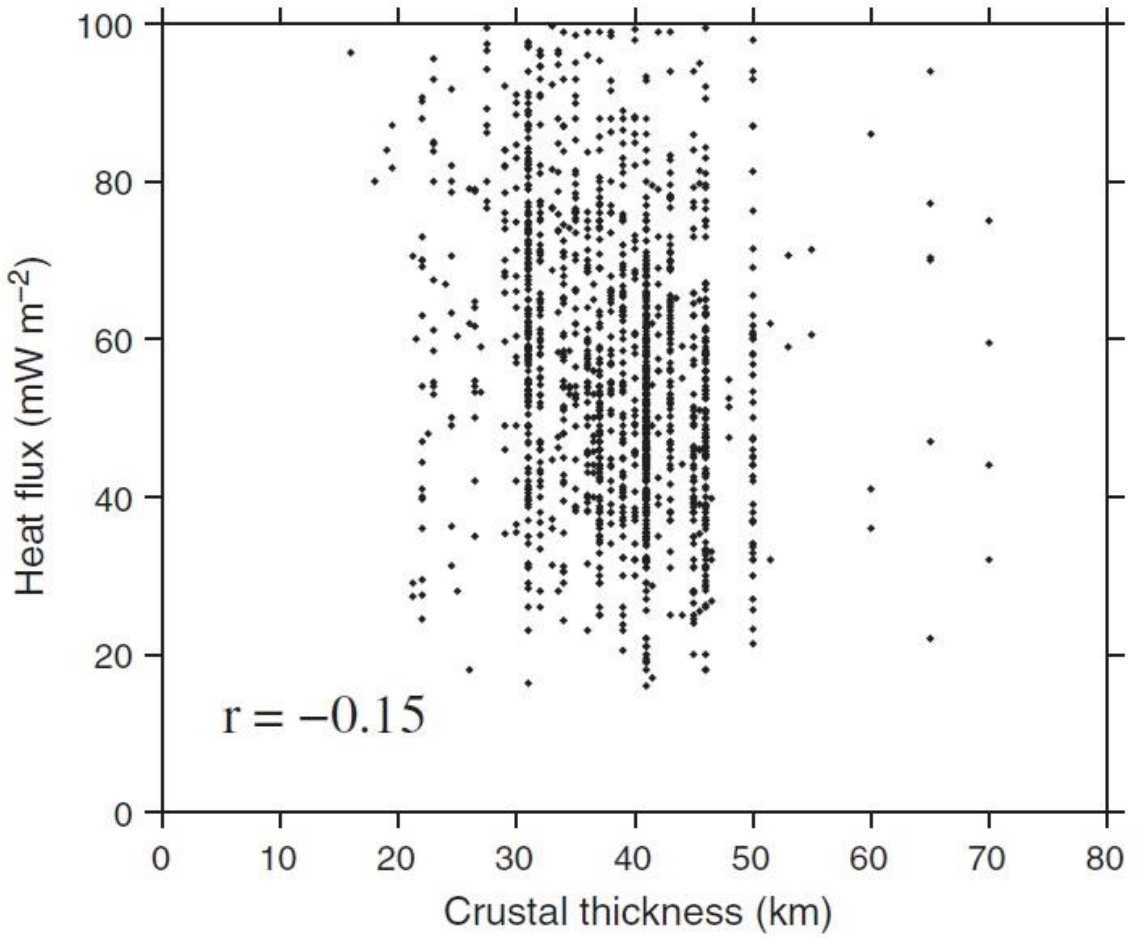

Moho Temperatures and Radiogenic Generation Distribution

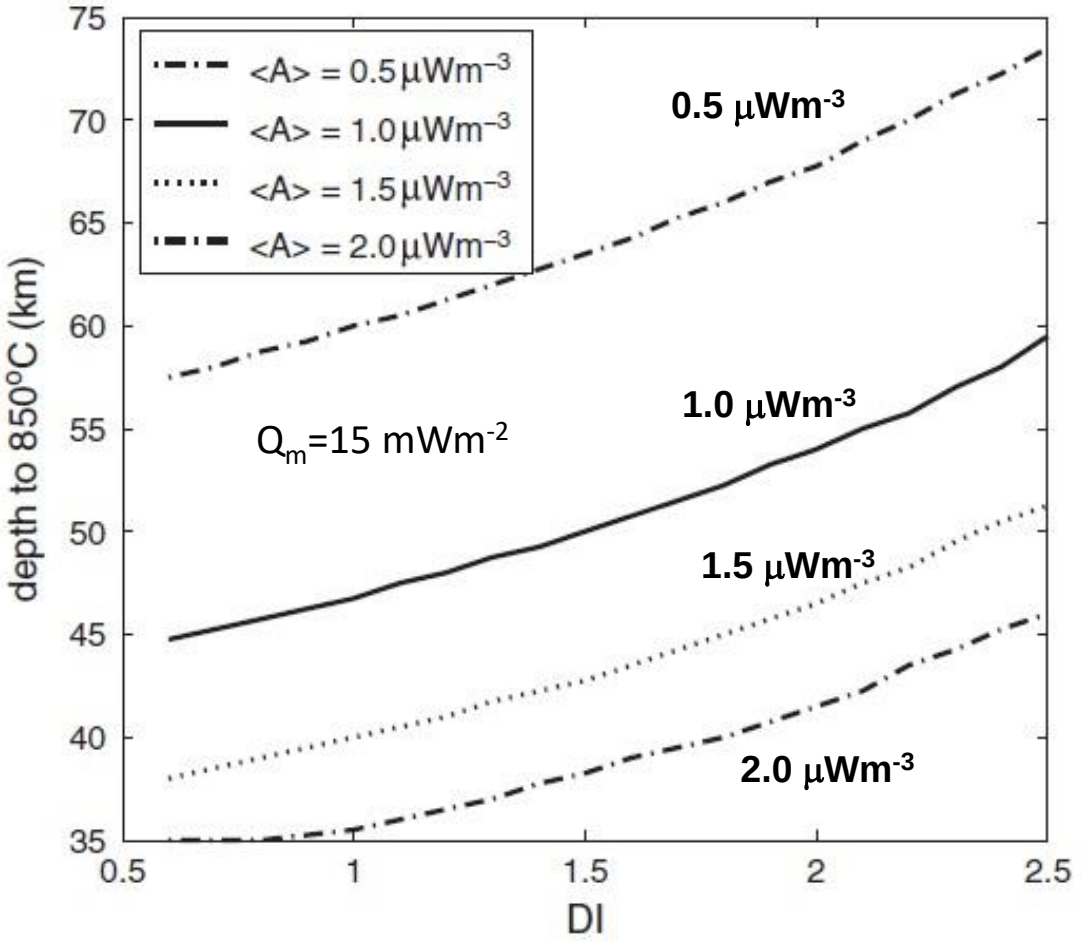

Mareschal and Jaupart, 2013, Tectonophysics, 609

No correlation between surface heat flux and Moho depth, since the crust is differentiated

Thermal Lithosphere (heat flow data, electromagnetic, and xenolith data) and Seismic Lithosphere

Thermal Lithospheric Thickness

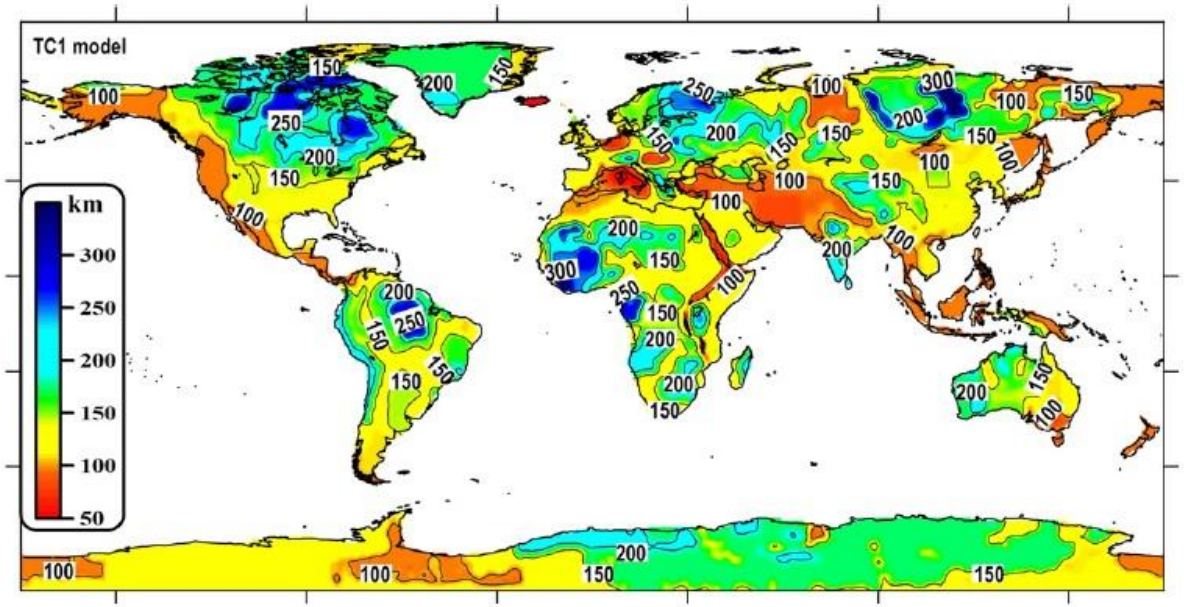

Lithospheric Thickness from surface-wave seismic tomography

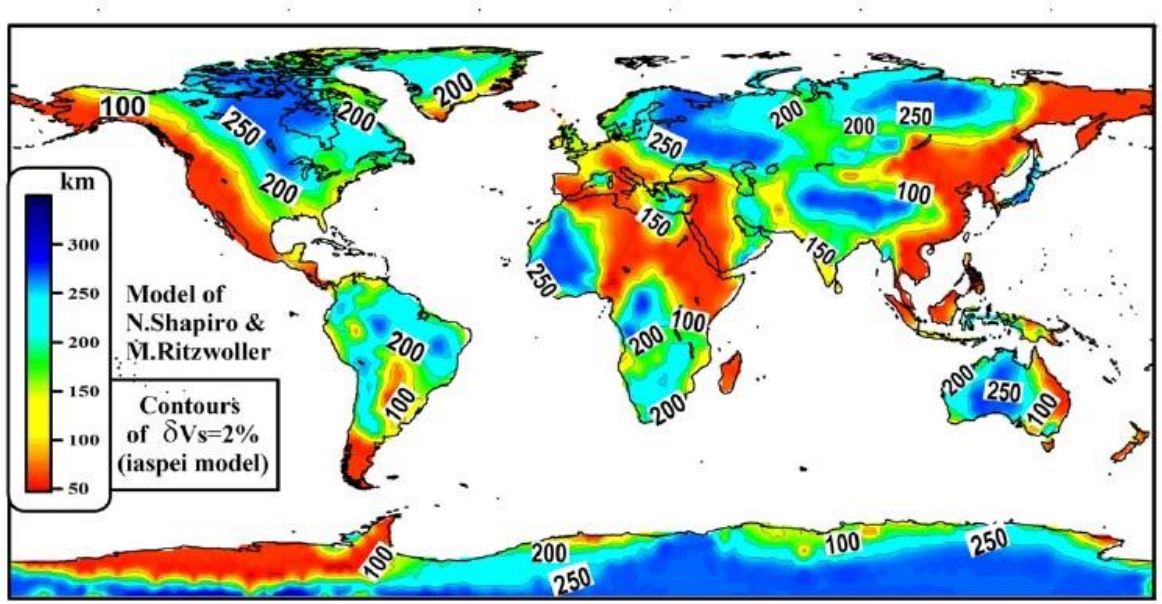

Artemieva, 2009, Lithos, 109

- **Thermal Lithospheric Thickness:** determined by the intersection of a lithospheric geotherm with a mantle adiabat Tm~ 1350°C or at T~ $0.8T_m$ (~ 1100°C), at the top of the transitional layer from high to low viscosity. It is usually 40-50 km shallower than the seismological boundary detected from seismic tomography (based of the convective boundary).
- **Seismic Lithospheric Thickness**: the lithospheric base is defined here as the depth where Vs velocity in the upper mantle is 2.0±0.5% higher.

Depth of the lithosphere: from conduction to convection

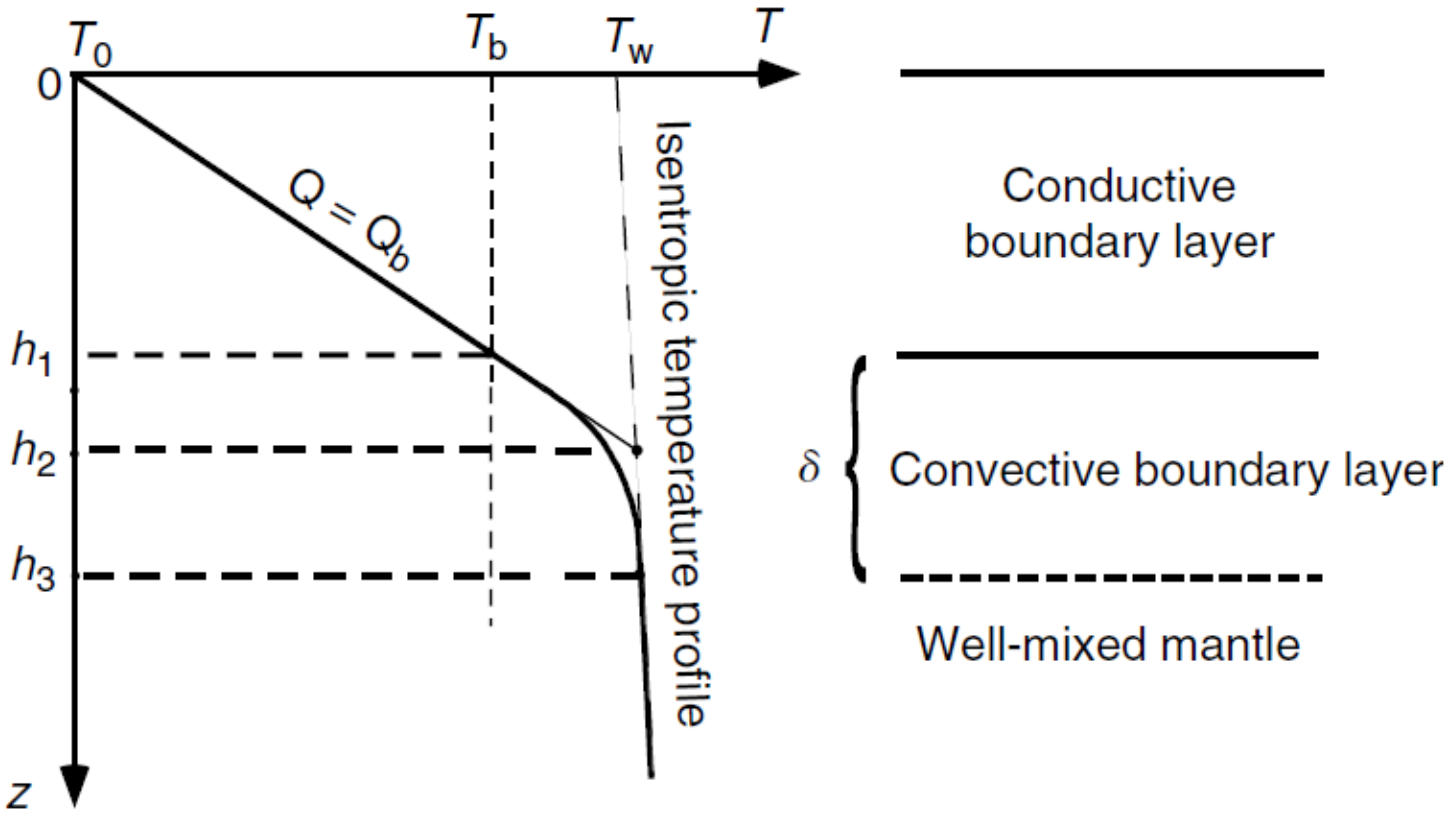

h_1= lower boundary of the conductive part (bottom of the thermal lithosphere).
h_2= intersection between the downward extrapolation of the conductive geotherm and the temperature profile for the convective mantle.
h_3= lower limit of the thermal boundary layer (transition between lithospheric regime and fully convective mantle regime).
T_0=temperature at the surface
T_b=temperature at the base of the lithosphere
T_W=temperature of well-mixed convective interior

Seismic velocity and temperature

Pn velocity

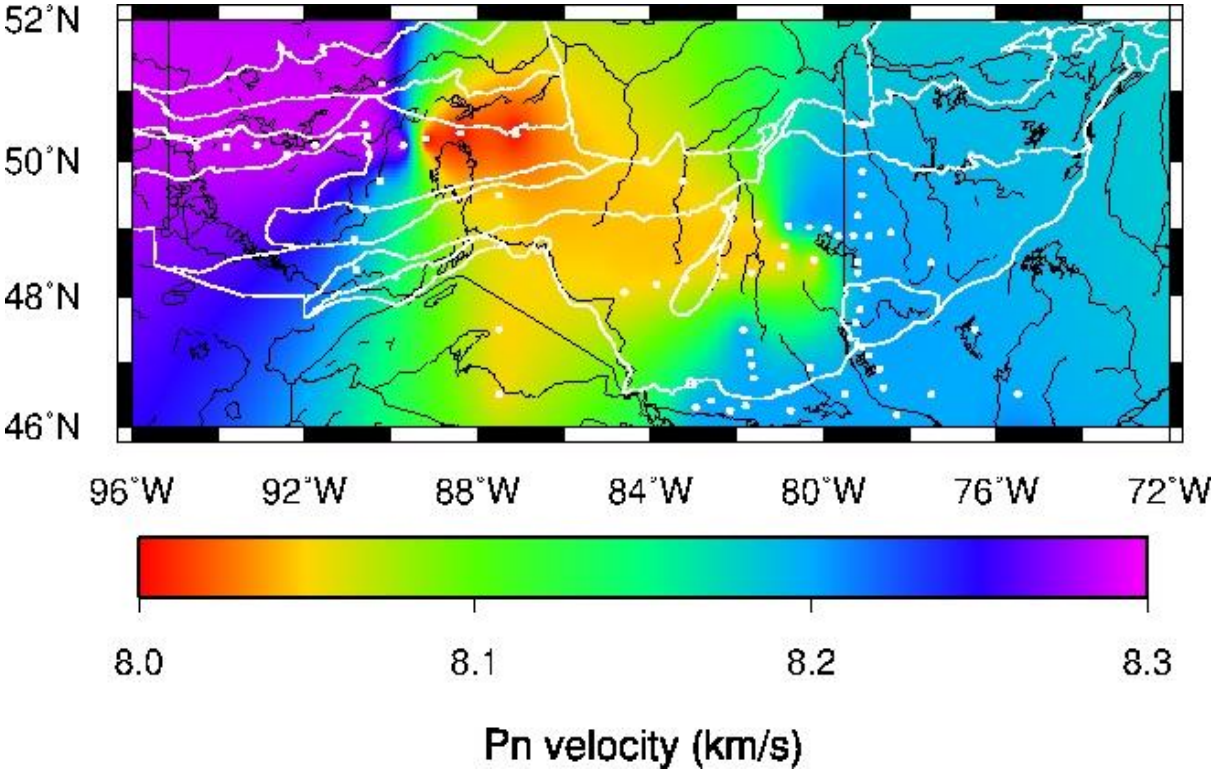

Heat Flow

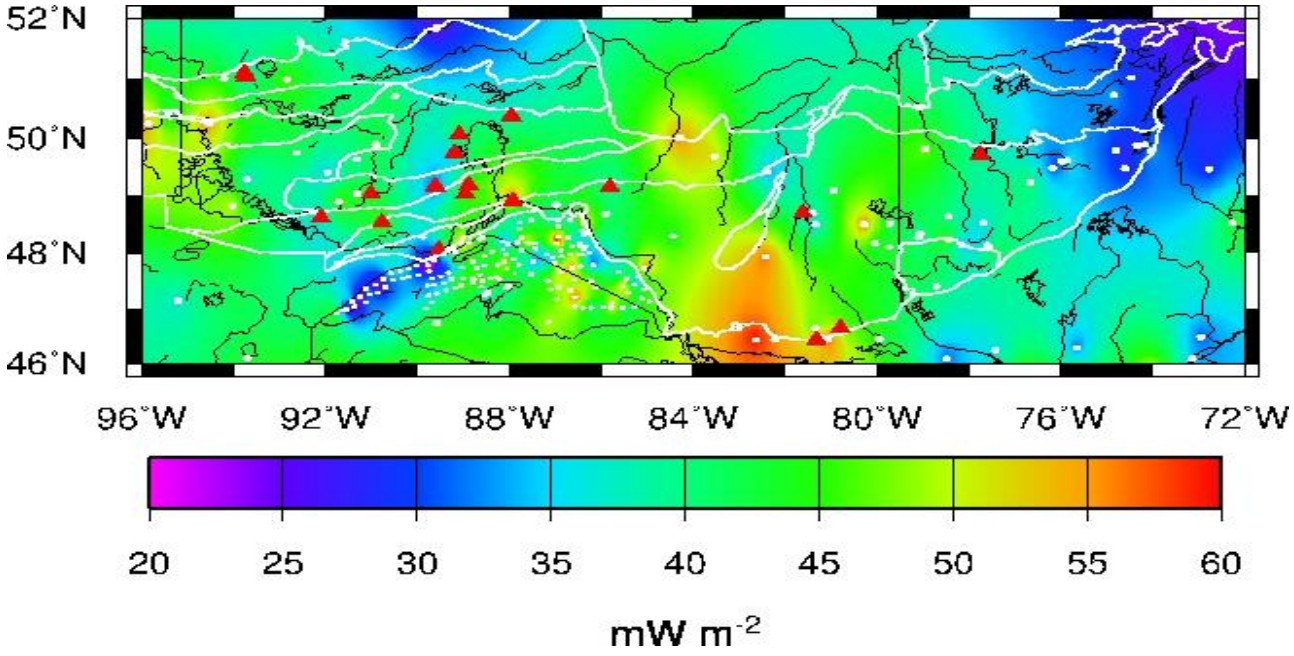

Seismic velocity and temperature

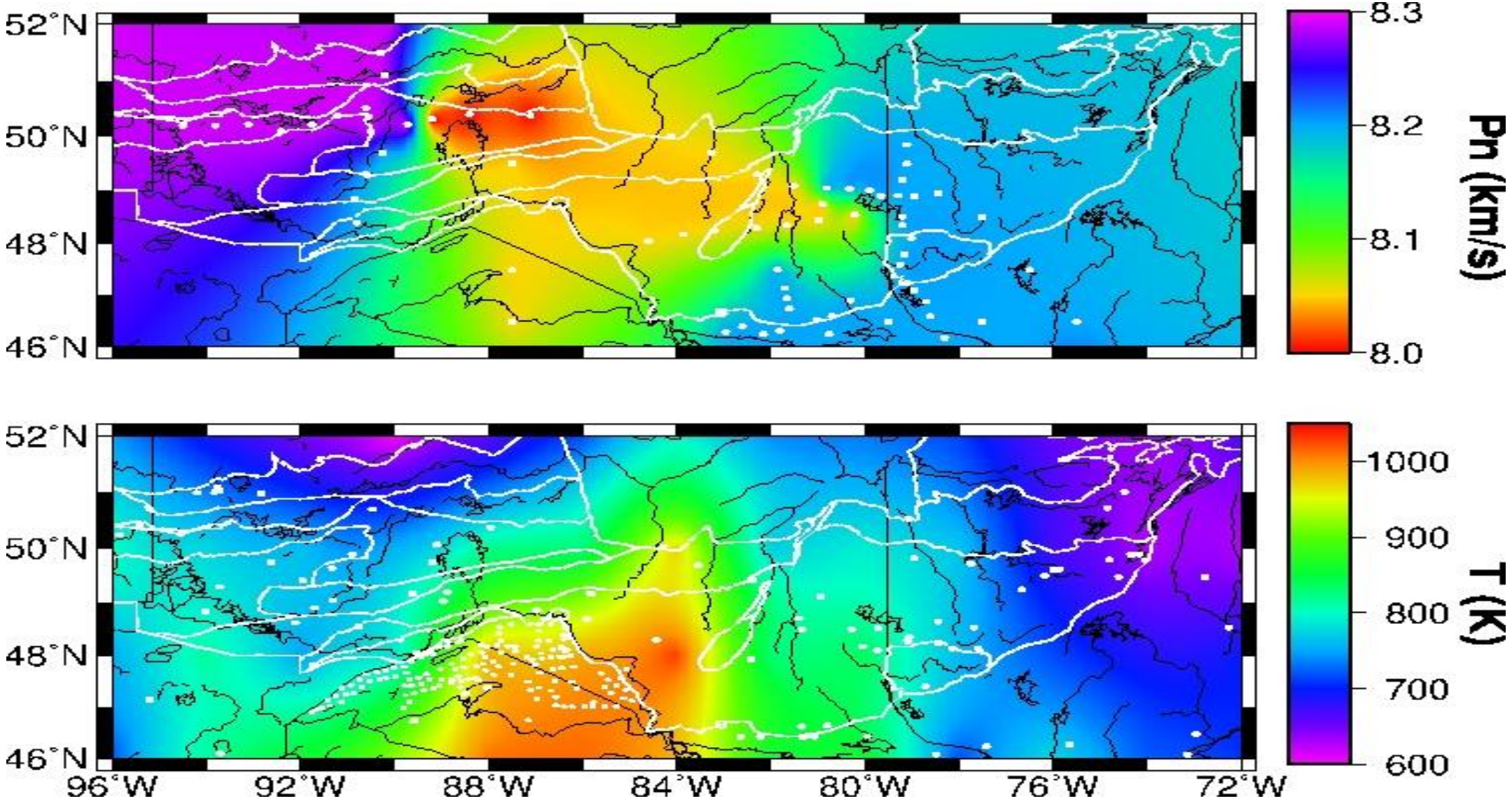

P-wave velocity as a function of temperature and composition

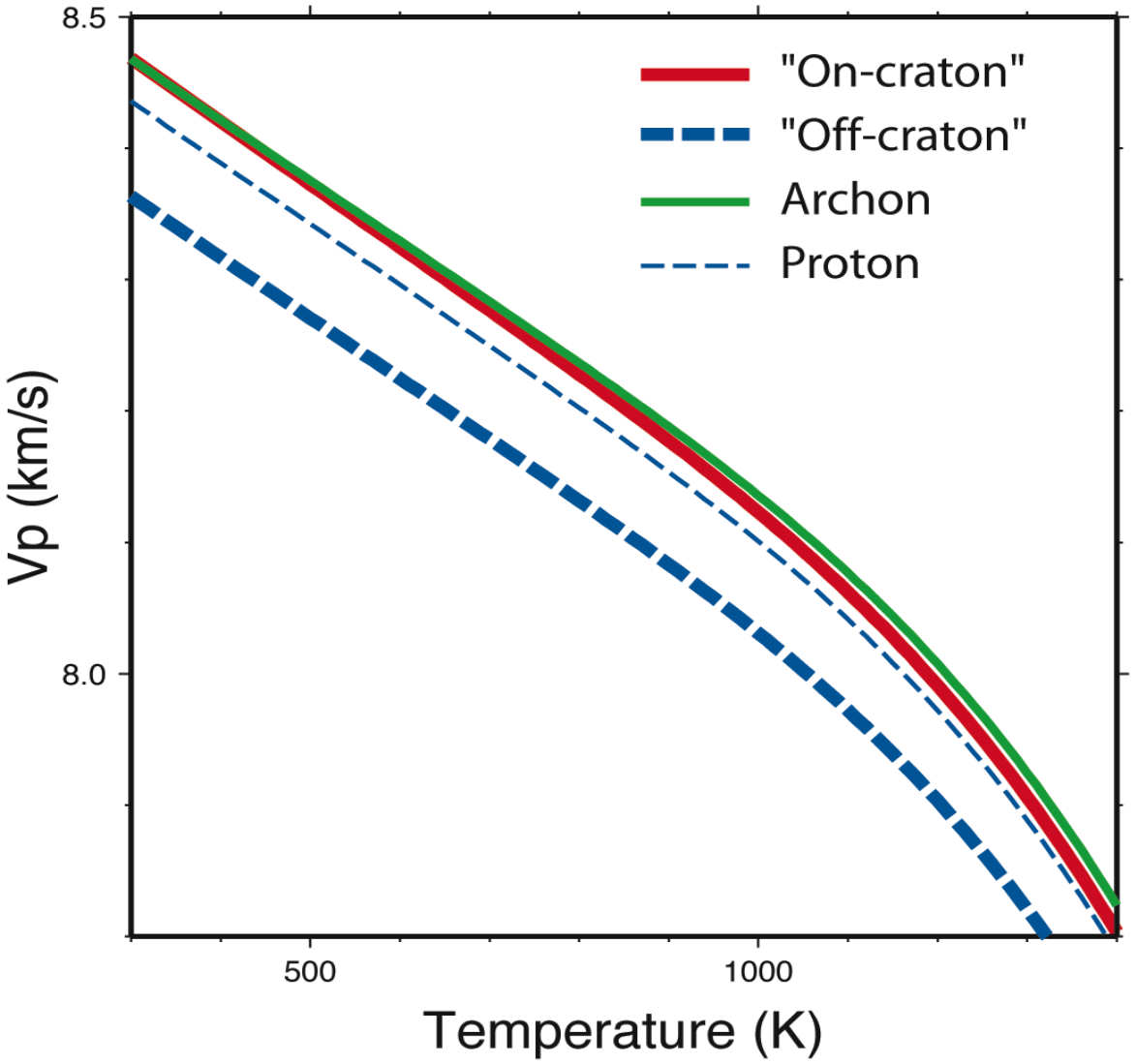

Temperature variations in depth constrained by xenoliths

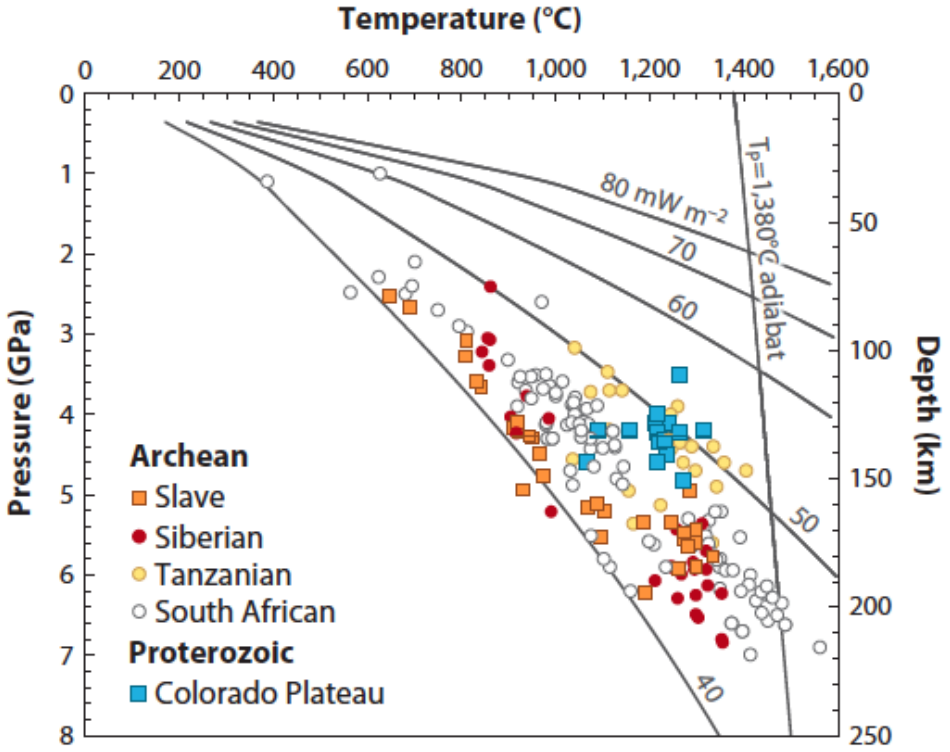

Lee et al., 2011, Annu. Rev. Earth Planet. Sci

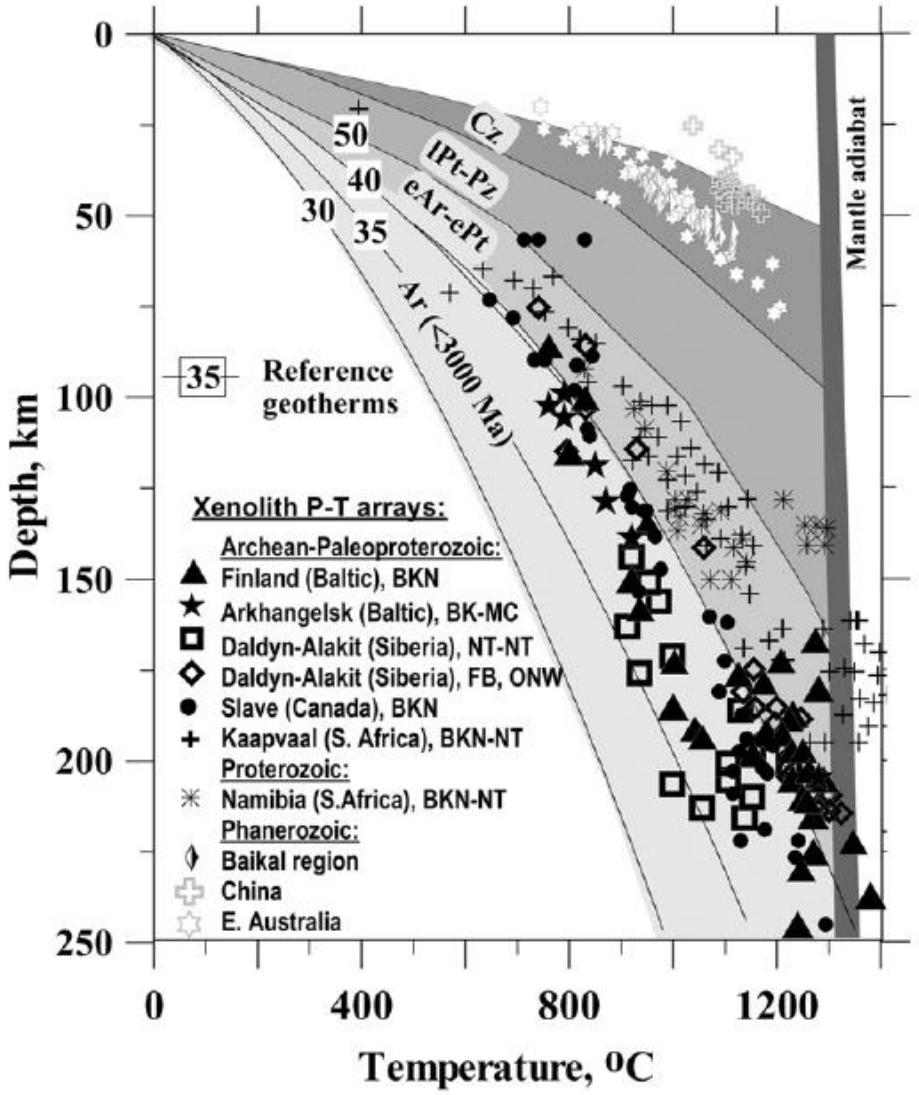

Artemieva, 2009, Lithos, 109

Issues for thermobarometry:

- **Pressures more uncertain than temperatures**
- **Some xenoliths were sheared just prior to quenching and do not represent conductive steady-state**
- **Some xenoliths may have been transported upward along adiabat**

No Steady-state conditions

Heat flow > 90 mWm^2 imply melting in the crust or a weak lithospheric mantle
(other heat transport mechanisms are effective in tectonic active areas)

Crustal thickness variations imply changes of crustal heat production and deformation (change of temperature distribution)

- Erosion or crustal extension initially cause steeper geotherms and enhanced heat flux and later the reduced crustal thickness and possible injection of basaltic melts (depleted in radioelements) leads to a lower heat flux than initial.
- Crustal thickening causes the geothermal gradient and the heat flux to decrease at first and then to increase due to higher crustal heat production (e.g., Tibet and Alps).
- Heat flux may record shallow processes such as the cooling of recently emplaced plutons. The anomalously high heat flux in the Basin and Range Province (about 110 mWm^2) and the high elevation (about 1750 m) is consistent with an extension of 100% and presence of shallow magma intrusions.

- ***crustal thinning causes subsidence and reduces heat flux***

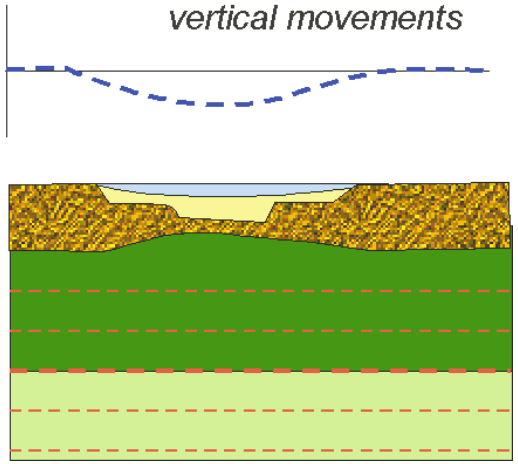

- ***crustal thickening causes uplift and increases heat flux***

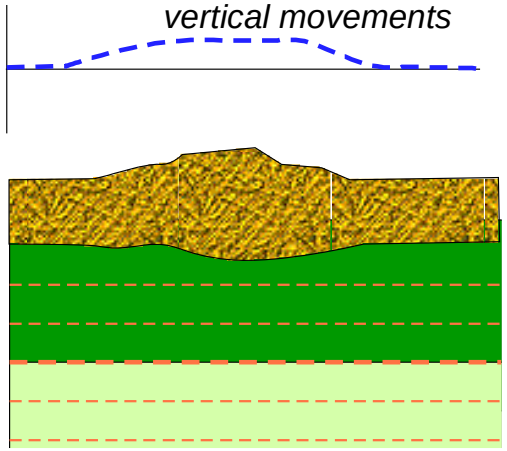

Crustal temperatures return to equilibrium with local heat sources in less than 100 My.
Mantle lithosphere re-equilibrate much slower. For thick lithosphere, such transients may last as long as 500 My